

**METHODOLOGY AND ALGORITHMS FOR
PEDESTRIAN NETWORK CONSTRUCTION**

by

Piyawan Kasemsuppakorn

B.Sc. in Statistics, Chulalongkorn University, Thailand, 1998

M.Sc. in Info Sys Mgt, The National Institute of Development Administration, Thailand, 2000

Submitted to the Graduate Faculty of
School of Information Sciences in partial fulfillment
of the requirements for the degree of
Doctor of Philosophy

University of Pittsburgh

2011

UNIVERSITY OF PITTSBURGH
SCHOOL OF INFORMATION SCIENCES

This dissertation was presented

by

Piyawan Kasemsuppakorn

It was defended on

September 8, 2011

and approved by

Burcu Akinci, PhD, Professor, Department of Civil and Environmental Engineering,
Carnegie Mellon University

Dan Ding, PhD, Assistant Professor, School of Health and Rehabilitation Sciences

Stephen Hirtle, PhD, Professor, School of Information Sciences

Vladimir I. Zadorozhny, PhD, Associate Professor, School of Information Sciences

Dissertation Advisor: Hassan A. Karimi PhD, Associate Professor,
School of Information Sciences

Copyright © by Piyawan Kasemsuppakorn

2011

METHODOLOGY AND ALGORITHMS FOR PEDESTRIAN NETWORK CONSTRUCTION

Piyawan Kasemsuppakorn, PhD

University of Pittsburgh, 2011

With the advanced capabilities of mobile devices and the success of car navigation systems, interest in pedestrian navigation systems is on the rise. A critical component of any navigation system is a map database which represents a network (e.g., road networks in car navigation systems) and supports key functionality such as map display, geocoding, and routing. Road networks, mainly due to the popularity of car navigation systems, are well defined and publicly available. However, in pedestrian navigation systems, as well as other applications including urban planning and physical activities studies, road networks do not adequately represent the paths that pedestrians usually travel. Currently, there are no techniques to automatically construct pedestrian networks, impeding research and development of applications requiring pedestrian data. This coupled with the increased demand for pedestrian networks is the prime motivation for this dissertation which is focused on development of a methodology and algorithms that can construct pedestrian networks automatically.

A methodology, which involves three independent approaches, network buffering (using existing road networks), collaborative mapping (using GPS traces collected by volunteers), and image processing (using high-resolution satellite and laser imageries) was developed. Experiments were conducted to evaluate the pedestrian networks constructed by these approaches with a pedestrian network baseline as a ground truth. The results of the experiments indicate that these three approaches, while differing in complexity and outcome, are viable for automatically constructing pedestrian networks.

TABLE OF CONTENTS

PREFACE.....	XIV
1.0 INTRODUCTION.....	1
1.1 MOTIVATION	1
1.2 RESEARCH PROBLEMS, CHALLENGES, AND SIGNIFICANCE.....	9
1.3 RESEARCH OBJECTIVES AND CONTRIBUTIONS	10
1.4 ORGANIZATION OF THE DISSERTATION.....	11
2.0 PEDESTRIAN NETWORK.....	12
2.1 CATEGORIZATION OF PEDESTRIAN PATHS	14
2.2 VECTOR DATA MODEL.....	17
2.3 PEDESTRIAN NETWORK DATABASE STRUCTURE.....	18
2.4 DATA NEEDS ANALYSIS	21
3.0 BACKGROUND AND RELATED WORK	24
3.1 BACKGROUND	24
3.1.1 Applications.....	24
3.1.1.1 Pedestrian Navigation Systems/Services.....	25
3.1.1.2 Navigation Systems for Individuals with Special Needs	28
3.1.1.3 Urban Planning.....	31
3.1.2 Digital Map Data Providers	33

3.2	RELATED WORK.....	36
3.2.1	Map Generation Using GIS Tools	36
3.2.2	Map Generation Using GPS Traces	37
3.2.3	Map Generation Using Image Processing.....	42
4.0	PEDESTRIAN NETWORK CONSTRUCTION APPROACHES	45
5.0	NETWORK BUFFERING	49
5.1	DATA SOURCES	51
5.2	DATA PREPARATION.....	52
5.3	NETWORK CONSTRUCTION (NB ALGORITHM)	52
6.0	COLLABORATIVE MAPPING APPROACH	56
6.1	DATA SOURCE	56
6.2	DATA PREPARATION.....	57
6.3	NETWORK CONSTRUCTION (CM ALGORITHMS).....	59
6.3.1	Pre-Processing.....	61
6.3.2	Significant Point Filtering.....	62
6.3.3	Pedestrian Network Construction.....	67
7.0	IMAGE PROCESSING.....	73
7.1	DATA SOURCES	76
7.1.1	Orthoimages	76
7.1.2	LiDAR (Light Detection and Ranging).....	77
7.2	DATA PREPARATION.....	79
7.3	NETWORK CONSTRUCTION (IP ALGORITHMS).....	89
7.3.1	Object Filtering.....	89

7.3.2	Pedestrian Path Region Extraction	96
7.3.3	Pedestrian Network Construction.....	101
7.3.4	Raster-To-Vector Conversion.....	108
8.0	EVALUATION.....	111
8.1	EVALUATION METHODOLOGY	111
8.2	PEDESTRIAN NETWORK BASELINE AND THE STUDY AREA	114
8.3	EVALUATION OF THE NETWORK BUFFERING APPROACH.....	118
8.4	EVALUATION OF THE COLLABORATIVE MAPPING APPROACH	124
8.5	EVALUATION OF THE IMAGE PROCESSING APPROACH.....	130
8.6	EVALUATION DISCUSSION.....	136
9.0	RECOMMENDATION	140
10.0	CONCLUSIONS AND FUTURE RESEARCH	153
10.1	CONCLUSIONS.....	153
10.2	FUTURE RESEARCH.....	156
	APPENDIX A	159
	BIBLIOGRAPHY	167

LIST OF TABLES

Table 2-1. Pedestrian path types	14
Table 2-2. Pedestrian path types, characteristics, and connection information	16
Table 2-3. Examples of pedestrian path types	18
Table 2-4. Summary of pedestrian network data quality criteria.....	23
Table 3-1. Summary of selected pedestrian navigation systems/services	25
Table 3-2. Summary of selected navigation systems/services for individuals with special needs	28
Table 3-3. Summary of urban planning research projects	31
Table 3-4. Examples of digital map data providers	33
Table 7-1. Characteristics of roads and pedestrian paths.....	73
Table 7-2. The statistics of training samples for two groups.....	84
Table 7-3. Statistics of training samples for four classes.....	85
Table 7-4. Error matrix for the classification result using 1-band (LiDAR intensity)	87
Table 7-5. Error matrix for the classification result using 3-band (RGB)	87
Table 7-6. Error matrix for the classification result using 4-band (RGBI).....	87
Table 8-1. Definition and formula for evaluation criteria.....	113
Table 8-2. The characteristics of pedestrian network baseline	116
Table 8-3. Environment settings and characteristic of 10 tiles.....	117

Table 8-4. Parameters for the experimentation (Network buffering)	118
Table 8-5. Example of gap distance for each direction of travel and number of lanes	119
Table 8-6. Statistics results of network buffering approach	121
Table 8-7. Statistic results of network buffering approach (Environment setting).....	122
Table 8-8. Data source and parameters used in collaborative mapping	124
Table 8-9. Statistics results of collaborative mapping approach	129
Table 8-10. Statistics results of Collaborative Mapping approach (Environment setting).....	129
Table 8-11. Details of Orthoimage and LiDAR point cloud	131
Table 8-12. Statistics results of image processing approach	133
Table 8-13. Statistics results of image processing approach (Environment settings).....	134
Table 9-1. Comparison of development complexity of the three approaches	140
Table 9-2. Comparison of evaluation results	143
Table 9-3. Comparison of evaluation results based on three environment settings.....	146
Table A-1. GPS traces used in the experiment	164
Table A-2. Results of three evaluation metrics.....	166

LIST OF FIGURES

Figure 1-1. Main components of a navigation system.....	2
Figure 1-2. Route calculated by using road network and pedestrian network.....	4
Figure 1-3. Examples of research areas in urban planning.....	6
Figure 1-4. Comparison between average PRD values for road and pedestrian networks.....	8
Figure 2-1. A conceptual of model of the real world (adapted from Lo and Yeung (2006))	12
Figure 2-2. A pedestrian network database structure.....	19
Figure 3-1. Example applications requiring pedestrian networks	24
Figure 4-1. The proposed pedestrian network construction approaches.....	46
Figure 4-2. Steps of three algorithms for pedestrian network construction.....	47
Figure 5-1. Examples of constant width buffering and variable width buffering.....	49
Figure 5-2. Data preparation and NB algorithm for pedestrian network construction	50
Figure 5-3. Digital road networks from three different map providers	52
Figure 5-4. Examples of the radial parameter.....	54
Figure 5-5. The calculated geometries of sidewalk segments	54
Figure 6-1. Public GPS traces available in Pittsburgh, PA.....	58
Figure 6-2. Public walking GPS traces (left) and public bike traces (right).....	58
Figure 6-3. Three steps of the CM algorithms.....	60
Figure 6-4. Example result after pre-processing.....	62

Figure 6-5. Steps of significant point filtering.....	63
Figure 6-6. 12-direction chain code and an example.....	65
Figure 6-7. Examples of significant point filtering.....	67
Figure 6-8. Steps of pedestrian network construction	68
Figure 6-9. An example of a generated pedestrian path segment.....	69
Figure 6-10. An example of merged significant points and paths (in circle A).....	70
Figure 6-11. An example of geometric update of merged pedestrian path.....	71
Figure 6-12. Examples of validating network topology	72
Figure 7-1. A pedestrian network model and context relations	74
Figure 7-2. Steps of the IP approach.....	75
Figure 7-3. Example of orthoimage in the University of Pittsburgh's main campus.....	77
Figure 7-4. The laser scanning technique (Renslow, 2001).....	77
Figure 7-5. Example of LiDAR point cloud in the University of Pittsburgh's main campus.....	78
Figure 7-6. An example of TIN representing DSM in the University of Pittsburgh main campus	80
Figure 7-7. A 3D view of DSM	80
Figure 7-8. Example of DSM, DEM, Last-Return surface, and LiDAR intensity image of the same location	81
Figure 7-9. An example of training sample for pedestrian paths and non-pedestrian paths groups	83
Figure 7-10. The histogram of the training samples.....	84
Figure 7-11. Examples of histograms for four classes.....	85
Figure 7-12. Examples of classified class "Concrete" represented by white areas	88

Figure 7-13. Steps of object filtering algorithm.....	90
Figure 7-14. Example of building detection result	92
Figure 7-15. An example of road detection result	93
Figure 7-16. Building and road filtering.....	94
Figure 7-17. Parking lot detection	95
Figure 7-18. Flowchart of pedestrian path area extraction	97
Figure 7-19. Examples of pedestrian path regions extraction.....	100
Figure 7-20. Algorithm to link the broken pedestrian path centerlines	102
Figure 7-21. Scanning direction and area of an end point	103
Figure 7-22. An example of candidate linking points and calculation likelihood function.....	104
Figure 7-23. Two examples of linking paths between two end points	105
Figure 7-24. Algorithm for crosswalk linking.....	106
Figure 7-25. An example of crosswalk linking.....	107
Figure 7-26. Three steps of pedestrian network construction.....	108
Figure 7-27. Algorithm for edge tracing.....	109
Figure 7-28. Examples of selected edge pixels to represent the geometries of lines.....	110
Figure 7-29. Georeferencing image space to coordinate space	110
Figure 8-1. Matching principle (adapted from Wiedemann (2003))	112
Figure 8-2. The pedestrian network baseline generated by field survey and manual digitization	115
Figure 8-3. Ten tiles in the study area.....	117
Figure 8-4. Examples of constructed pedestrian networks based on the network buffering approach.....	120

Figure 8-5. Evaluation result of constructed pedestrian network (using network buffering).....	121
Figure 8-6. Errors from network buffering approach	123
Figure 8-7. GPS points of walking GPS traces in the study area	125
Figure 8-8. Constructed pedestrian networks with different number of traces.....	127
Figure 8-9. Constructed pedestrian networks in 10 tiles of the study area	127
Figure 8-10. An example of evaluation process (Collaborative Mapping)	128
Figure 8-11. The generated path segments in the blocked and open sky area.....	130
Figure 8-12. An example of splitting orthoimage.....	131
Figure 8-13. The evaluation process (image processing)	133
Figure 8-14. Errors from image processing approach	135
Figure 8-15. Percentage distribution of pedestrian path types.....	136
Figure 8-16. Pedestrian Path types and the three approaches.....	137
Figure 8-17. Average values of geometrical and topological correctness of the three approaches in the study area	138
Figure 8-18. Completeness percentages of pedestrian path types and the recommended approaches.....	139
Figure 9-1. The criteria and quality result of the network buffering approach.....	148
Figure 9-2. The criteria and quality result of the collaborative mapping approach.....	149
Figure 9-3. The criteria and quality result of the image processing approach.....	151
Figure A-1. Flowchart of verification of sidewalks and crosswalks using GPS traces	160
Figure A-2. An example of GPS point segmentation	161
Figure A-3. Pseudocode of side determination.....	162
Figure A-4. Examples of establishing sides of a road segment	163

PREFACE

First and foremost, I would like to express my deepest gratitude to my advisor, Dr. Hassan Karimi, for all the invaluable advices and insights that made this dissertation possible. I greatly appreciate all the support and suggestions from my dissertation committee members, as well as the School of Information Sciences, for their supports. I am also thankful for my friends in the Geoinformatics Laboratory for their opinions and suggestions. I would really like to thank my mom, brothers, and sisters for their never-ending support and encouragement. Lastly, I would like to thank the University of the Thai Chamber of Commerce for providing the financial support for my graduate studies in the United States.

1.0 INTRODUCTION

1.1 MOTIVATION

The availability of ubiquitous computing devices and wireless networks along with the advancements of high accuracy satellite-based positioning systems have paved the way for new services capable of providing location-sensitive information to mobile users (Theodoridis, 2003). These types of services are termed Location-Based Services (LBSs) and are changing the way people live and work by allowing mobile users to send and receive digital content anytime and anywhere. LBS providers are engaged in a variety of business opportunities by creating innovative services such as mobile guides and navigation, shopping assistants, emergency services, and social networking, to name a few (Wang et al., 2008). Car navigation systems, a very popular application of LBSs, are being used by a large number of people around the world. Navigation systems popularity is primarily due to the fact that they make the essential and everyday task of traveling much easier and safer by simply providing vehicle's current location as well as routes to selected destinations. Car navigation systems would not be possible without advancements in positioning and mobile computing devices. Furthermore, technology trends today are advancing into many new and exciting areas providing opportunities that would not have been possible just a short time ago.

In order to understand the motivation for this research, it is necessary to underline the importance of a digital map database in a navigation system. Generally, a navigation system is constructed by the integration of six main components: positioning, map matching, routing, geocoding, interface, and digital map database, as shown in Figure 1-1.

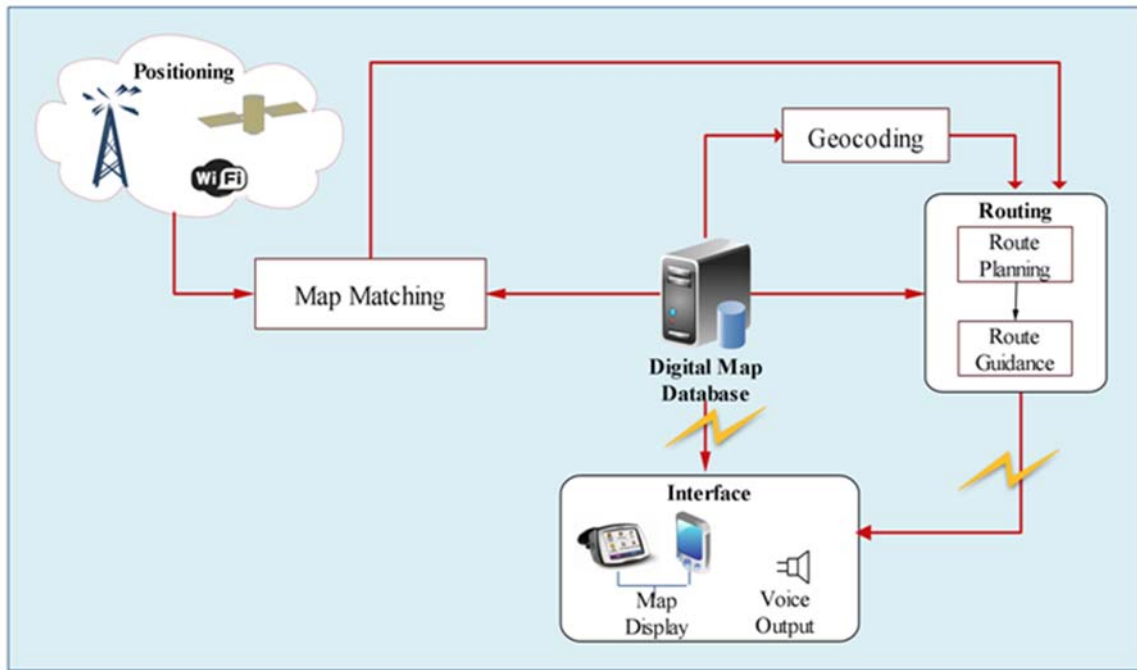


Figure 1-1. Main components of a navigation system

The digital map database component represents driving environment (e.g., road network) and is the backbone of a navigation system (Kasemsuppakorn and Karimi, 2008, Steiniger et al., 2006) as it provides essential map-related data to most other components. The positioning component estimates user’s current location by using Global Positioning System (GPS), among other possible positioning technologies, which may be inaccurate due to errors such as multipathing or attenuation. This position information is then fed to the map matching component which first finds the road segment on which the user is and then snaps the estimated position to the segment. The road segment is found by searching a digital map database (Quddus, 2006). The routing component, which is used for planning and guidance (Zhao, 1997), invokes

the geocoding component to find the coordinates for the desired destination in order to compute a route to it from current location (obtained from the map matching component). Given an address, such as a destination, the geocoding component uses the map database to find its coordinates (e.g., latitude/ longitude). The interface component displays user's current location and computed routes using the digital map database as a visual reference to orient the user.

With the success of car navigation systems, road network databases are now well developed and widely available for many countries in North America, Europe, and Asia. Data sources for road network databases are provided by government agencies, e.g., the U.S. Census Bureau's Topographically Integrated Geographic Encoding and Reference (TIGER), non-profit organizations, e.g., Pennsylvania Spatial Data Access (PASDA), and commercial mapping companies, e.g., NAVTEQ. Today, with the increasing capabilities of mobile devices, navigation system functionality can also be extended into handheld devices such as mobile phones, assisting pedestrians, especially disabled individuals, with travel related tasks, called pedestrian navigation services. Unlike motorized vehicles, pedestrian movement takes place along pedestrian paths, not along the street lanes and are not constrained by the boundaries of the road. A major difference between road and pedestrian network models is that road networks used for navigation are generally based on road centerlines which are of no, or little, use to pedestrians traveling along pedestrian paths such as sidewalks (Elias, 2007, Gaisbauer and Frank, 2008, Holone et al., 2007, Stark et al., 2007, Walter et al., 2006). Furthermore, not all pedestrian path segments are adjacent to roads and can be substituted by road networks. Therefore, roads do not adequately represent pedestrian navigation environments and their use for assisting pedestrians result in poor performance and errors. Such differences between roads and pedestrian paths are the reasons why road networks are inappropriate for assisting pedestrians with their navigation

needs (Elias, 2007, Hampe and Elias, 2003, Pressel and Weiser, 2006), especially in navigation applications that require reliable assistance, e.g., assisting people with disabilities who require specialized guidance for mobility.

Compared to road networks, pedestrian networks of many countries are not available, or are provided by commercial mapping companies at significant costs. As a result, navigation systems intended for use by pedestrians resort to road networks as their main data source (Gaisbauer and Frank, 2008), with such disclaimers as “the routes may be missing sidewalks or pedestrian paths”. We conducted an experiment to demonstrate the issues of using a road network as a substitute for a pedestrian network for computing routes. We computed the shortest routes using Dijkstra’s algorithm between three pairs of buildings within the University of Pittsburgh’s main campus, by using both a road network and a pedestrian network. The road network was derived from NAVTEQ and the pedestrian network was manually digitized from satellite imagery using the technique described in Kasemsuppakorn and Karimi (2008). The results of this experiment are shown in Figure 1-2, where the thick solid line is the route computed based on the road network and the dashed line is the route calculated based on the pedestrian network.



Figure 1-2. Route calculated by using road network and pedestrian network

In Figure 1-2, the route computed based on the road network starts and ends at the road segments that are closest to the origin and destination, respectively, and the route computed based on the pedestrian network, which contains more details and is denser than the road network, provides realistic walking paths to the destination. For example, the route in Pair 2 was computed based on the pedestrian network, starts right at the origin point and arrives right at the destination point and it is much shorter than the route computed based on the road network. This simple experiment demonstrates that for computing relevant routes in pedestrian navigation services, navigation aids for handicapped or elderly people, and LBSs such as tourism or recreational trips, pedestrian networks are needed.

Another application area that requires a pedestrian network is urban planning. A common objective in urban planning projects is to make cities more “walkable”, helping increase the physical activity of its inhabitants and at the same time decrease traffic congestion and pollution. Southworth (2005) defined “walkability” as the extent to which the built environment encourages walking by providing pedestrians a safe, comfortable, convenient and appealing travel corridor. The most common factors that influence an individual’s decision to walk rather than drive to a destination generally include personal health and fitness, pedestrian-friendly routes, and route distance (Southworth, 2005).

Figure 1-3 presents two areas related to urban planning: auditing pedestrian environment and evaluating pedestrian network connectivity. These two areas are related to pedestrian environments and require pedestrian networks.

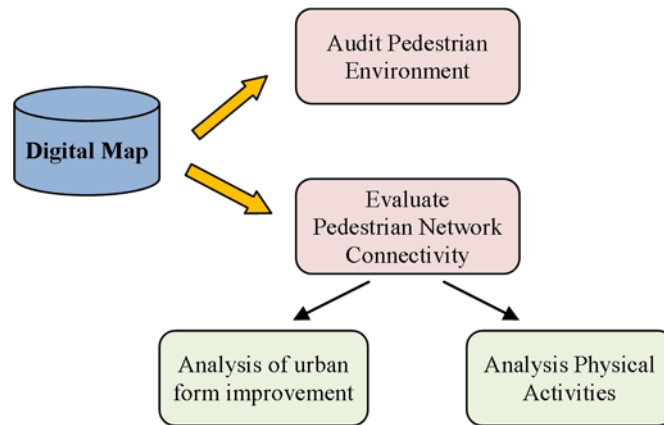


Figure 1-3. Examples of research areas in urban planning

Auditing pedestrian environment's aim is to develop methodologies that collect information and analyze the walking environment by looking at pedestrian facilities such as sidewalk, walkway, and/or trail. Common auditing instruments today include handheld technology such as Personal Digital Assistants (PDAs) which allow auditors to incorporate surveyed data directly into a database (Clifton et al., 2007). A digital map database, which is served as a base map for survey data entry at a given location, is an essential component in auditing pedestrian environment. The main advantage of employing a digital map on mobile Geospatial Information System (GIS) is that it speeds up analysis and decision making by using the up-to-date and accurate spatial data.

Urban planning requires pedestrian networks to examine pedestrian network connectivity. It has been shown that evaluation of network connectivity and accessibility has significant associations with physical activities such as walking (Humpel et al., 2002). A high degree of connectivity usually results in shorter travel distances and more route choices (Handy et al., 2003), both of which greatly benefit pedestrians. There are various indices to measure network connectivity such as Pedestrian Route Directness (PRD), Link Node Ratio (LNR), or Intersection

Density. These indices require a pedestrian network for calculations. The resultant indices are then used to analyze and improve the urban form as well as provide health experts with data points for physical activity analysis.

In the absence of pedestrian networks for many areas, most pedestrian auditing and accessibility/connectivity studies substitute pedestrian networks with road networks on the assumption that all streets have sidewalks while completely ignoring pedestrian walkways not adjacent to streets (Handy et al., 2002). Such a substitution does not often guarantee the type of data required for measurements in auditing and accessibility/connectivity studies because pedestrian networks usually have a much finer resolution than road networks do. Research by Chin et al. (2008) studied the differences between road and pedestrian networks and how the differences between them influence the walkability index. The pedestrian network in this study included parks and walkways and was manually digitized from aerial photos. The Pedsheds, LNR, and PRD are the methods used to measure network connectivity. The result showed that using a pedestrian network offers a more realistic means of measuring level of connectivity than a road network does.

In order to demonstrate how the differences in road and pedestrian networks influence the walkability index, the experiment in Chin et al. (2008) using the PRD method was replicated. PRD is the ratio between the actual route distance travelled and the Euclidean distance between specific origins and destinations within a network (Randall and Baetz, 2001). The lower value of PRD indicates better connectivity because it is believed that people are willing to walk to a destination if the route is short and straight. We compared walkability, using the PRD metric, between a road network and a pedestrian network within the University of Pittsburgh's main campus. We computed the shortest routes between pairs of campus buildings by using both a

road network and a pedestrian network. Four walking distance ranges were <500, 500-700, 700-900, and >900 m. Five routes within each walking distance range were computed using both networks. The total number of sample routes in each network (road network and pedestrian network) is equal to 20 and the average PRD values of those routes based on each walking distance range were calculated as illustrated in Figure 1-4.

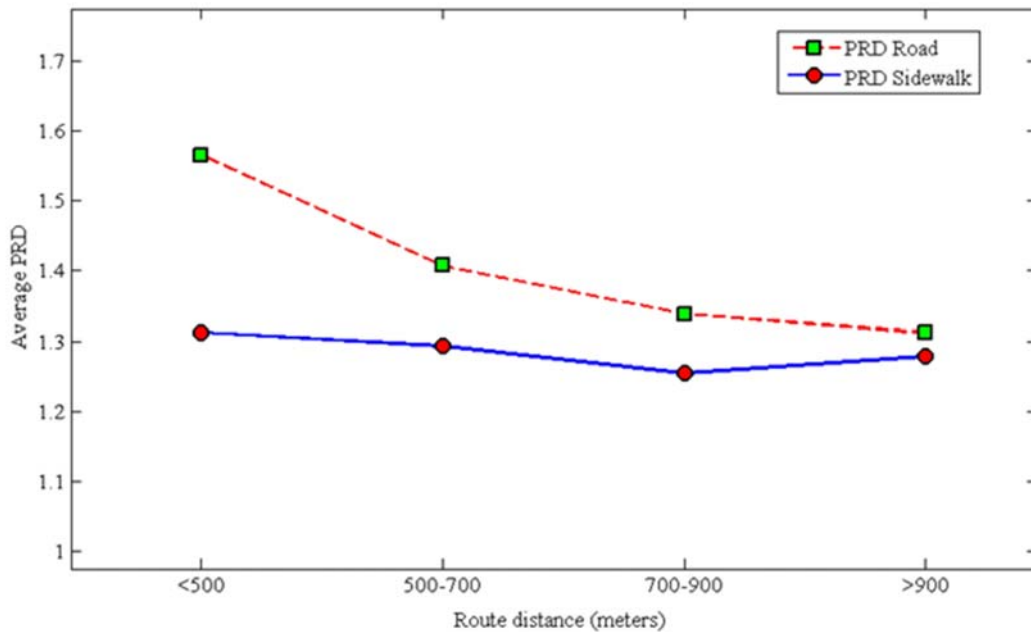


Figure 1-4. Comparison between average PRD values for road and pedestrian networks

The result from this experiment showed that using a pedestrian network has the average PRD value lower than the road network for all walking distance ranges. This means that using a pedestrian network in the analysis produces higher connectivity result. In urban planning and physical activities, using a pedestrian network in the evaluation process should produce more realistic results than the road network does.

Despite the growing demand for pedestrian networks, they are currently not publicly available and compared to road networks little attention has been paid to them. Currently,

researchers requiring pedestrian networks for studies generate their own data. One major problem with this approach is that the produced data is very specific and only useful for a particular scenario and chosen area. This and other observations indicate that there is an absolute need for developing new methodologies and techniques for acquiring and maintaining pedestrian networks; this is an important area of study for further advancements in pedestrian-centric LBS applications.

1.2 RESEARCH PROBLEMS, CHALLENGES, AND SIGNIFICANCE

As mentioned earlier, there are many applications that require pedestrian networks, but published papers focusing on collection, construction, and maintenance of these databases are scarce. Furthermore, pedestrian networks are not publicly available or are provided by commercial mapping companies at significant costs impeding research and development in applications needing such data. In this dissertation, possible data sources and a new methodology and algorithms for pedestrian network construction are investigated and developed. This research is challenging because of the complexity of pedestrian networks and the difficulty of extract information from noisy data sources. Pedestrian networks are complex as they usually exist in urban areas and include multiple types of paths. Possible data sources to construct pedestrian networks are road networks, GPS traces, and satellite imageries. Generally, these data sources, especially in urban areas, contain noises that impede network construction; for instance, the pedestrian path areas appearing in the images are often influenced by neighboring objects (e.g., buildings, shadows). Therefore, approaches that can automatically construct pedestrian networks

and can handle noises are needed. In this dissertation, the following research questions are addressed:

- What are the properties of pedestrian networks?
- What data should a pedestrian network base map contain?
- What are suitable approaches to automatically construct pedestrian networks?
- What are the evaluation criteria and how to measure the quality of pedestrian networks?

1.3 RESEARCH OBJECTIVES AND CONTRIBUTIONS

In this dissertation, a new methodology and algorithms to construct pedestrian network are investigated and developed. The objectives of this dissertation are:

- To develop a methodology for recommending a suitable approach for constructing pedestrian networks in a given area and a set of criteria
- To develop and evaluate techniques for collecting raw pedestrian data
- To develop and evaluate techniques for generating pedestrian paths from raw data
- To develop and evaluate algorithms for constructing pedestrian network from generated pedestrian path segments

While pedestrians may travel indoors as well as outdoors, this research focuses on outdoor pedestrian networks. The main contributions of this dissertation are:

- Analysis and categorization of pedestrian path types
- Techniques to collect raw pedestrian data
- Algorithms to generate pedestrian path segments and construct pedestrian networks

- A methodology to recommend a suitable approach for constructing pedestrian networks

1.4 ORGANIZATION OF THE DISSERTATION

This dissertation is organized as follows. Chapter 2 provides a definition of pedestrian networks and an analysis and categorization of pedestrian path types and pedestrian network database structure. Chapter 3 provides backgrounds on applications requiring pedestrian network and digital map data providers, as well as related work on existing techniques for map generation using GIS tools, collected GPS points, and image processing. Chapter 4 discusses the pedestrian network construction approaches. Chapter 5 discusses the data source and details of the algorithm in the network buffering approach. Chapter 6 discusses the data source and details of the algorithm in the collaborative mapping approach. Chapter 7 provides details of data sources, data preparation and network construction using the image processing approach. Chapter 8 describes the evaluation methodology, the pedestrian network baseline, the study area and the evaluation results by the three approaches. Chapter 9 provides the recommendation methodology. Finally, the conclusions and future research are discussed in Chapter 10.

2.0 PEDESTRIAN NETWORK

This chapter begins by describing terminologies used within this dissertation. A *pedestrian* is “any person who is afoot or who is using a wheelchair or a means of conveyance propelled by human power other than a bicycle” (WashingtonStateLegislature, 2003). A *pedestrian network* is a topological map that delineates the geometric relationship between pedestrian path segments. A *pedestrian path segment* is a segment describing any pathway that is designed for a pedestrian in order to improve pedestrian safety, reduce potential accidents, and promote mobility and accessibility. The digital representation and organization of a pedestrian network is discussed in the following. In general, a geographic representation conceptually models real-world objects into a computer data representation (data model and database level) as illustrated in Figure 2-1.

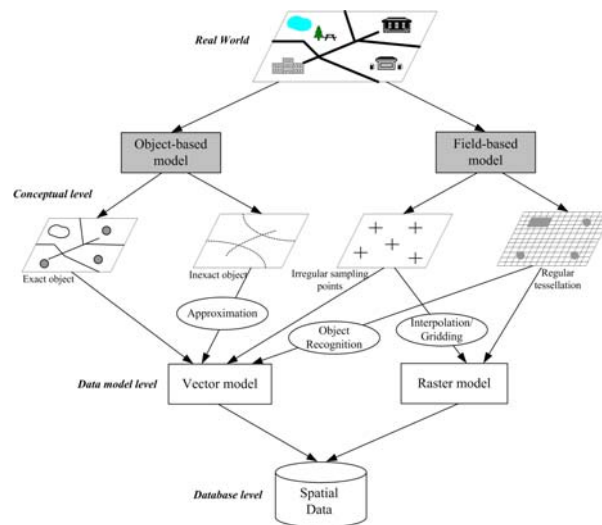


Figure 2-1. A conceptual of model of the real world (adapted from Lo and Yeung (2006))

At the conceptual level, a model basically represents user's perception of the real world and tends to be tailored to a specific application. The concept starts by clarifying what objects are deemed necessary to be represented by a data model because real-world geographic objects are varied and complicated. Two distinct approaches for representing the real-world objects in a geospatial database are the object-based model and the field-based model (Lo and Yeung, 2006). The object-based model represents geographic space as an empty space occupied by discrete and identifiable objects. Spatial objects represent discrete objects with well-defined boundaries called "exact objects" such as buildings or roads. The field-based model conceptualizes spatial phenomena that vary continuously over space such as elevation, temperature, air pressure, or concentration of pollutants. Generally, these spatial phenomena are represented as surfaces containing field values and modeling as 3D, or 2.5D. There is no exact criterion to select one model over the other; however, the choice of a model sometimes depends on the data available. For example, one would adopt the field-based model if the observed data is from satellite imagery or adopt the object-based model if the input data are points collected using a GPS receiver.

Even though a conceptual model allows us to view real-world objects in a certain way, it is not designed for the computer data representation. Basically, two steps are required to prepare digital spatial data: choosing a spatial data model (data model level) and organizing geometric objects (database level) (Chang, 2010). There are two spatial data models, vector and raster, that are widely employed to represent spatial data. The vector model is best suited to represent discrete objects, whereas the raster model is best employed to represent spatial features that are continuous over a large area (Chang, 2010). Since a pedestrian network base map mostly represents man-made features, which are discrete objects, we consider only the vector data

model in this dissertation. The vector model generally represents phenomena as a collection of three geometric primitives: points, lines, and polygons. However, only points and lines are required in pedestrian network databases. A point, the simplest type of vector data, is specified by a pair of coordinates with respect to a reference coordinate system, and a line is represented by at least two connected points. Locations of features are purely geometric and do not contain relationships among objects (non-topological data). Therefore, there is considerable redundancy in this data model. For example, the places where two polylines connect have duplicate points. The database level involves geometric objects, attributes, and spatial relationships organized in such a way that computer can access, interpret, and process. At this level, vector data must be properly structured, explicitly store spatial relationships (topology) between geometric elements, and link spatial and non-spatial data.

2.1 CATEGORIZATION OF PEDESTRIAN PATHS

In this dissertation, seven types of pedestrian path segments are distinguished. Name and description of each type are explained in Table 2-1.

Table 2-1. Pedestrian path types

Path Types	Description
1. Sidewalk	A path designed for pedestrian traffic alongside a road
2. Pedestrian Walkway	A path not necessary at the side of a road such as a walkway between buildings, or a foot path to the plaza
3. Accessible Path/Ramp	A part of pedestrian walkway, but specifically at the entrance of the buildings or ramp for disabled group
4. Crosswalk	A facility that is marked off on a road to indicate where pedestrians should cross, generally at an intersection

Path Types	Description
5. Pedestrian Bridges	A grade-separated crossing that is constructed over the roadway
6. Pedestrian Tunnels	A grade-separated crossing that is an below-ground passageway
7. Trails	A path that is mostly designated as recreational such as running trails or natural trails

A sidewalk, the most common structure, is a paved walkway along the side of a road, whereas a pedestrian walkway is not along the side of a road. An accessible entrance is a part of a pedestrian walkway and is the actual entrance to a building. A path marked off on a road indicating where pedestrians should cross, generally at intersections, is called a crosswalk. The pedestrian bridge is a grade-separated crossing that is constructed over the roadway, while the pedestrian tunnel is a grade-separated crossing that is a belowground passageway. A trail is a path that is mostly designed for recreational activities such as running trails or natural trails. In addition to the seven main pedestrian path types, we also identify one subtype of pedestrian path, stairs, which is a facility normally located on main path types (e.g., pedestrian walkway, building entrance, or trail). Stairs is a series of steps designed to fill the gap in elevation. The physical characteristics, on-path man-made objects and off-path man-made objects, of each pedestrian path type are described in Table 2-2. We also provide the inner junction information to describe the connection between pedestrian path types. Unlike a road network, a pedestrian network is found mostly in urban areas and in some areas there may be more than one pedestrian network. Ideally, to provide complete navigation assistance for different modes of transportation, a pedestrian network should connect with a road network and a public transportation network in a given area, as described in Table 2-2 (outer junction).

Table 2-2. Pedestrian path types, characteristics, and connection information

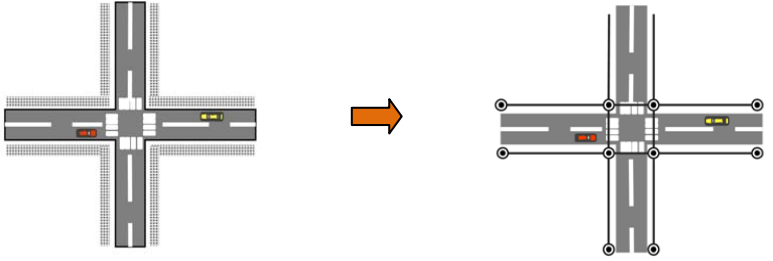
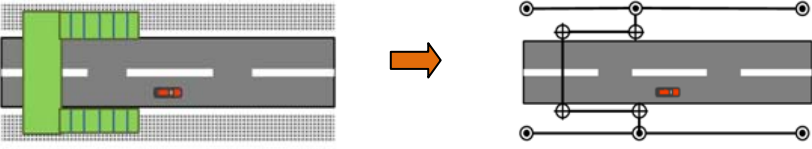
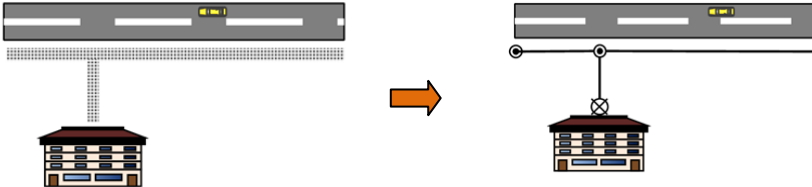
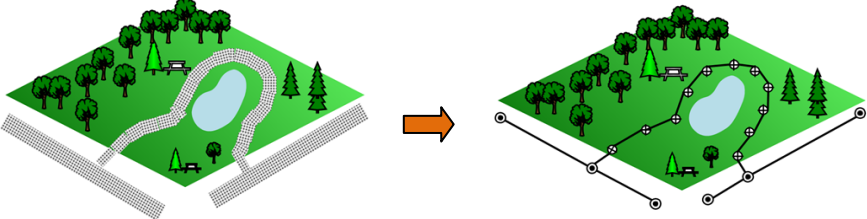
Type	Characteristics		On-Path man-made objects	Off-Path man-made objects	Inner Junction	Outer Junction
Sidewalk	Location	ground Side of roads	Fire hydrants Telephone poles Street signs Streetlights Traffic lights Parking meter Mail box Garbage can Tree Bus stop	Road edge/curb Cars Parking lots Grass Trees	- Crosswalk - Walkway - Building entrances - Pedestrian bridge - Pedestrian tunnel - Trail	- Road network - Public Transportation Network (connect through bus stop)
	Surface	concrete Asphalt				
	Shape	Continuous/ elongated				
	Stairs	No				
Crosswalk	Location	Ground On roads, mostly at the intersections	Cars Bus Traffic light	Bus stop Street sign	Sidewalk	-
	Surface	Asphalt Color: white/ yellow (two stripes/ zebra crossing)				
	Shape	short stripe				
	Stairs	No				
Building entrance	Location	Ground Attached to the building	Garbage can	Buildings	Sidewalk Pedestrian walkway	Hallway Network
	Surface	concrete				
	Shape	Short				
	Stairs	yes/no				
Pedestrian walkway	Location	ground	Seating place Garbage can Streetlights	Buildings Grass Tree	Sidewalk Trail	Road Network (connect through parking lot)
	Surface	concrete Asphalt Brick Stone				
	Region	continuous/ elongated open space area				
	Stairs	yes/no				
Pedestrian Bridges	Location	Above ground (over the road)	-	-	Sidewalk	Sky train network
	Surface	Concrete				
	Region	Short				
	Stairs	Yes				
Pedestrian Tunnels	Location	Underground (under the road)	-	-	Sidewalk	Subway Network

Type	Characteristics		On-Path man-made objects	Off-Path man-made objects	Inner Junction	Outer Junction
	surface	Concrete				
	Region	Short				
	Stairs	Yes				
Walking Trails	Location	Ground	-	Trees Grass	Sidewalk Pedestrian walkway	-
	Surface	Concrete Asphalt Soil				
	Region	Continuous/ elongated				
	Stairs	Yes/no				

2.2 VECTOR DATA MODEL

The vector data model for representing pedestrian networks can model complex spatial objects from basic graphical elements, allows explicit topological representation between objects, and is suitable for many types of computations such as routing. The pedestrian path types defined above can be represented by two basic graphical elements: point and line. A point, defined by a pair of coordinates, is used for identifying a topological junction of two or more lines (marked as \odot in Table 2-3), or the location of objects such as an accessible entrance of a building (marked as \otimes in Table 2-3). A line, described by a start point, an end point, and a list of shape points (marked as \oplus in Table 2-3), is used to represent pedestrian paths for all seven types as depicted in Table 2-1. Examples of pedestrian paths and their corresponding vector data are shown in Table 2-3.

Table 2-3. Examples of pedestrian path types

Pedestrian path types	Vector data
Sidewalk Crosswalk	
Pedestrian Bridge Pedestrian Tunnel	
Accessible/ Building Entrance	
Pedestrian Walkway Walking Trail	

2.3 PEDESTRIAN NETWORK DATABASE STRUCTURE

A network generally refers to “a type of mathematical graph that captures relationships between objects using connectivity” (Kothuri et al., 2007). An object in the network is represented by a node (point) and the relationship between two objects is represented by a link (line). Topology stores the line connectivity information. Spatial data include geometric information (e.g., longitude, latitude, or shape), and non-spatial data include the descriptive element of geographic

features such as name and length. A pedestrian network database contains both geometric and topologic information. The Open Geospatial Consortium, Inc. (OGC, 2003), an international consortium of companies, government agencies, and universities, has been producing worldwide standards for spatial data including Simple Feature Specification for storing, retrieving, and updating simple geospatial features. A pedestrian network database designed based on OGC's Simple Feature Specification can be used by many Database Management Systems (DBMSs) that employ and follow OGC's standards including Oracle Spatial (Kothuri et al., 2007), Microsoft's SQL Server (Microsoft, 2008), ESRI's ArcGIS Geodatabase (ESRI, 2008), and the Postgres extension PostGIS (PostGIS, 2009). Also, today's DBMSs enable efficient management of geographic data by supporting spatial data attribute types, spatial operations in query language, and spatial indexing methods. The overall structure of a pedestrian network database using the Unified Modeling Language (UML) (Ambler, 2005) is illustrated in Figure 2-2.

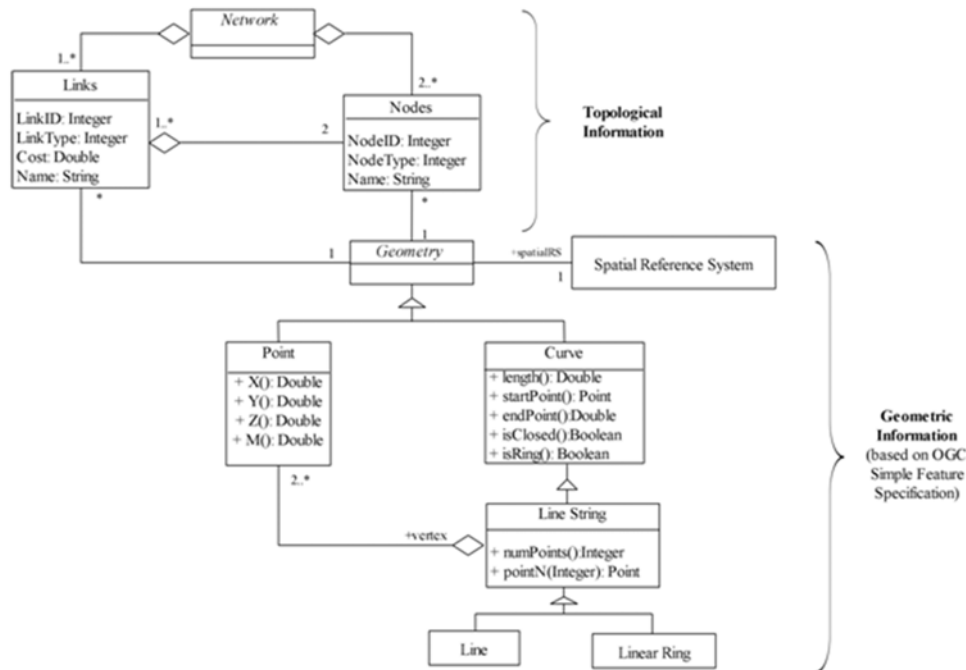


Figure 2-2. A pedestrian network database structure

In this UML, a class is represented by a rectangle divided into three compartments. The topmost compartment shows the name of the class, the middle compartment contains a list of attributes and the bottom compartment contains a list of operations or methods. We do not include methods in this diagram since we focus on the data structure. Solid lines with action labels indicate associations between two classes. Symbols at end of each line represent multiplicity of association; for example, “0..1” indicates zero or one instance; “2..*” indicates at least two instances. The hollow diamond shape represents an association with an aggregation relationship indicating that one class is a part of another class. For example, a line string is composed of two or more points or vertices. The triangular arrowhead represents an inheritance relationship between superclass and subclass. An arrowhead points from subclass to superclass implying that subclass inherits common attributes and methods defined in superclass.

As shown in Figure 2-2, the geometry class hierarchy is derived from OGC’s Simple Feature Specifications which are based on 1D geometry with linear interpolation between vertices. Geometry is a root class and is associated with a spatial reference system that describes the coordinate space. All geometry classes include basic methods (e.g., dimension, boundary), spatial relation methods (e.g., equals, intersects, within), and spatial analysis methods (e.g., distance, buffer, difference). The base geometry class has subclasses for points, curves, polygons, and geometry collections (OGC, 2003). Only point and curve geometric objects based on OGC are included in pedestrian network database structure to represent points and lines. A point is a 0-dimensional geometry that represents a single position in coordinate space by using an x-coordinate value and a y-coordinate value. A point value may include a z-coordinate value and an m-coordinate value, but these are not required in pedestrian network databases. The z-coordinate generally represents altitude or elevation and the m-coordinate basically represents a

scalar measurement. A curve is a 1-D geometric object representing the continuous image of a line. One subclass of a curve is a line string, representing a sequence of points and line segments connecting them. At least two distinct points form a line string. Two subclasses of a linear ring include a line and a linear ring. A line is a linear edge between two points, whereas a linear ring is a closed line string (start point is equal to end point). Geometric curve objects generally contain start and end points as well as length of the associated spatial reference.

Since the geometry class has no explicit declaration of topological information, node and link classes are added to describe the connectivity between nodes in a pedestrian network. The node class describes all nodes in the network that represent junctions, end points, and entity points. Each node has a unique numerical identifier, type of node (e.g., junction, entity point), and name of node (e.g., building name). The link class describes all links in the network that represent the pedestrian path segments between two nodes. Unlike road segments, pedestrian segments are undirected links that can be traversed in either direction. Each link has a unique numerical identifier, type of link (e.g., crosswalk, sidewalk), name of link (e.g., street name), cost for traversing the link (e.g., distance, slope). As shown in Figure 2-2, both nodes and links have geometric information associated with them. Each link connects only two nodes and each node might be connected by one or multiple links. Therefore, each link also contains the identifiers of the two nodes it connects.

2.4 DATA NEEDS ANALYSIS

Today, spatial data play an important role in planning, design, analysis, and administration of transportation systems and facilities. Many applications require high quality and reliable spatial

data in order to support various analyses. Generally, there is a lack of quality standards in spatial data because different applications have dissimilar needs (Chrisman, 1983). In other words, the quality of data depends on their fitness for a particular purpose. The U.S. National committee for Digital Cartographic Data Standards identified five general elements for spatial data quality: positional accuracy, attribute accuracy, completeness, logical consistency, and lineage (Chrisman, 1991). As discussed in Chapter 1, a pedestrian network is mainly employed in pedestrian-related navigation systems and measuring network connectivity for urban planning. For navigation systems, the correctness of the network and the locations of map features have a great impact on route computation and route guidance. The spatial road network data requirements of car navigation systems can be used as a starting point for determining the data requirements of pedestrian network data since both network data support navigation functions. Elements of spatial road network data quality include geometrical and topological errors, correctness of feature classifications (e.g., junction, roundabout), and how up-to-date features are (Quddus et al., 2009). Moreover, car navigation systems are very sensitive to spatial data as reported by State Departments of Transportation (NRC, 2003). For urban planning purposes, correctness of the network also significantly impacts computation of network connectivity index.

In this dissertation, the quality of pedestrian networks is determined by four evaluation criteria: geometrical completeness, geometrical correctness, topological completeness, and topological correctness. These four criteria are selected as they are commonly used in the literatures of road network extraction. Geometrical completeness refers to the degree to which map features describe real-world pedestrian paths. In other words, it refers to the missing pedestrian path segments in a database. Geometrical correctness represents the percentage of geographic features, which is matched with actual pedestrian paths. Network quality is

determined by two criteria: topological completeness and topological correctness. Topological completeness means the degree to which geographic features represent connection nodes. Therefore, the percentage of topological completeness decreases with increasing fragmentation of the pedestrian paths. In other words, a map with a high topological completeness means high number of pedestrian path intersections represented in the map. On the other hand, topological correctness refers to the accuracy of connection nodes. The percentage of topological correctness decreases with an increase in the number of incorrect connection nodes. Table 2-4 presents a summary of the criteria needed to measure quality of pedestrian network base map. These criteria are chosen based on the needs of navigation and urban planning applications. The optimum or near-optimum value of each criterion indicates that the pedestrian network is of high quality, thus the ideal pedestrian network base map. Moreover, spatial data should include a document explaining data sources, methods used to construct spatial dataset, and the construction time. This additional information will assist application developers in deciding the suitability of the database for the underlying applications.

Table 2-4. Summary of pedestrian network data quality criteria

Criteria	Definition	Range value	Optimum value
Geometrical completeness	The degree to which pedestrian path segments describing the actual pedestrian paths are included in the constructed dataset	[0;1]	1
Geometrical correctness	The percentage of the constructed pedestrian networks, which is in accordance with the baseline	[0;1]	1
Topological completeness	The presence or absence of connection nodes in a dataset	[0;1]	1
Topological correctness	The degree to which constructed features represent correct connections	[0;1]	1

3.0 BACKGROUND AND RELATED WORK

3.1 BACKGROUND

3.1.1 Applications

In this section, two main categories of applications that require pedestrian networks, navigation systems/services and urban planning, are discussed. Figure 3-1 shows general characteristics of these two applications.

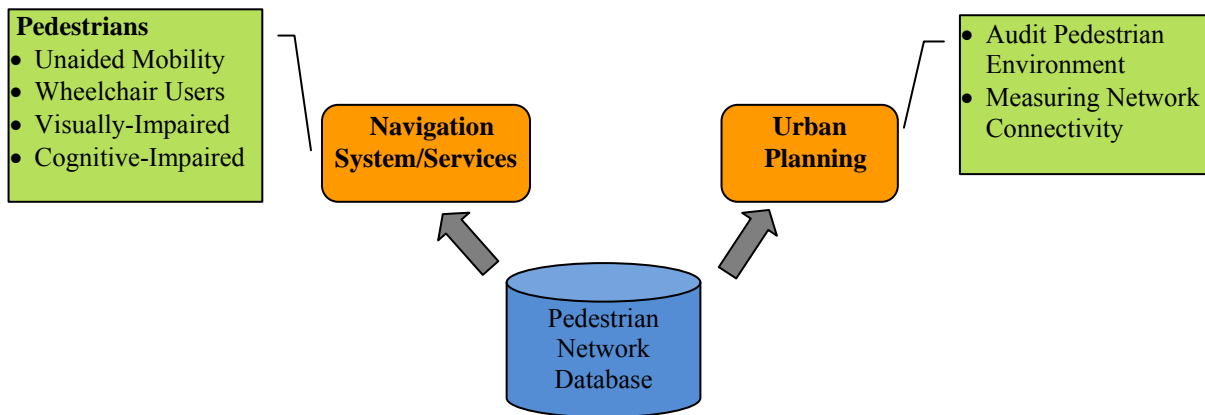


Figure 3-1. Example applications requiring pedestrian networks

The concept of navigation has been expanded from car navigation into pedestrian navigation for all pedestrians including mobility, visually, and cognitively impaired. This expansion is primarily stemmed from the technological advancements that have made devices and applications possible for use by pedestrians. Development of Internet-capable mobile

devices, portable positioning devices, and communication capabilities have paved the way for developing specialized applications on suitable devices geared towards assisting pedestrians and disabled individuals. Most LBS applications developed for pedestrians (general population and individuals with special needs) require pedestrian networks for route planning and visualization. However, in some cases people with special needs, in particular wheelchair users, require an even more detailed base map which might include information such as sidewalk’s surface type, sidewalk’s width, or locations of stairs (Kasemsuppakorn and Karimi, 2009b).

Urban planning applications also require pedestrian networks for modeling, analysis, and planning. It is believed that good physical layout and design of a city (urban area) can lead to a reduction in total transportation costs and automobile usage as well as promotion of physical activity resulting in more livable communities (Leslie et al., 2007). Network connectivity is one parameter that measures the built environment for conduciveness to physical activity and requires pedestrian network for analysis. Digital pedestrian networks can also serve as a base map for entering survey data on pedestrian facilities or pavement maintenance at a given location. Using digital pedestrian networks can speed up analysis for auditing pedestrian environment by using up-to-date and accurate spatial data.

3.1.1.1 Pedestrian Navigation Systems/Services

Table 3-1 provides data, data sources, and data acquisition techniques used by five commercial systems and two research projects related to pedestrian navigation systems/services.

Table 3-1. Summary of selected pedestrian navigation systems/services

Authors	Area	Data	Data Sources	Techniques
Navitime (Arikawa et al., 2007)	Mobile-based Commercial Pedestrian Navigation	<ul style="list-style-type: none"> • Sidewalk Network • Road network 	Data-supply companies (Japan)	<ul style="list-style-type: none"> • Integrate all required data provided by various companies into a specific format

Authors	Area	Data	Data Sources	Techniques
	System (Japan)	<ul style="list-style-type: none"> • Public Transportation • Point of Interest (POI) • Weather/ Traffic 		
Google (2010)	Web-based route services	<ul style="list-style-type: none"> • Road Network • Pedestrian Network 	Google Maps	<ul style="list-style-type: none"> • Provide pedestrian routes based on road network and pedestrian network (if available)
MapQuest (2011)	Web-based route services	<ul style="list-style-type: none"> • Road Network 	NAVTEQ and Open source data	<ul style="list-style-type: none"> • Provide pedestrian routes based on road network
Bing (2011)	Web-based route services	<ul style="list-style-type: none"> • Road Network 	NAVTEQ	<ul style="list-style-type: none"> • Provide pedestrian routes based on road network
Nokia Maps (2008)	Mobile-based Commercial Pedestrian Navigation System (Europe)	<ul style="list-style-type: none"> • Road Network • Landmark 	OviMaps ^{Beta}	<ul style="list-style-type: none"> • Provide pedestrian routes based on road network data or provide a straight line between origin and destination
Walter et al. (2006)	Route Calculation	<ul style="list-style-type: none"> • Graph representation of the walkable space for both indoor and outdoor 	Raster Image	<ul style="list-style-type: none"> • Image pre-processing • Skeletonizing algorithms • A* algorithm • Smoothing techniques
Elias (2007)	Database	<ul style="list-style-type: none"> • Road Network • Buildings • Indoor plan 	ATKIS (Authoritative Topographic-Cartographic Information System)	<ul style="list-style-type: none"> • GIS analysis and Geometric Integration (e.g. conflation techniques)

Navitime (Arikawa et al., 2007) is a commercial mobile pedestrian navigation system in Japan that provides users with navigation assistance for different modes of transportation such as walking, driving, or riding trains. One necessary dataset in NaviTime is sidewalk network that is used to compute suitable walking routes. Sidewalk networks are provided by the commercial mapping companies in Japan.

Google Maps (2010), MapQuest (2011), and Bing Maps (2011) are popular Web Mapping Services (WMSs) that provide map-based services for pedestrian navigation with

walking direction mode (beta version). Google Maps delivers walking routes based on road network and pedestrian network (if the data is available) with the disclaimer: “the route may be missing sidewalks or pedestrian paths”. For MapQuest and Bing Maps, pedestrian routes are based on road networks.

Nokia Map 2.0 (2008) is a commercial mobile navigation system that supports both cars and pedestrians. Users are able to find their current location, nearby points of interest, and receive real-time car and pedestrian navigation assistance. The required data sources are a road network, points of interests, and public transportation information, which are provided by Ovi MapsBeta. However, routes for pedestrians are computed based on road networks, which may not contain pedestrian paths or false positives in cases where there is no sidewalk adjacent to the street.

Walter et al.,(2006) conducted research with the purpose of determining alternative approaches to computing shortest routes for pedestrians based on raster maps. The authors confirm that the data used in vehicle navigation is inappropriate for pedestrian navigation and methods of collecting data for pedestrian navigation need to be investigated. To compute routes, pre-processing and skeletonizing techniques were employed to generate an undirected graph from raster images for both indoor and outdoor environments.

Elias (2007) presented a method for creating a pedestrian-tailored geospatial database for indoor and outdoor environments using already existing geospatial datasets available in Germany. Three steps were implemented to generate the pedestrian geospatial database: data selection, GIS analysis, and geometric integration. However, results from this research showed that the method created paths that did not exist, such as phantom paths from a building to the street.

3.1.1.2 Navigation Systems for Individuals with Special Needs

While navigation systems for disabled are being explored by many researchers, at the time of this writing there is no commercial navigation system for disabled individuals. Table 3-2 provides data, data sources, and data acquisition techniques used by eight research projects.

Table 3-2. Summary of selected navigation systems/services for individuals with special needs

Authors	Area	Data	Data Sources	Techniques
Drishti (Helal et al., 2001)	Wireless Navigation System (Visually-impaired)	<ul style="list-style-type: none"> • Building location • Streets • Walkways • Campus building plan 	University of Florida Physical Plant Division (UFPPD)	<ul style="list-style-type: none"> • Digitized the centerline of walkways
MAGUS (Beale et al., 2006)	Web-based Wheelchair Navigation System	<ul style="list-style-type: none"> • Sidewalk Network • Obstacles 	Ordnance Survey Land Line Data Aerial Photography	<ul style="list-style-type: none"> • Manually digitized and incorporating local knowledge
U-Access (Sobek and Miller, 2006)	Web-based Navigation System	<ul style="list-style-type: none"> • Sidewalk Network • Accessible Entrances • Obstacles 	University of Utah Facilities Management Department Center of Disabilities Services	<ul style="list-style-type: none"> • Adding stairs and curb cuts by using GPS-based • Convert GIS data to SVG file format
Karimanzira et al., (2006)	Adaptive routing (Wheelchair and visually-impaired)	<ul style="list-style-type: none"> • Street network • Sidewalk Network • Obstacles simulation data 	N/A	N/A
Ourway (Holone et al., 2007)	Mobile-based Navigation Prototype (Physically-impaired)	<ul style="list-style-type: none"> • Road Network • Sidewalks and paths 	OpenStreetMap (OSM) project	<ul style="list-style-type: none"> • Supplementing the existing network by field survey and manually editing
ODILIA (Mayerhofer et al., 2008)	Navigation System Concept (visually-impaired)	<ul style="list-style-type: none"> • Sidewalk Network • Landmarks (e.g. public buildings, shops, restaurants) • Obstacles 	N/A	<ul style="list-style-type: none"> • Modeled with the support of GIS
RouteCheckr (Volker and Weber, 2008)	Personalized Routing	<ul style="list-style-type: none"> • Sidewalk network • Annotation on safety rating 	University map from local land surveying office	<ul style="list-style-type: none"> • Manually preprocessing to generate the digital format
Kasemsuppakorn and Karimi (2009b)	Personalized routing (Wheelchair)	<ul style="list-style-type: none"> • Sidewalk Network • Obstacles 	Aerial Photography	<ul style="list-style-type: none"> • Manually digitized and incorporating local knowledge

Drishti (Helal et al., 2001) is a wireless pedestrian navigation system for the visually and mobility impaired, which aims to provide users with optimized routes based on specified preferences and to guide them from one location to another. The required dataset includes

building locations, streets, walkways, parkings, and building plans. The centerline of walkways was manually digitized and the building dataset for the University of Florida's campus was provided by University of Florida Physical Plant Division (UFPPD).

MAGUS (Beale et al., 2006) is a web-based navigation service that guides wheelchair users in urban areas. Its route planning requires a pedestrian route network with very high-resolution details such as slope, surface type, and curb cuts of each sidewalk segment in order to calculate suitable routes. The pedestrian network base map was manually digitized using the Ordnance Survey land line data and aerial photo as backdrops and incorporated field survey or knowledge from local people.

U-Access (Sobek and Miller, 2006) is a web-based routing tool that provides pre-trip planning and shortest feasible routes to given destinations for people with three ability levels: unaided mobility, aided mobility, and wheelchair users. Spatial data creation includes a peripatetic network, an aided mobility network, and a disabled network with accessible building entrances. Data sources for U-Access include the University of Utah's Facilities Management department and Center of Disability services. However, the network base map acquisition process is not explained in detail.

Karimanzira et al., (2006) developed a travel aid to assist the visual/limb/hearing impaired for pre-trip planning in urban areas. A mathematical model and various machine learning techniques were used to generate routes tailored to the needs of disabled pedestrians. The spatial database used in this research was created for the test area in Georgenthal, Germany. However, details of the spatial data acquisition and creation for this project are no provided.

Ourway (Holone et al., 2007) is a mobile pedestrian navigation prototype with special emphasis on the physically impaired like wheelchair users or parents with baby strollers. The

pedestrian base map, used for route planning, was constructed through the OpenStreetMap Project, where users can add pedestrian paths to the system and give a rating on the path. The complete pedestrian base map of the downtown area of Halden in Southern Norway was constructed through field survey and the existing network was manually edited.

ODILIA (Mayerhofer et al., 2008) is a navigation system prototype for the visually impaired. The system requires a high-resolution pedestrian navigable map that is geometrically accurate, topologically consistent, up-to-date, and complete. A pedestrian path network was manually constructed in the testing area of Graz with the support of GIS.

RouteCheckr (Volker and Weber, 2008) is a client/server system for collaborative multimodal annotation of geographical data and personalized routing for the mobility impaired. The objective of multimodal annotation is to allow users to annotate existing geographical data with their own information such as safety rate. This additional information would be useful for optimal route computation. However, a navigable network that includes sidewalks and footpaths is required by this system. The data for the university campus and the area surrounding the main railway station was manually created.

Kasemsuppakorn and Karimi (2009b) developed a personalized routing system for wheelchair users that considers user's aversion to certain sidewalk obstacles when computing routes. In this project, sidewalk centerlines were manually digitized using satellite images and the University of Pittsburgh's campus buildings and accessible entrances were incorporated into the base map.

3.1.1.3 Urban Planning

This section reviews the required data by five research projects, two are related to pedestrian audit instrument and three related to measuring network connectivity for urban planning. Table 3-3 provides data, data sources, and data acquisition techniques used by five research projects.

Table 3-3. Summary of urban planning research projects

Authors	Area	Required data	Data Sources	Techniques
Randall and Baetz (2001)	Measuring Pedestrian Connectivity	<ul style="list-style-type: none"> • Pedestrian Network • Buildings and Point of Interests 	N/A	N/A
Schlossberg (2006)	Pedestrian Audit instrument	<ul style="list-style-type: none"> • Street Network with road type 	<ul style="list-style-type: none"> • TIGER Street • Street network from METRO 	<ul style="list-style-type: none"> • Create pedestrian skeleton from using GIS tools and street network
Clifton et al. (2007)	Pedestrian Audit instrument	<ul style="list-style-type: none"> • Street Network • Sidewalk Network 	TIGER Street	<ul style="list-style-type: none"> • Manually editing sidewalk network based on street center lines
Titheridge et al. (2007)	Measuring Pedestrian Accessibility	<ul style="list-style-type: none"> • Street Network • Pedestrian Network • Bus stops • Buildings • Road crossings 	Integrated Transport Network (ITN) road centerline	<ul style="list-style-type: none"> • Field survey • Network buffer method • Network link method
Chin et al., (2008)	Measuring Network Connectivity	<ul style="list-style-type: none"> • Street Network • Pedestrian Network 	<ul style="list-style-type: none"> • TIGER Street network • Aerial Photography 	<ul style="list-style-type: none"> • Manually digitized for pedestrian network

Randall and Baetz (2001) provided a methodology and a prototype for urban planners to evaluate pedestrian network connectivity and to generate retrofitting alternatives for the pedestrian environment in suburban neighborhoods. Route distance and PRD were used to measure network connectivity. The analysis requires a pedestrian network consisting of sidewalks and paved pedestrian paths. However, the pedestrian network acquisition process is not explained in detail.

Schlossberg (2006) explored how street networks around transit stops and schools can be visually and quantitatively analyzed to provide useful planning and evaluation tools for

pedestrian environments. This study explained how to use GIS tools for street classification analysis to remove inaccessible pedestrian paths and for connectivity analysis to measure intersection intensity.

Clifton et al., (2007) developed and tested a complete environmental audit methodology called Pedestrian Environmental Data Scan (PEDS). PEDS was designed to evaluate pedestrian environments with walking paths/sidewalks quality as one of its items. The pedestrian path data, which was generated by using the street network as the starting point, is needed to audit the pedestrian environment. Segments of pedestrian facilities that are not adjacent to roadways are added and segments inaccessible to pedestrians are removed from the street network.

Titheridge et al., (2007) developed a GIS-based tool named AMELIA to measure pedestrian accessibility to services and facilities at the micro data level. The pedestrian network database, composed of footways and crossings, was set up for the city of St Albans in the UK for the prototype testing. The network buffer and the network link method were used to automatically generate pedestrian paths. The network buffer generates approximate sidewalks and the network link creates additional paths that connect the centroid of the buildings to the nearest footpaths. Building's centroids were used because the actual locations of entrances to the buildings were not available.

Chin et al., (2008) studied the differences between road and pedestrian networks and how the differences in these networks influence the walkability index. The pedestrian network in this study included parks and walkways and was manually digitized from aerial photos. The Pedsheds, LNR, and PRD methods were used to measure network connectivity. The results showed that using a pedestrian network offers a more realistic means of measuring connectivity levels than a road network does.

3.1.2 Digital Map Data Providers

Digital map data providers are those organizations that create and provide digital map data and other map related content. Data providers can be grouped into three categories: government and non-profit agencies, commercial mapping companies, and community mapping organizations. Digital map data created by government agencies such as the U.S. Geological Survey (USGS) are available for free or at a nominal cost, whereas data created by commercial mapping company such as Tele Atlas can be purchased at costs and are subject to strict copyright laws. The third group is community mapping which aims to provide free access to current digital map data, often considered to be expensive through other providers. Its motivation is driven by the lack of publicly-available geographic data and the rapid development of mobile positioning technology and online communities (Goodchild, 2007). The concept of community mapping is to allow any user in the community to add important information to a particular area of a map by collecting and editing their own GPS traces, digitally tracing aerial images, or obtaining data from other free sources (Hakley and Weber, 2008). Table 3-4 presents examples of data providers in the three groups. The coverage area and the focus of the data content are also included.

Table 3-4. Examples of digital map data providers

Group	Examples	Coverage Area	Transportation Contents
Government and non-profit organization	TIGER/Line 2009 by “U.S. Census Bureau” (Bureau, 2011)	<ul style="list-style-type: none"> • United States • American Indian Area-based 	Digital base map for geographic features of <ul style="list-style-type: none"> • Roads • Railroads • Rivers • Lakes
	State Data (e.g., PASDA (2011))	<ul style="list-style-type: none"> • U.S. States 	Digital base map for geographic features of <ul style="list-style-type: none"> • Street Centerlines • Railroads

Group	Examples	Coverage Area	Transportation Contents
			<ul style="list-style-type: none"> • Rivers
Commercial Mapping Company	NAVTEQ (2010)	<ul style="list-style-type: none"> • 78 Countries 	Digital base map for geographic features of <ul style="list-style-type: none"> • Streets (called “NAVSTREET”) • Traffic • Landuse (e.g., Railroads, Buildings) • Pedestrian Geometry and POI called “Discover Cities” (available in some cities)
	Tele Atlas (TomTom, 2010)	<ul style="list-style-type: none"> • 90 Countries 	Digital base map for geographic features of <ul style="list-style-type: none"> • Roads and related navigation information (called “MultiNet”) • Integrate sidewalks and buildings features into road networks called “Urban Maps” (available in some cities)
Community Mapping (data depends on contributors; therefore, it might not be complete)	OpenStreetMap (OSM, 2010)	<ul style="list-style-type: none"> • Global area 	Digital base map for geographic features of <ul style="list-style-type: none"> • Roads • Footway • Cycle way • Railway • Subway
	WikiMapia (2011)	<ul style="list-style-type: none"> • Global area 	Digital base map for geographic features of <ul style="list-style-type: none"> • Roads • Railroads • Ferry, Rivers

The government agencies in each country generally serve as the primary source of geographic data. The USGS and the U.S. Census Bureau are examples of federal sources, which serve as the primary civilian mapping agencies in the United States. TIGER, a digital base map for geographic features of roads and address ranges, railroads, rivers, and lakes, is provided and maintained by the U.S. Census. State government sources, supported by universities, state agencies, or non-profit groups, are also important GIS data providers at the state level. Pennsylvania Spatial Data Access (PASDA) is an example of a state agency that provides many map datasets including digital base map for transportation in Pennsylvania. At the time of this writing, there are no government agencies that provide digital base map data for pedestrian networks.

NAVTEQ and Tele Atlas (TomTom) are examples of commercial mapping companies that provide digital maps and related information for many parts of the globe with focus on navigation and LBS applications. Bing Maps and MapQuest are examples of online mapping portals that employ digital map data from NAVTEQ under a restricted license. Tele Atlas is a major data provider for Google Maps and Google Earth. Both companies supply comprehensive map data at the street level, however, constructing pedestrian networks is currently in early stages and the pedestrian networks are not publicly available.

The impetus for community mapping is driven by the lack of publicly-available geographic data and the rapid development of mobile positioning technology, location-awareness, and online communities (Gillavry, 2006). Advanced technologies provide individuals with easy access to devices capable of recording and sharing geographic data through mobile social networking. There has been a dramatic growth in the number of active users of mobile social network sites with forecasted growth from 54 million in 2008 to nearly 730 million in 2013 (Holden, 2009). The reason for this can be attributed to people wanting to meet new friends, to get in touch with their networks, to get comments on their uploaded content, and to utilize location services. Dong et al. (2009) analyzed the structure of mobile social networks and confirmed that it is a typical “scale-free network” that the degree of connectivity distribution almost fits the power law distribution like other social networks. Considering the success of mobile social networking and the rapid adoption of mobile devices by a wide variety of users, it is feasible to conceive a mobile social network where members, among other activities, participate in building alternative map data with free access. OpenStreetMap (OSM) and WikiMapia are extensive and effective projects that currently facilitate access to collaboratively collected map data for the whole world. OSM also provides editing tools for manually adding

and editing pedestrian paths, such as sidewalks, crosswalks, or walkways. The benefit of community mapping is that it provides a free resource for data in large geographic areas. However, the availability and quality of data relies heavily on the network of people to collect and edit map data. Geographic features provided by current community mapping sites are mainly related to street data.

3.2 RELATED WORK

This section summarizes a review of related work for existing techniques used in map data generation. The map generation techniques are divided into three categories: (1) GIS-based tools, (2) GPS traces, and (3) image processing.

3.2.1 Map Generation Using GIS Tools

The existing techniques reviewed in this category were employed by researchers that generated their own data for testing purposes.

The first technique is “Road Network Proxy” that uses portions of the available road networks as a proxy and supplements them by manually adding and removing paths that are not included in the existing road networks. The advantages of this technique are that it uses road networks, which are widely available, the process is fast, and it is not labor intensive. The main disadvantage is that the computed routes might not be accurate because the network does not contain all the possible paths between pairs of origin and destination.

The second technique is “Manual Digitization” which uses satellite or aerial images as a backdrop and tools such as GIS software. Manual digitization or vectorization refers to the process of converting satellite or raster images into vector data. This technique is popular because of the availability of high-resolution raster images for wide areas and the availability of easy-to-use tools to generate data from images. Today, there are many sources of high-resolution raster images such as USGS, e.g., a 0.305 m natural color orthoimages (USGS, 2009) covering many urban areas. Research studies in Beale et al. (2006), Holone et al. (2007), Chin et al. (2008), and Kasemsuppakorn and Karimi (2009b) employed manual digitization and validated the results by field survey or local knowledge. The advantage of this technique is its ability to create a pedestrian network base map, which includes such required elements as walking pathways or trails. However, this technique is generally suitable for a small area as it requires field survey in order to complete and validate the data collection process.

3.2.2 Map Generation Using GPS Traces

With the availability of GPS-enabled mobile devices and the rapid growth of mobile users, a new and potentially large source of GPS data is emerging. Mobile users, using their mobile phones, can now collect GPS traces of where they are and where they have been in a simple manner. A variety of LBSN web sites, such as OSM (2010) and WikiLoc (2010), provide their members with a set of tools to contribute GPS traces. There is also the “Data Recycling” (Guo et al., 2007) method which allows collection and accumulation of in-vehicle GPS traces through car navigation systems. Nowadays, there are various methods for collecting large amounts of raw GPS data and there has been much research on extracting useful information from such data. Research on extracting GPS data includes mining of locations of interest or travel sequences,

e.g., see Lee and Cho (2007), studying human behavior and users' mobility, e.g., see Zheng et al. (2008), and updating existing maps or generating new map data. Of these GPS data extraction projects, existing techniques for updating and generating road map data are the closest to the work presented in this dissertation and can be used as a good starting point. In the remainder of this section, two groups of research projects, updating and refining maps using GPS traces and generating maps from scratch using GPS traces, are overviewed.

The first group addresses the problem of automatically updating and refining existing maps using GPS traces. Existence of map data is required as a priori knowledge and is updated or improved by using GPS traces. While distance, speed or direction noise filtering methods are common in map refinement algorithms for GPS data, different approaches are employed to extract and generate road features. Guo et al. (2007) examined two conditions, the necessity of update of the target roads and the number of available GPS traces on them. If these two conditions are met, the least squares approximation method, to extract road feature points, and the spline curve fitting method, to approximate road centerline, are used. The result of their study confirmed that the extracted road centerlines quickly converge to a stable position as the number of GPS traces increases. Rogers et al. (1999) proposed an approach that generates road centerlines and augments them with lane information. In this approach, geometry of each road segment is improved by iteratively performing a weighted average on an existing road map with each GPS trace. A hierarchical agglomerative clustering method groups centerline offsets into lanes and averages them to find lane centerlines. The results showed that it is possible to generate an accurate road centerline with existing commercial maps and few high-precision GPS traces. Ekpenyong et al. (2009) presented an approach to extend existing road maps with specific road type information such as specifying private roads or roundabouts. In this approach, the

Snap-Drift Neural Network was used to group GPS traces into road types based on speed, horizontal and vertical curvature, and bearing between successive points. The results show that the approach is able to detect road change and achieves a high percentage of road type classification accuracy. Niehoefar et al. (2009) presented a high-level architecture for a road map generation system consisting of trace recording, trace uploading and map generation algorithms. Davies et al. (2006) presented a different approach for generating map data through image processing techniques. Instead of using GPS points, they were converted to a raster data set using histogram and a Voronoi graph to compute road centerlines and a directed graph for route calculation. The results showed that the approach is able to detect road change; however, the generated map has some skewed junctions due to GPS errors. In short, the research in this group is focused on updating geometry, topology, and attribute information of existing road networks.

While the work presented in this dissertation is to generate map data from scratch using collected GPS traces, the vehicle trajectory data exploration used in Ekpenyong et al. (2009) for road type detection provides useful guidelines of processing information obtained from GPS data. Example GPS data include change in travel direction which can be used to detect the shape of pedestrian paths.

Unlike the first group, the second group aims to generate road maps from scratch using GPS traces. In other words, the map generation process is independent of any existing road map data. Edelkamp and Schroedll (2003) and Schroedll et al. (2004) extended the work by Rogers et al. (1999) to identify common segments in several GPS traces and estimated road centerlines for each segment by using the weighted least-squares spline with a suitable number of control points. They also improved the lane clustering algorithm in Rogers et al. (1999) to handle lane splits and merges. The experimental results showed that the proposed method can both

automatically generate digital road maps from GPS traces and improve on initial maps when they are available.

Worrall and Nebot (2007) discussed line and arc models for roads that provide a simple digital map representation and a technique for extracting a set of road waypoints using GPS data. The technique is composed of two steps: clustering and linking. The clustering step groups GPS data into regions of similar position with similar headings and the linking step connects those clusters to form the road structure. The results from this approach showed a close match between the GPS data and the aerial images of the same area. Bruntrup et al., (2005) also included travel time information in the graph, which is useful for calculating fastest routes between pairs of origins and destinations on the map. The most common process in Bruntrup et al. (2005) and Cao and Krumm (2009) is clarification of multiple GPS traces belonging to the same road with the same direction. Bruntrup et al., (2005) claimed that their algorithm could correctly determine most road structures except for narrow roads and mini-roundabouts. Cao and Krumm (2009) calculated routes from their generated map and compared them with those produced by Bing Maps using the same pairs of origins and destinations. The results showed matches with moderate accuracy in most cases.

Castro et al., (2006) presented an approach to generate road centerlines for two-lane rural highways using GPS traces collected on both lanes. The two-lane rural highway centerline and the width of a lane of the highway are estimated by GPS point interpolation. The centerline estimation was further refined using the parametric cubic spline to smooth out any further errors. The result showed that the maximum error from the generated road centerline is 1 m. However, the GPS traces used in their work were collected from vehicles driven at an approximate speed of 80 km/h, which is much faster than walking and produces less GPS error.

Fathi and Jrumm (2010) introduced an approach that is different from the aforementioned research in that the process begins with finding road intersections instead of finding road shape geometry. The “local shape descriptor”, a 2D circular window, slides over the GPS points and detects the intersection by using the Adaboost classifier. The locations of the detected intersections are then refined by iteratively matching the points in the model and the ones in the data, until convergence. Finally, the road centerline is formed by connecting those intersections. The results showed that the detected intersections deviated from their ground truth intersections by approximately 4.6 m.

Chen and Cheng (2008) and Shi et al. (2009) employed an image processing technique to generate road maps from GPS traces. The vehicle trajectories are first transformed to a road network bit map. Morphological operations were used to extract road network skeleton from road network bit map. The extracted road network skeleton was then used to find road junctions and elaborate the road network graph. To validate the algorithm, they overlaid their results on Google Earth and found a satisfying match between the two. The research in this group suggests that it is feasible to extract road centerlines, road network graph, and peripheral information such as lanes or road type by using only GPS traces. However, single GPS trace or a small number of GPS traces is insufficient to accurately represent road information.

The major difference between the research discussed above and this dissertation is that the former needs driving GPS data and the latter needs walking GPS data. This difference can pose significant challenges as GPS accuracy while walking is more susceptible to the multipath problem than driving is. This is because pedestrian paths are closer to buildings than roads are, and buildings are one main source of interference with GPS signals in urban environments. Also,

pedestrian path features are different from road features requiring development of new techniques for their extraction.

3.2.3 Map Generation Using Image Processing

Cartographic object extraction from remotely-sensed data is a challenging research topic that has been approached in many different ways. Compared to the relatively high number of research projects that are focused on extracting cartographic objects (e.g., roads, buildings), extraction of pedestrian networks from images is in its infancy. Walter et al., (2006) proposed an algorithm for semi-automatic pedestrian path extraction from raster images. The proposed algorithm has two steps to create an undirected graph representing pedestrian paths from raster images. The first step (pre-processing) generates a binary raster map, where “1” represents a pedestrian path and “0” represents an obstacle. Human input is required to select pixels on the map, which are considered walkable areas. The second step (skeleton) generates pedestrian paths from a binary raster map and employs morphological image processing operations. The limitation of this algorithm is that it requires manual input from human to indicate the pixel of walkable area.

Given that there is little research directly related to pedestrian network data extraction and that pedestrian networks are in many ways similar to roads (i.e., characteristics), existing automatic urban road network extraction techniques, which are a good starting point for further research in pedestrian network extraction, are overviewed.

Hinz and Baumgartner (2003) proposed an automatic road extraction approach in complex urban scenes using high-resolution imagery with context based analysis. The non-building areas are first extracted by detecting the building outlines followed by detecting the valleys between them. In the non-building areas, the road lane markings, which are thin bright

lines, are extracted and form the road segments. Limitations of this approach are the influence of large vehicles on the extraction process and the weakness of the model at complex road intersections (e.g., the location where a highway, several main and minor roads converge). The authors emphasize the importance of a feature model and context model for feature extraction in urban areas.

Hu et al. (2004) developed an automatic urban road extraction method that integrates LiDAR data and high-resolution satellite imagery. The method starts by detecting the primitives of the roads and the contextual targets, such as parking lots, from the LiDAR data using both intensity and height information. Detected trees and grasslands are eliminated by using morphological operations on color images. Road strips are extracted using an iterative Hough transform algorithm with the assumption that urban roads exist in a grid structure. The authors indicated that integrating multiple sources of data would definitely improve the extraction results in the urban area.

Karimi and Liu (2004) developed a set of algorithms to automatically extract road data from satellite images and vectorize the extract data for use in GIS and Intelligent Transportation Systems (ITS) applications. The automate procedure includes a set of algorithms: region growing, edge detection, image enhancement, vectorization, and georeferencing. Three 1-m resolution satellite images from different areas were tested and the running time of the procedure was analyzed.

Zhu et al. (2005) extracted roads from IKONOS satellite images by using a line segment match method and a mathematical morphology. This method assumes that roads have a darker color compared with surrounding areas and that roads are straight or slightly curved. This method begins by recognizing road and non-road pixels classified by morphological leveling that

combines opening and closing operations. Then the line segment matching method finds parallel line segments corresponding to roads. Lastly, the mathematical morphology is employed to generate the road network. The assumption about the road model can induce some problems in different situations, e.g., color of road is darker than surrounding features.

Wang et al., (2006) employed a machine learning algorithm to extract urban road features from the Quickbird satellite imagery. They first extracted lane markings by using the algorithm by Hinz and Baumgarther (2003). Road and non-road scenes were collected using small rectangular windows and were used to calculate three types of features: coverage ratios, direction consistency of lane markings, and local binary patterns. These features were then input to the AdaBoost learning algorithm for training classifiers. Finally, roads were extracted with a sliding window using the learned result and road connectivity. The limitation of this approach is the weakness of the algorithm at road areas without lane markings.

Clode et al., (2007) discussed a method for automatic detection and vectorization of roads using only LiDAR data. The method consists of two steps. First, the LiDAR points are classified into “road” or “non-road” using both height and intensity information and a hierarchical classification technique. Second, the road centerlines and road width are extracted by employing the Phase-Coded-Disk (PCD) method on the classified binary image. The final result is the road centerline with width and direction information. The method was applied to two urban test sites and the results showed an acceptable quality. However, the method is susceptible to parked cars and data noise.

4.0 PEDESTRIAN NETWORK CONSTRUCTION APPROACHES

While pedestrian network databases are required by a variety of different applications, they are not publicly available; in some areas they are available through commercial mapping companies at significant costs. Despite the fact that road and pedestrian networks overlap in content, the two are dissimilar in scale and details and are not irreplaceable for most applications. Moreover, research on pedestrian network construction and maintenance is scarce. In this dissertation, three approaches for automatically constructing pedestrian networks are investigated and developed, in order to understand their challenges, issues, and performances. The approaches were chosen based on research conducted in the automatic road network construction field and available data sources. Based on the performance of these three approaches, a recommendation methodology (Chapter 9) for pedestrian network construction for a given set of resources and locations is provided.

In general, the approaches that were chosen for pedestrian network construction consist of two main steps (1) data preparation and (2) network construction, as shown in Figure 4-1. The data preparation step is the process of assembling, preparing, and collecting raw data from a variety of sources such as people, road networks, and images. Raw data, such as a GPS trajectory, which is a series of GPS points on a path, are needed to generate the geometries of pedestrian path segments. The network construction step generates pedestrian path segments, composed of points and lines. Geometric elements and relationships among them (i.e., topology)

of pedestrian networks are explicitly stored. The pedestrian network data explicitly stores geometric elements and spatial relationships among geometric elements.

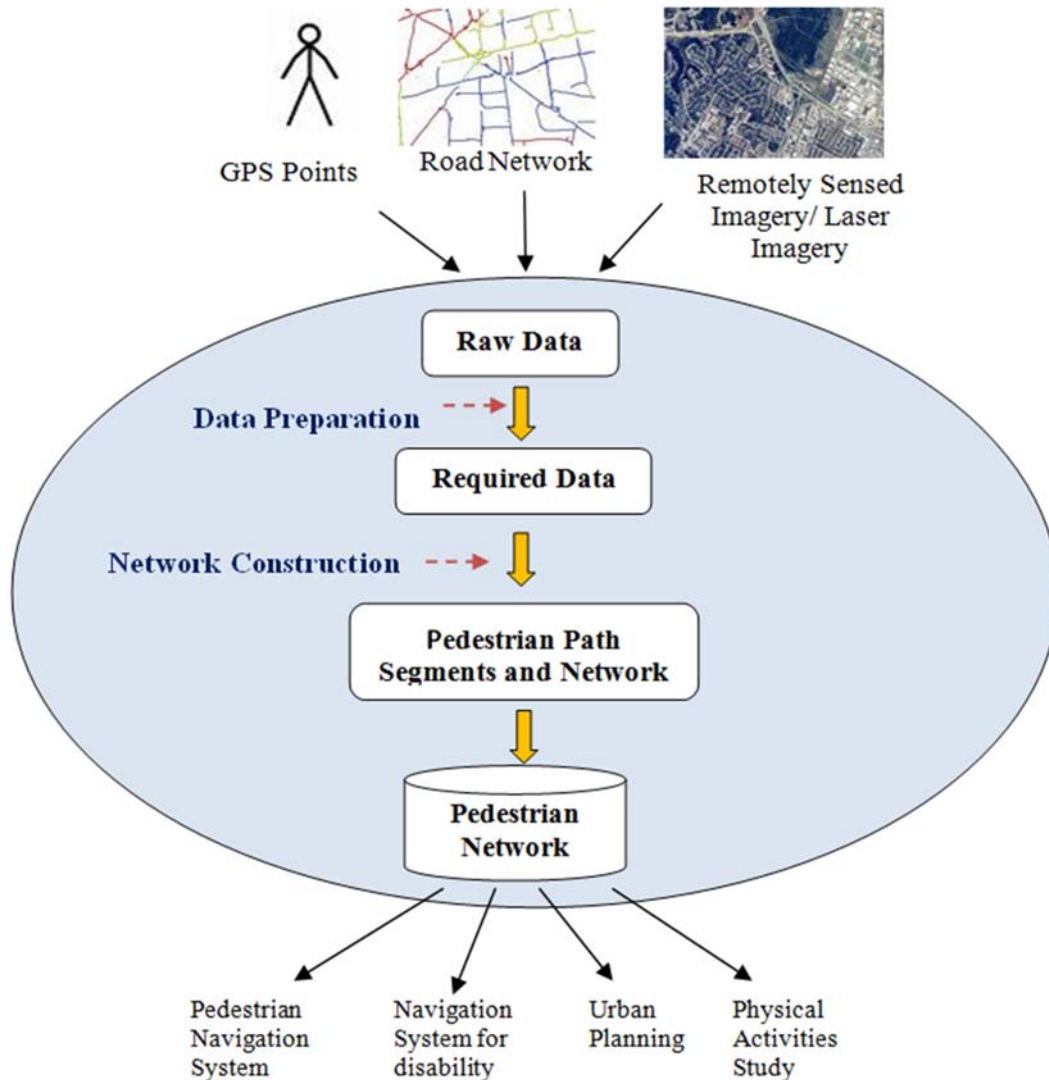


Figure 4-1. The proposed pedestrian network construction approaches

The approaches chosen for this dissertation include network buffering (Chapter 5), collaborative mapping (Chapter 6), and image processing (Chapter 7). These approaches are implemented and tested for completeness and correctness (Chapter 8). An overview of the steps and data sources for each approach is shown in Figure 4-2.

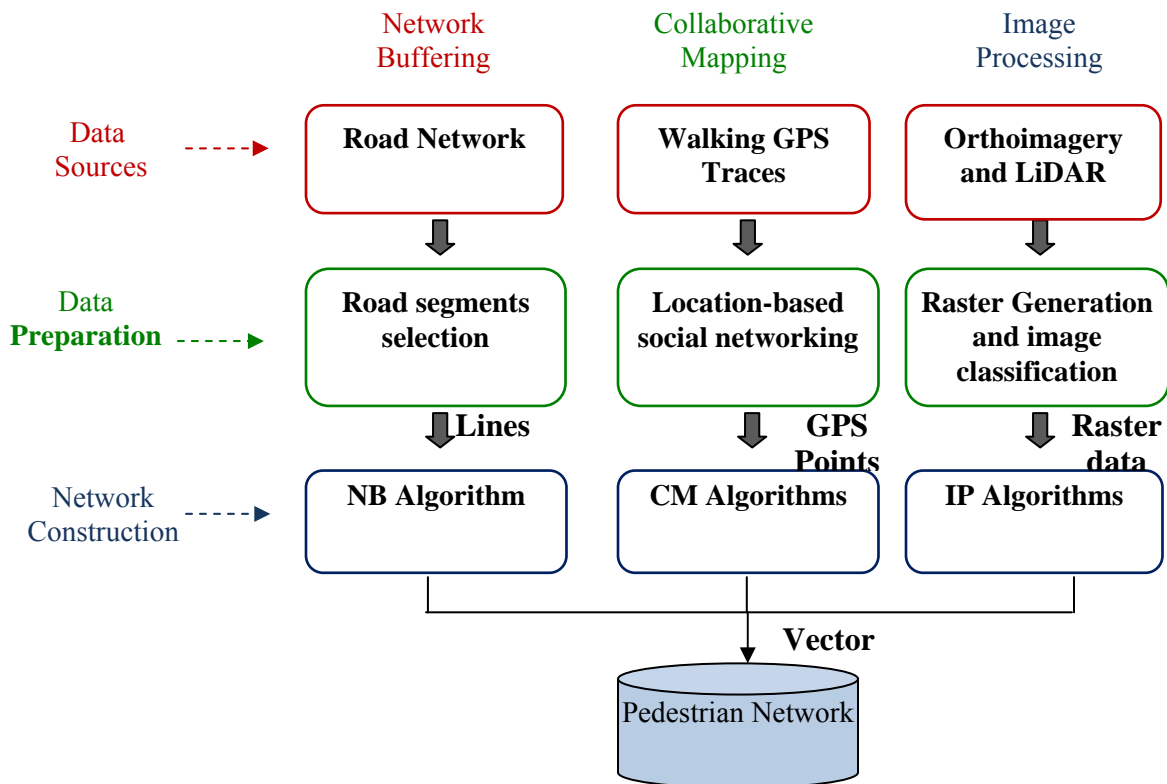


Figure 4-2. Steps of three algorithms for pedestrian network construction

Network buffering is the most common operation in cartographic modeling. Using road network as a reference, buffering generally results in polygons whose boundaries are on both sides of each road segment. These boundaries are considered as the approximate locations of sidewalk segments. The assumption to construct pedestrian networks based on a network buffering approach is that pedestrian path segments only exist along roads. The data preparation step of the approach involves selection of road segments that most likely have adjacent sidewalks where pedestrians would travel. There are situations where roads may not have adjacent sidewalks such as alongside highways. The network construction step of the approach involves calculating the geometries of pedestrian path segments and connecting them through the

algorithm called “NB Algorithm”. One advantage of network buffering is that it only requires road networks, which are widely available, as input.

Collaborative mapping is the aggregation of web mapping and user-generated content from a group of people. The pedestrian network construction algorithm based on the collaborative mapping approach aims to automatically construct pedestrian network from collected walking GPS traces. The data preparation step involves collecting GPS traces on walking paths. GPS traces (raw GPS data) are collected by GPS receivers or GPS-enabled mobile phones. This step is labor intensive, as it requires a number of volunteers to travel a particular area and record their GPS traces. The network construction step of the approach involves generating pedestrian path segments and constructing the network from raw GPS traces through the algorithms called “CM Algorithms”.

Image processing is an approach to analyze, enhance, and extract features from digital images, such as remotely-sensed imagery or laser imagery. The data preparation step involves raster generation and image classification. The network construction step employs the generated raster and classified image to extract and generate pedestrian path segments and to form a network by connecting adjacent segments through the algorithms called “IP Algorithms”.

5.0 NETWORK BUFFERING

A buffer zone is an area that is within a specified distance from a map feature such as points or lines (Smith et al., 2007). A network is made up of many line segments and their buffering areas are usually handled independently of each other. Two types of buffers are constant width buffers and variable width buffers. Figure 5-1b shows an example of a constant width buffer that identifies a region with a fixed distance away from the road segments in Figure 5-1a. Figure 5-1c presents an example of a variable width buffer in which a different buffer width is used for each line segment based on attributes such as number of road lanes.

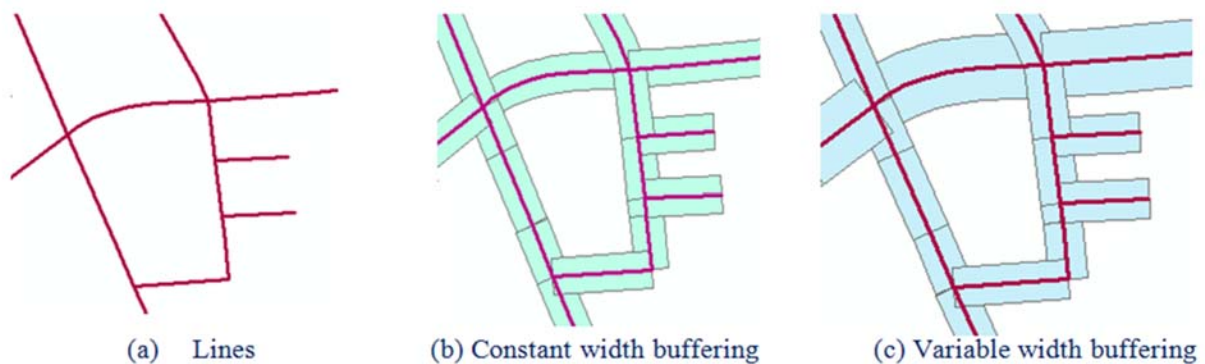


Figure 5-1. Examples of constant width buffering and variable width buffering

Line buffering is considered as a potential technique to estimate the location of pedestrian paths and to construct pedestrian networks, using the road network as a reference. Road segments are buffered using the variable width method, since each road segment might have a different width and number of road lanes.

The details of the pedestrian network construction algorithm based on network buffering approach are illustrated in Figure 5-2

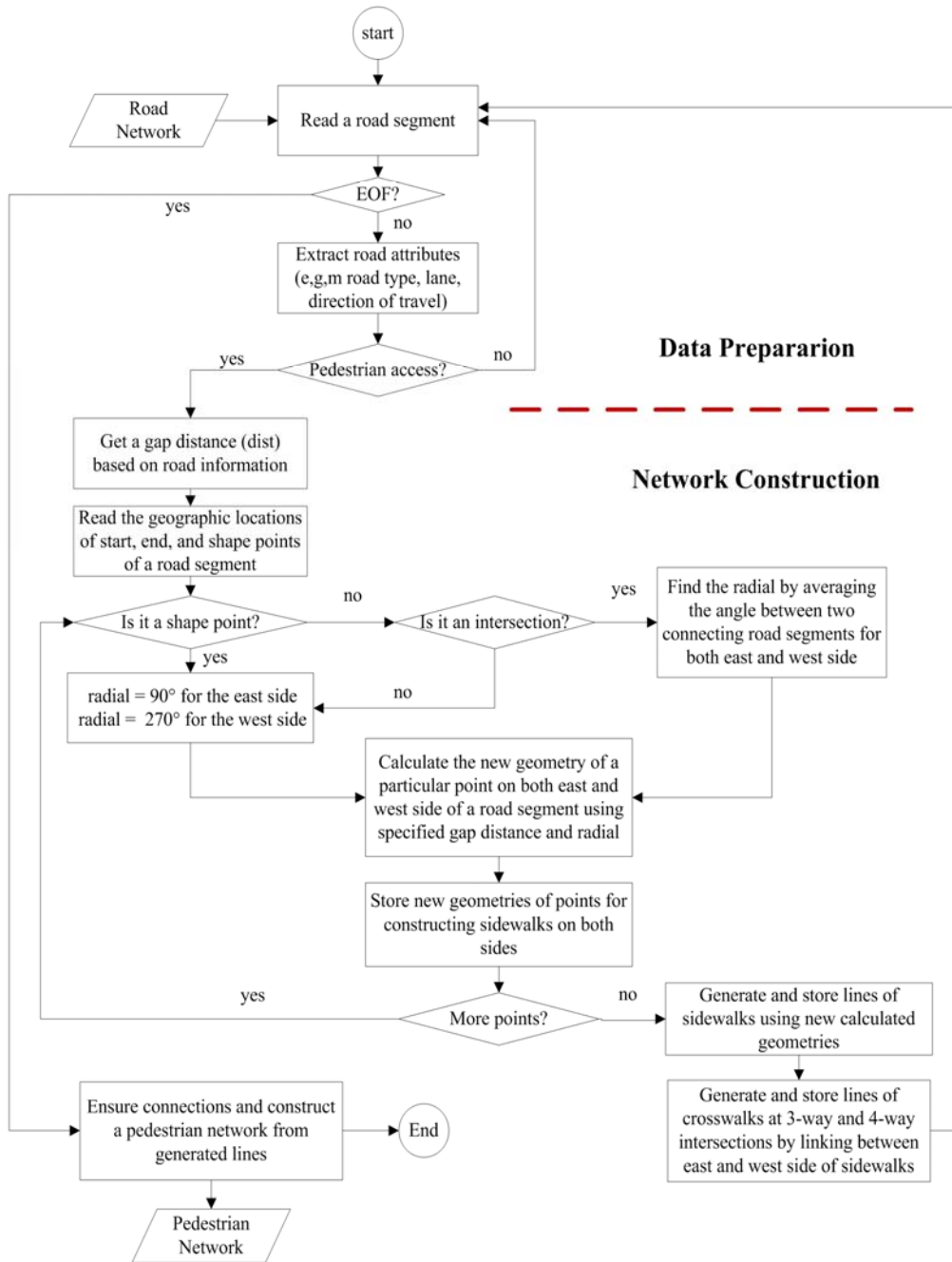


Figure 5-2. Data preparation and NB algorithm for pedestrian network construction

The algorithm is able to construct only two pedestrian path types, sidewalk and crosswalk. However, sidewalks and crosswalks constitute bulk of pedestrian paths and share

common characteristics, i.e., they are generally along road features. For this, a road network is used to construct pedestrian networks with the assumptions that sidewalks are in parallel on both sides of road segments and crosswalks are located at every road intersections (e.g., 3-way or 4-way). Data source for this algorithm is described in Section 5.1. The algorithm has two main components: data preparation and network construction, described in Section 5.2 and 5.3, respectively.

5.1 DATA SOURCES

The input data for the algorithm is a road network. Road network data include road geometry, network topology, and road attributes. Sources of road network of the University of Pittsburgh's main campus include TIGER/Line, provided by the U.S. Census Bureau, Allegheny Street centerlines, provided by PASDA, and the NAVSTREETS road network, provided by NAVTEQ. Each source may have a different quality data since several techniques are typically used to generate a road network database. Figure 5-3 shows two examples of a road network from three different providers (i.e. PASDA, TIGER/Line 2009, and NAVTEQ), overlaid and verified with 0.3 m resolution natural color orthoimages obtained from the USGS. TIGER/Line provides the lowest positional accuracy as shown in the figure where some street centerlines intersect buildings. NAVTEQ provides a higher resolution and positional accuracy for cul-de-sac features than the other two data sources, see the figure on the right. However, NAVTEQ data are available at significant costs and their usage is subject to copyright laws, while the PASDA and TIGER are free or available at nominal cost.

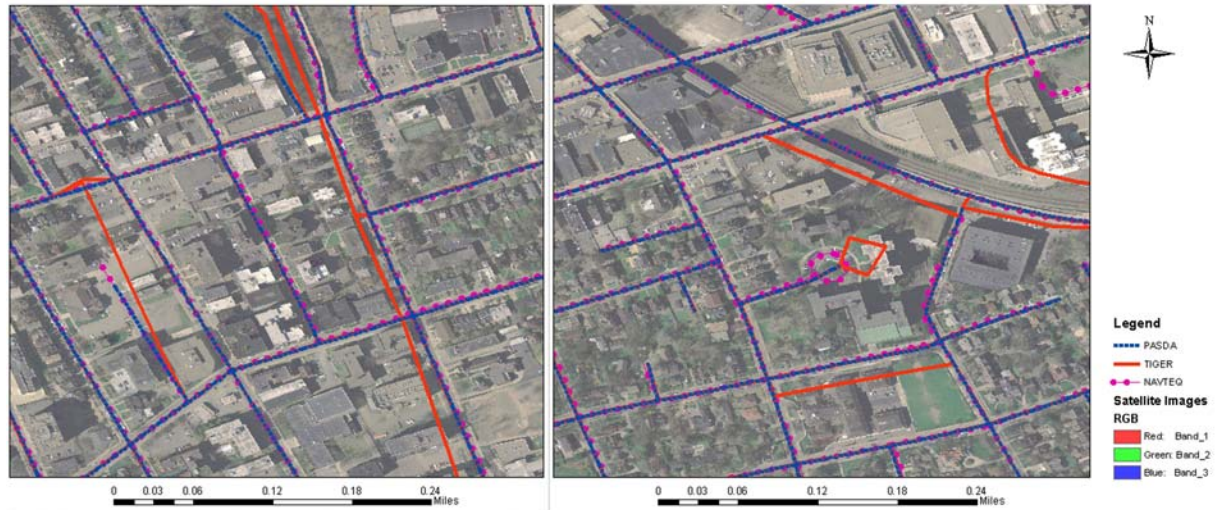


Figure 5-3. Digital road networks from three different map providers

5.2 DATA PREPARATION

The purpose of data preparation is to collect road segments that most likely have sidewalks along both sides. Road attributes can be used in filtering candidate road segments. For instance, road class and speed in NAVSTREETS, major road in Allegheny Street Centerlines, and road type in TIGER could be used to filter out road segments that are unlikely to have adjacent parallel sidewalks.

5.3 NETWORK CONSTRUCTION (NB ALGORITHM)

The purpose of network construction is to generate geometries of sidewalks and crosswalks along both sides of selected road segments and to construct pedestrian networks from generated sidewalks and crosswalks. Once road segments are filtered, geometries of sidewalks are

calculated. Each road segment's start point, end point, and shape points are extracted and used to calculate the geometry (latitude and longitude) of the shape points along pedestrian paths by using the great circle navigation formula (Williams, 2008):

$$newlat = a \sin(\sin(lat) * \cos(dist) + \cos(lat) * \sin(dist) * \cos(radial)) \quad (5.1)$$

$$newlng = lng + a \tan 2(\sin(radial) * \sin(dist) * \cos(lat), \cos(dist) - \sin(lat) * \sin(newlat)) \quad (5.2)$$

In Equations 5.1 and 5.2, three parameters required for calculating the geometry of a pedestrian path: start point, gap distance, and radial. A start point with latitude (lat) and longitude (lng), can be one of the points at either end of the segment or a shape point along the path of a road segment. The distance (dist) refers to the gap between a road segment and a pedestrian path segment. The gap distance between roads and sidewalks can be estimated using road attributes together with the standards minimum road width and sidewalk width. Examples of road attributes to determine the gap distance are number of lanes (included in NAVTEQ and PASDA data) and direction of travel (included in NAVTEQ data). The American Association of State Highway and Transportation Officials specifies a minimum lane width of 4.267 m (including 0.61 m for inner shoulder width) and a minimum outside shoulder width of 3.048 m to provide refuge for disabled vehicles and bicyclists (AASHTO, 2005). The Institute of Transportation Engineers (ITE) recommends a minimum sidewalk or walkway width of 1.829 m, which allows two people to pass alongside comfortably (Center, 2009). Based on these standards, the gap distance along each side of a road centerline is approximated, by summation of road width, shoulder width, and sidewalk width for each lane category and by taking into account road segment's direction of travel. Radial is the direction from a start point, expressed as the angle measured from north in a clockwise direction. East (90°) and West (270°) are degrees for calculating geometry of shape points and 2-way intersection point on the east and west sides, respectively. For intersection points

(a 3-or 4-way connection), radial is derived by averaging the bearing of two intersecting road segments. Figure 5-4 shows examples of radial parameter for both shape points (a) and the intersection point (b). For example, if two road segments intersected where the bearing of road segment A is 0° East and the bearing of road segment B is 90° East, then the resulting radial would be 45° East.

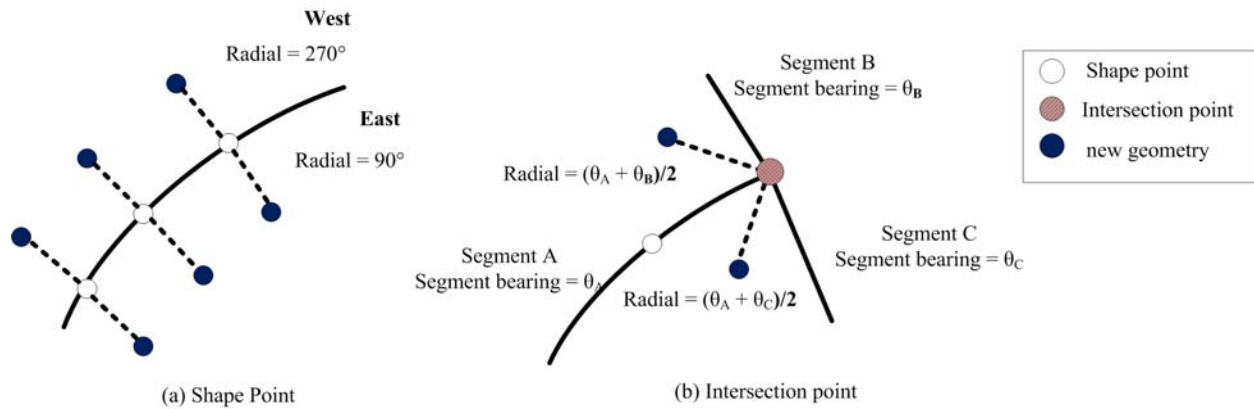


Figure 5-4. Examples of the radial parameter

An example of calculating geometry of sidewalk segments using great circle navigation formula is shown in Figure 5-5.

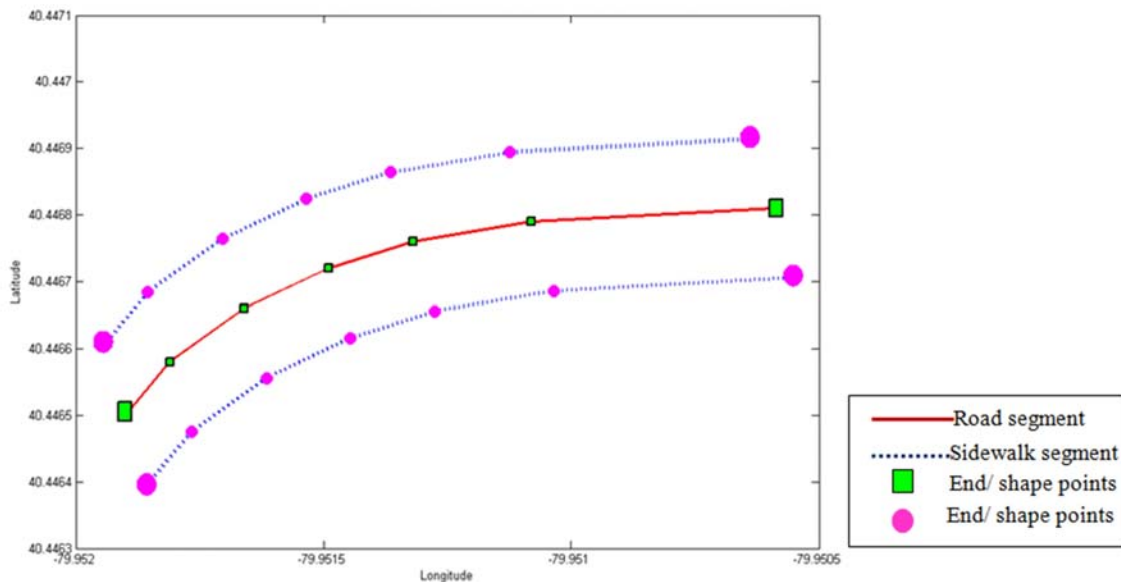


Figure 5-5. The calculated geometries of sidewalk segments

The red curve is a road segment with end points and shape points marked as green rectangles. The dashed blue curves are sidewalk segments along the east and west sides of a road segment which were calculated using the great circle navigation formula. After calculating the sidewalk segment geometries, the crosswalk segments are generated by linking the end point (intersection) of the east side and the west side of the sidewalk segment. Once all sidewalk segments and crosswalk segments are generated from road segments and the network topology is validated, by checking whether start and end nodes of connected segments coincide, the pedestrian network is constructed.

6.0 COLLABORATIVE MAPPING APPROACH

Collaborative mapping, or community mapping, is “an initiative to collectively create models of real-world location online that anyone can access and use to virtually annotate locations in space” (Gillavry, 2006). Its goal is to create a copyright-free and/or an alternative data source for geographic data. This chapter provides details of the pedestrian network construction algorithm based on GPS traces, collected through collaborative mapping. The data source required in the algorithm is discussed in Section 6.1. The algorithm consists of two main steps, data preparation, explained in Section 6.2 and network construction (CM algorithms), discussed in Section 6.3.

6.1 DATA SOURCE

Data required in this approach are GPS traces. A GPS trace refers to a trajectory of a pedestrian travelling along pedestrian paths as recorded by a GPS receiver. The assumption is that GPS traces represent the pedestrian path segments travelled by contributors. Each contributor may provide more than one trace at different times, and over time, each pedestrian path segment might be covered by multiple GPS traces.

6.2 DATA PREPARATION

The data preparation step involves collecting GPS traces, which require contributors to walk in a particular area. Goodchild defines Volunteered Geographic Information (VGI) as a special case of user-generated geospatial content on the GeoWeb and discusses the role of people as sensors to monitor the world (Goodchild, 2007). The emergence of Web 2.0 has facilitated collaborative content and modification by establishing connection among people with common interests, (Murugesan, 2007). An appropriate Web 2.0 technology, coupled with GPS-enabled mobile phones, portable digital maps, and free WMSs such as Google Maps and Bing Maps, provides users with easy access to location information and enables them to supply their own location content. Today, social networking services, such as Facebook and Friendster, have become extremely popular where people are able to post personal information, communicate and share information with other members. Location-Based Social Networking (LBSN), an extension of web-based social networking to mobile devices, where people can track and share location related information with each other is emerging.

Currently, there are several LBSN web sites (e.g., OSM¹, WikiLoc², everytrail³, and timatio⁴) that facilitate an environment where members of the network can participate in collaborative mapping projects or sharing leisure trips. These web sites provide tools for uploading GPS traces from walking, driving, or biking, collected by GPS devices or GPS-enabled mobile phones. The shared data can be downloaded, modified, and enriched by anyone. OSM is the most extensive and effective project that provides public GPS traces for mapping

¹ <http://www.openstreetmap.org/traces>

² <http://www.wikiloc.com/wikiloc/home.do>

³ <http://www.everytrail.com/>

⁴ <http://timatio.com/>

purpose, while the purpose of other websites is mainly for health and leisure services where GPS traces are a by-product of contributors' activities. Figure 6-1 and Figure 6-2 show the screenshot of public GPS traces available from OSM and Wikiloc.

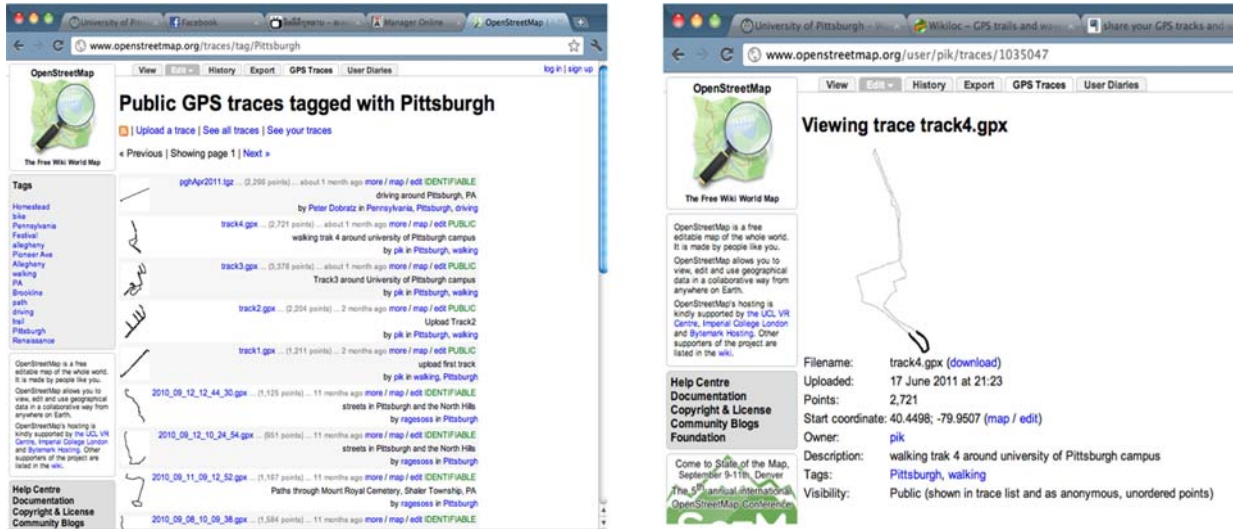


Figure 6-1. Public GPS traces available in Pittsburgh, PA

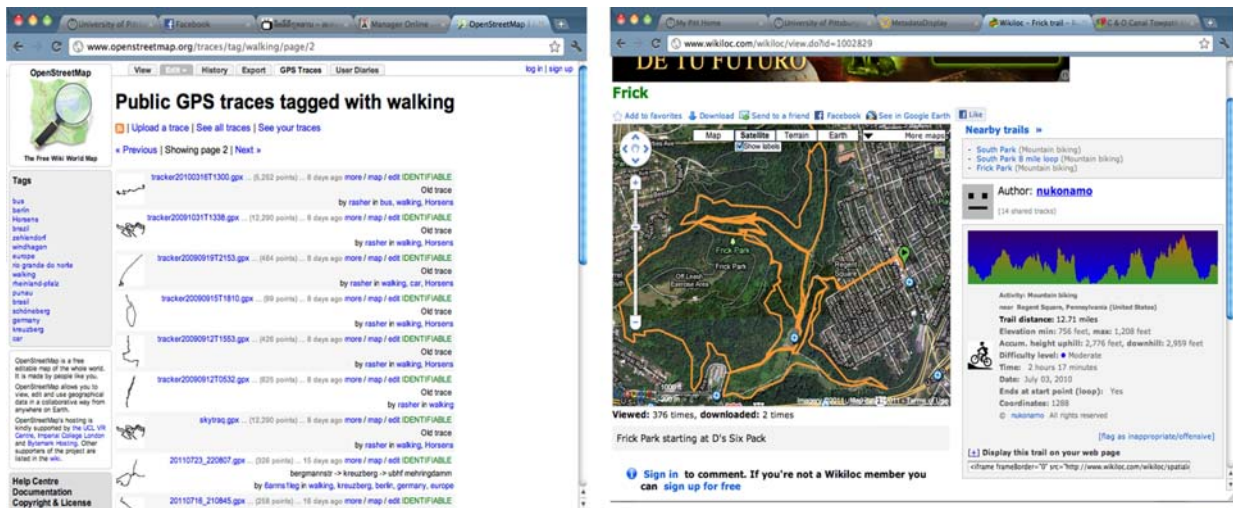


Figure 6-2. Public walking GPS traces (left) and public bike traces (right)

We searched for but could not find walking GPS traces in the University of Pittsburgh's area from OSM, Wikiloc, Everytrail, and timatio web sites. Therefore, we decided to collect data by volunteers, similar to the mapping parties found in the OSM project (Hakley and Weber,

2008) where large groups of people within a given area are offered guidance for collecting real-world data using GPS devices. Students in courses with location topics, such as GIS, are potential volunteers for collecting data as it helps them learn how GPS works and how to collect data with GPS. Other incentives for contributors include getting a community sense by exchanging information with other members in the community and deriving personal information from contributing valuable information, among others.

Although the LBSN approach is sound, it imposes certain constraints when collecting location data. Such constraints include walkable distance, complexity of mobile service, characteristics of the underlying area, and quality of GPS traces. Two of such constraints are related to human ability, while others are related to the environment. For walkable distance, the average human walking distance a day is around 2400 m in general (Frank et al., 2004); this implies that a large number of participants are needed to collect data in large areas. Maintaining up-to-date pedestrian network requires that members participate in repeated data collection. The closer the buildings are together, the narrower the streets are, and the closer the pedestrian footpaths are. Thus, a dense area (large number of pedestrian path segments) requires a larger number of volunteers than a sparse area does. Lastly, quality of GPS traces is affected by the types of GPS receivers at members' disposal and by the accuracy and continuity of GPS signals in some areas.

6.3 NETWORK CONSTRUCTION (CM ALGORITHMS)

This section discusses an algorithm to automatically construct pedestrian networks using multiple GPS traces collected by individuals on foot (Sinnot, 1984). The input to this algorithm

is walking GPS traces and the output is the constructed pedestrian network in a given area. A pedestrian network can be generated either manually or automatically. Manual generation means that contributors manually create and edit pedestrian paths using online GIS tools, such as JOSM (Java OpenStreetMap Editor), an online tool for creating and editing map based on GPS traces. Automatic generation means creation of map features from GPS traces without user intervention. The algorithm aims to process one raw GPS trace at a time and consists of three main steps: pre-processing, significant point filtering, and pedestrian network construction. Figure 6-3 highlights the input, the three steps, and the output of the CM algorithms.

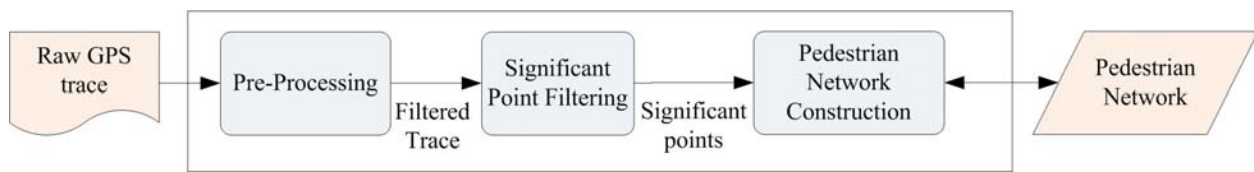


Figure 6-3. Three steps of the CM algorithms

The first two steps are concerned with preparing of individual GPS traces based on point-to-point property. The last step is concerned with incorporating new input traces to the already constructed paths stored in the database (initially empty) and consists of three tasks: (1) geometrical improvement of existing pedestrian paths, (2) generation of new pedestrian path features, and (3) construction of pedestrian networks. Details of these steps are described in the following.

6.3.1 Pre-Processing

Understanding quality of raw GPS traces is essential in constructing pedestrian networks; the lower the GPS accuracy, the lower the correctness of constructed pedestrian networks. This is particularly important as collected GPS traces usually contain errors due to the GPS Time-To-First-Fix (TTFF) problem, and the obscured GPS satellite signals. Generally, pedestrian paths are closer to buildings than roads are, and buildings are the main source of interference with GPS signals in urban environments. Therefore, GPS accuracy might be degraded while walking along pedestrian paths next to high-rise buildings. Moreover, because GPS data are constantly shifting, data recorded along the same path at different times may yield different accuracies. The pre-processing step aims to filter noises and outliers from GPS traces. In this step, GPS data, including latitude, longitude, time, speed, Horizontal Dilution of Precision (HDOP), and number of used satellites, are extracted. Serving as a filter, GPS observations with less than 4 satellites and HDOP greater than a threshold are considered as outliers and are eliminated. This task also eliminates the stored positions by GPS receivers when they are first powered up. The stored positions are the latitude and longitude (with no information on speed, HDOP, and number of used satellites) of the last location detected by the GPS receiver before it was powered off. Figure 6-4 shows a raw GPS trace (left side) and a filtered GPS trace (right side).

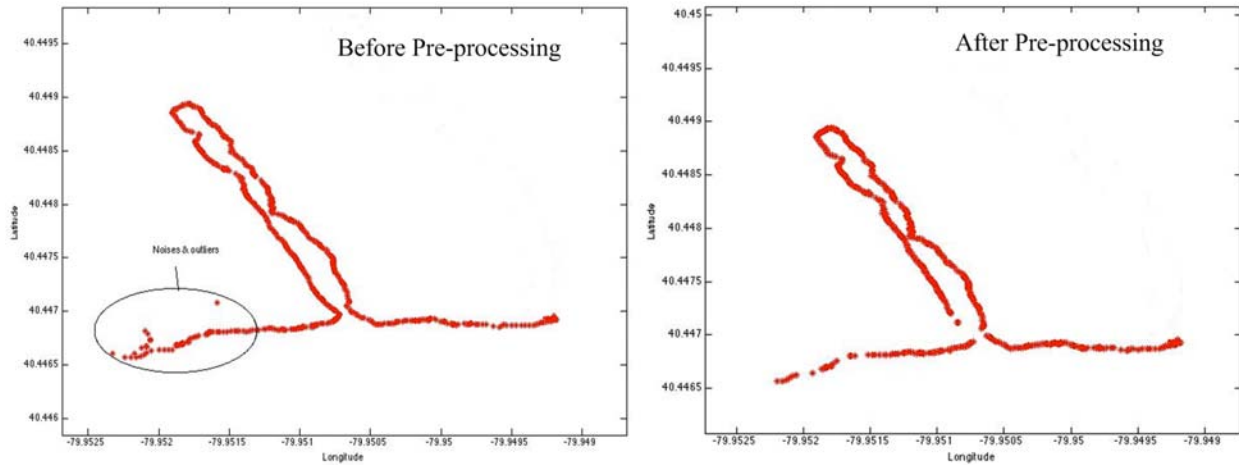


Figure 6-4. Example result after pre-processing

6.3.2 Significant Point Filtering

The objective of the significant point filtering step is to identify those GPS points that are important to determine the geometry of the underlying individual traces. A “significant point” refers to a GPS point with a high probability of determining the geometry of the walking path. For example, a GPS trace collected from an individual walking in a straight line would only need two significant points, start and end points, to represent the geometry of the GPS trace. This is a simple example and it is more challenging to identify the significant points for curved and irregular pedestrian paths from GPS traces. The input is the filtered GPS trace, obtained from the pre-processing step, and the output is the significant points of the GPS trace. Figure 6-5 shows input, output, and three tasks of the significant point filtering step.

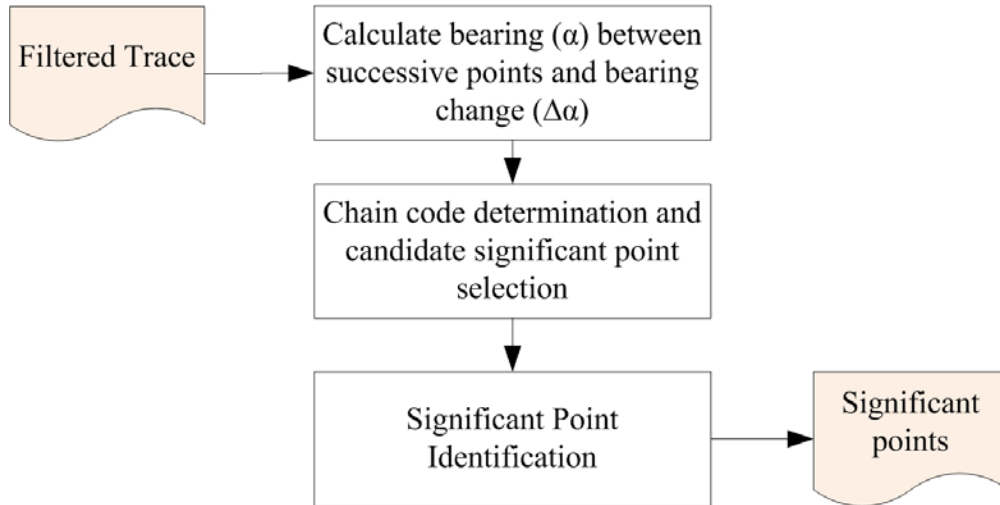


Figure 6-5. Steps of significant point filtering

The first task is to calculate bearing change ($\Delta\alpha$), which is used to identify significant points in the algorithm. To calculate bearing change, the bearing of successive points in a filtered GPS trace is required. Note that GPS receivers provide bearing information, but it is not employed in this task because it is not highly accurate, especially when travelling at speeds of less than 3.0 m/s (Ochieng et al., 2003). Bearing change ($\Delta\alpha$), i.e., the absolute value obtained from subtracting successive bearings, is calculated, using the great circle navigation formula (Williams, 2008), is calculated as follows:

$$Y = \sin(\Delta \ln g) * \cos(lat_2) \quad (6.1)$$

where $\Delta \ln g = \ln g_2 - \ln g_1$

$$X = \cos(lat_1) * \sin(lat_2) - \sin(lat_1) * \cos(lat_2) * \cos(\Delta \ln g) \quad (6.2)$$

$$\alpha = a \tan_2(Y, X) \quad (6.3)$$

where α is the bearing between two coordinates.

The second task (see Figure 6-5) is to select candidate significant points using the chain coding technique. Each GPS point now contains bearing between successive points and bearing change ($\Delta\alpha$). Given that bearing change is a real number ranging between 0° and 360° , it is difficult to set a threshold for candidate significant point selection. For example, consider a bearing change between 3° to 359° , the numerical difference between the values of the two numbers is very high but the actual change in direction is not. To address this problem, the chain coding technique to detect bearing change in the ordinal scale is employed. Chain coding is a common technique used to represent curves and recognized shapes of objects in image processing (Freeman, 1974). In our algorithm, a 12-direction chain code is chosen to represent bearing change in twelve direction intervals based on a counterclockwise direction starting from positive x-axis. A 12-direction is chosen because it is able to represent gently curves and angles of turns. The integer values, which range between 0 and 11, are used to represent direction of consecutive GPS points, as shown in Figure 6-6a. For instance, code 0 corresponds to bearing change from 0° to 15° and from 345° to 360° ; code 1 corresponds to bearing change from 15° to 45° . The values determined from chain coding are then used to eliminate those points with a bearing change of 0 and 6. This is because these codes do not represent any turn or curve, as can be seen in Figure 6-6a. Examples of chain coding and significant point selection are given in Figure 6-6b. In the figure, the bearing change from P_1 to P_2 and P_2 to P_3 is 10° which corresponds to chain code 0, thus P_2 is not considered a candidate significant point while P_3 is considered a candidate significant point because its bearing change represents a turn.

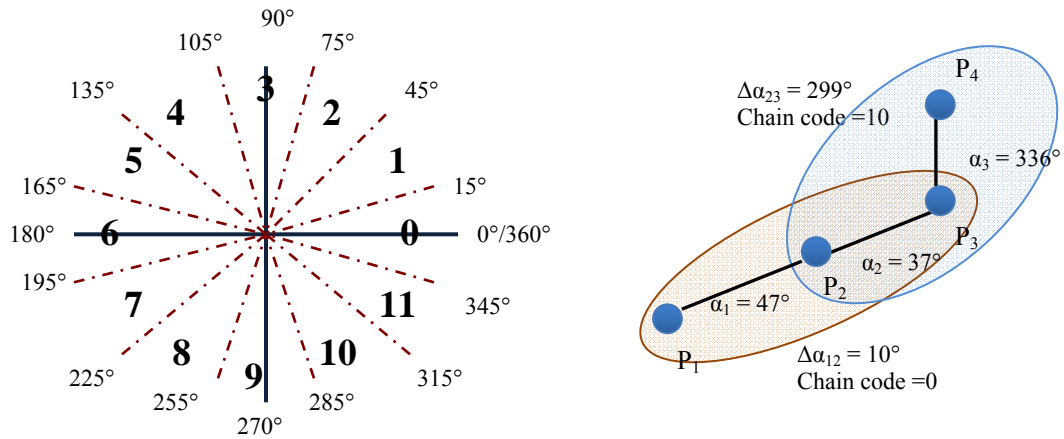


Figure 6-6. 12-direction chain code and an example

At this point, the algorithm has produced filtered GPS points along a walking trace that includes start, end, and candidate significant points. The selected GPS points from the chain coding task must be filtered further before they are considered significant points as they still may contain inaccuracies or may contain redundant data. A clustering analysis method is used to group candidate significant points to yield a significant point as the representative of each group. There are many types of clustering analysis, of which we chose the Partitioning Around Medoids (PAM) (Kaufman and Rousseeuw, 1987) method due to its robustness to noise and outliers. More specifically, PAM minimizes the dissimilarity (e.g., the geometrical distance) of the data points within a cluster, allows for a good clustering structure, and makes it possible to isolate outliers in most situations. PAM aims to find k representatives, called “medoids”, to minimize the objective function, which is the sum of the dissimilarities of all objects to their nearest medoid. PAM has two steps: (1) selecting sequentially k initial medoids and (2) swapping iteratively selected objects (medoid) with an unselected objects if the objective function can be reduced. This iterative process continues until the objective function can no longer be decreased (Kaufman and Rousseeuw, 1987). Considering PAM in our algorithm, the Euclidean distance function is used to compute the similarity between two candidate significant points, and the most

difficult task is the determination of a suitable number of clusters (k) since it cannot be known in advance. Kaufman and Rousseeuw (1990) suggest use of “Silhouettes” to validate quality of computed clusters and to determine which points lie well within their clusters and which do not. Each point i is represented by one silhouette (s_i), which is defined as follows:

$$S_i = \frac{[b(i) - a(i)]}{\max\{a(i), b(i)\}} \quad (6.4)$$

where $a(i)$ is average dissimilarity of point i to all other points within the same cluster and $b(i)$ is average dissimilarity of point i to all other points in the neighboring cluster

The value of s_i ranges between -1 and 1 where a value close to 1 means that the data is appropriately clustered, a value near zero means that the data is on the border of two clusters, and a value close to -1 mean that the data would be more appropriate for a neighboring cluster. The average silhouette width is the mean of s_i for all points i in a cluster and can be used to select a suitable number of clusters by choosing the number of clusters that yield the highest silhouette width.

To illustrate the entire process of significant point filtering, two examples are given in Figure 6-7. Figure 6-7a shows the filtered GPS points through the pre-processing step. Black rectangular points in Figure 6-7b represent candidate significant points chosen by the chain coding technique. As shown in the figure, candidate significant points are able to represent the shape of a pedestrian path; however, some redundant points can be removed without loss of information. Green circle points in Figure 6-7c represent the significant points obtained from PAM where candidate significant points were clustered. The number of GPS points after processing each task is also illustrated in the figure. At the end of this process, the significant points extracted from each trace are used as an input to the pedestrian network construction step.

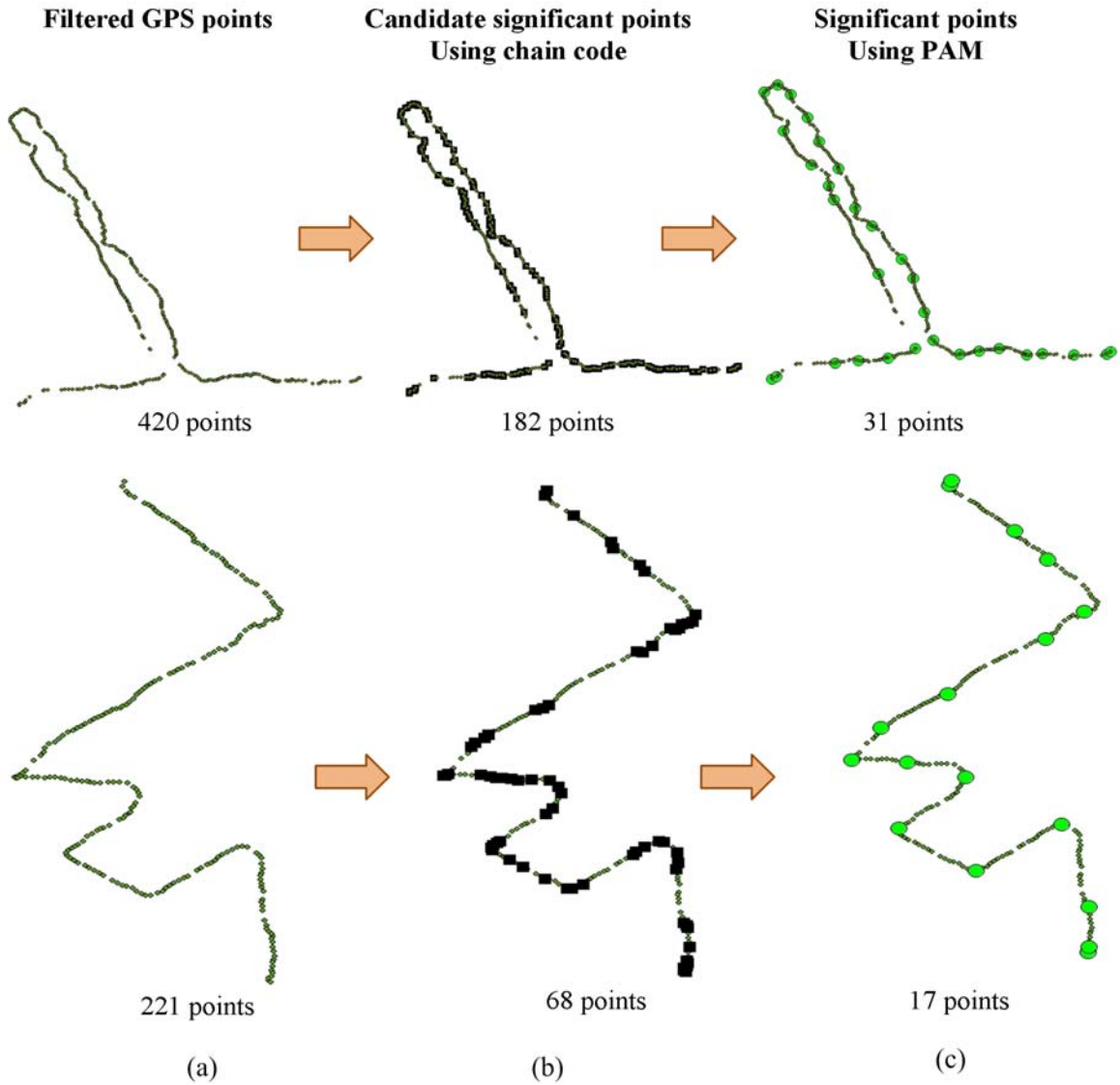


Figure 6-7. Examples of significant point filtering

6.3.3 Pedestrian Network Construction

Initially, the pedestrian network is empty and over time is incrementally extended/refined by collected GPS traces. The input is the significant points of a GPS trace, obtained from the previous step, and the output is the pedestrian network. Figure 6-8 shows the flowchart of this step.

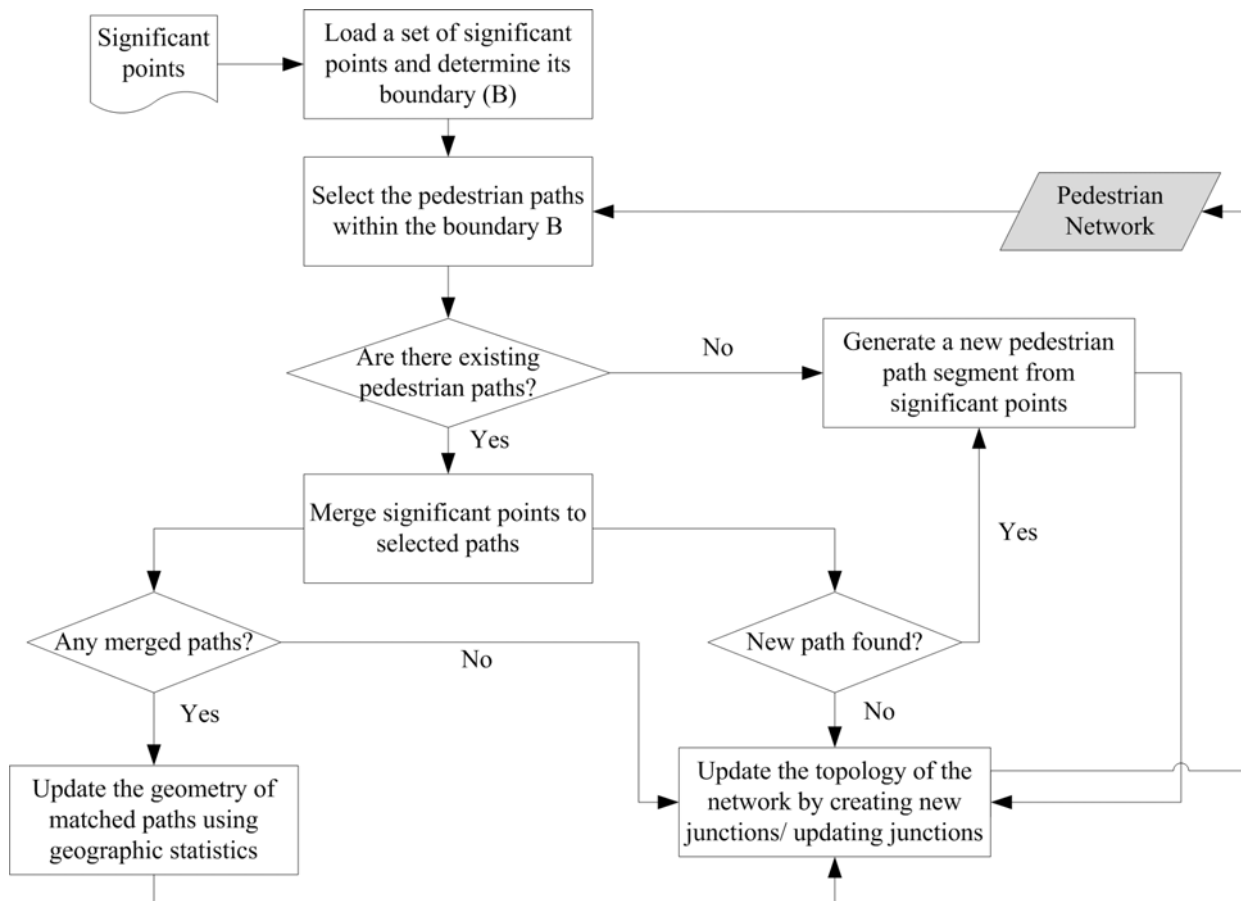


Figure 6-8. Steps of pedestrian network construction

This step begins by loading the set of significant points of a GPS trace and defining its map boundary. Then the algorithm decides the next task based on the following three conditions: (1) generating a new path segment, (2) merging and improving existing path segments, and (3) generating a new path segment and improving existing path segments. Within the defined map boundary, if there is no existing pedestrian path segments (called EPs), the new pedestrian path segment is detected and the next task is to generate the geometry of a new pedestrian path segment by connecting the given significant points. The new generated path is subsequently added to existing pedestrian network. An example is shown in Figure 6-9.

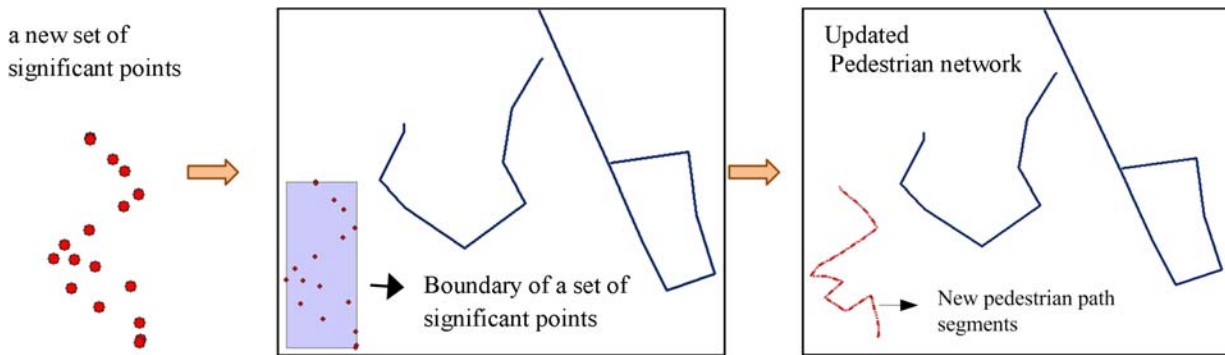


Figure 6-9. An example of a generated pedestrian path segment

On the other hand, if there are EPs within the boundary, a set of significant points are compared to the geometry of EPs in order to decide whether they should be merged or not. Given a set of significant points, several cases are possible. For instance, some significant points are merged to EPs and others represent a new path; all significant points are merged to EPs; and all significant points form a new path. The set of significant points are decided to merge and improve EPs when all the following three conditions are satisfied: (1) the shortest distance from a significant point to the closest EP is smaller than a predetermined threshold (called merged points); (2) there are at least two merged points on a particular EP segment; and (3) the directions of a curve drawn by contiguous merged points and a particular EP are nearly parallel. If consecutive significant points do not satisfy those three criteria, they form a new path and will be used to generate new geometry. Figure 6-10 shows an example of a new set of significant points (highlighted in circle “A”) considering as merged points. However, the significant points in circle “B” do not satisfy all the criteria for merging in that the direction of curve on merged points is almost perpendicular to the existing line. In this example, only significant points in circle “A” are merged to the existing line (called merged path) and other points contribute to the new pedestrian path.

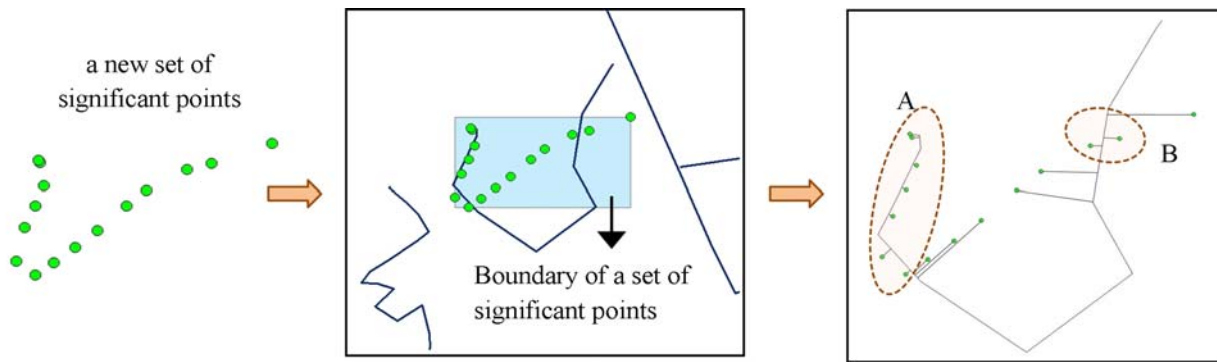


Figure 6-10. An example of merged significant points and paths (in circle A)

In a case where pedestrian path segments are close to each other, such as parallel sidewalks along narrow roads, to which pedestrian path segment the significant points belong to is not clear. To deal with this problem, the previous travelled path can be used to determine the next paths based on connectivity. Another possible way to determine the right path is to use the result by majority of merged points.

Once points are merged, the next task is to improve the geometry of the merged pedestrian paths by applying statistics. The geometrical improvement process begins by extracting shape points (including start/end points) of the merged path. Each merged significant point is then grouped to the closest shape points of the merged path. The new geographic locations of shape points are identified by calculating the mean position of geographic points in the group. However, there could be a case where the significant point itself could represent a new shape point of the merged path, if its geographic location is not close to existing shape points (i.e., distance to the closest shape point is larger than the threshold). An example of the geometrical improvement process is illustrated in Figure 6-11. Figure 6-11a shows the geometric location of shape points (green rectangle) of the merged path and the location of merged significant points (red circle). Figure 6-11b shows the new shape points (black triangle) of the merged path, which are derived from the mean position of geographic points in the group (each

circle). Figure 6-11c shows the geometry of the old path (solid blue line) and the new path (dashed red line) after overlaying the merged data on a raster image. As shown in the figure, the geometry of new path (after merging 2 GPS traces) is more accurate than the geometry of the old path (using one GPS trace).

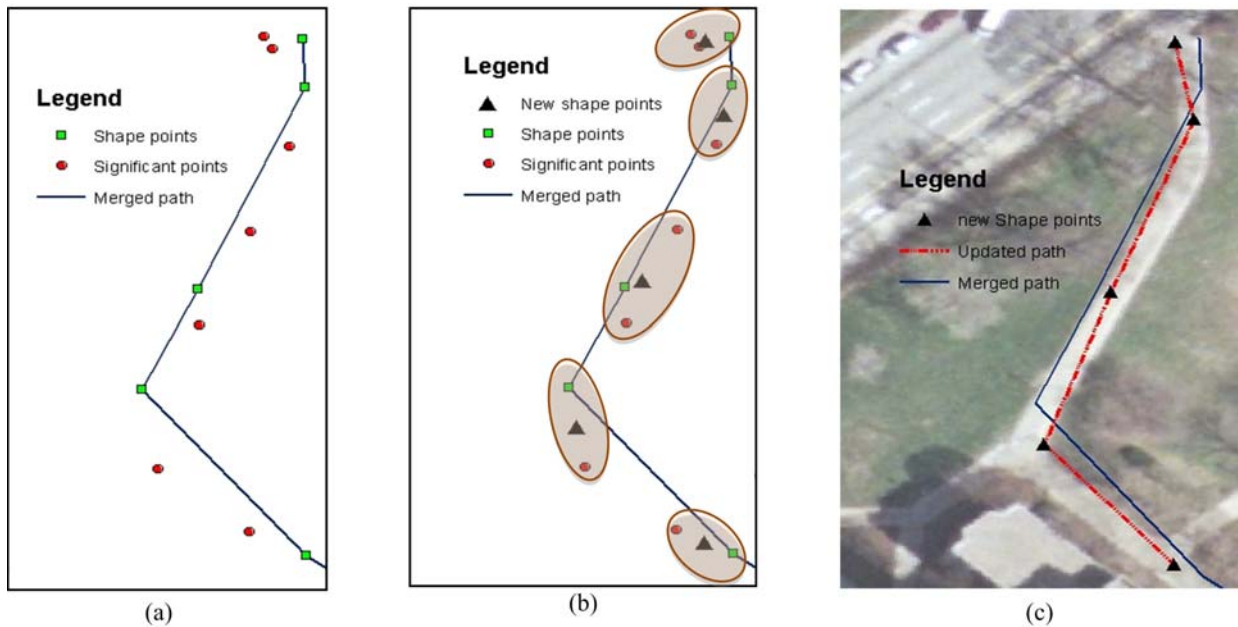


Figure 6-11. An example of geometric update of merged pedestrian path

The last task of constructing pedestrian network is to update the topology of the network. After generating new geometry of a pedestrian path, new intersection points are created when either newly generated path intersects with EPs or there is a gap smaller than the minimum width of the pedestrian path between the end points of the newly generated paths and EPs. In the former case, the intersection points are used to split the lines and ensure the connectivity between them. The short lines after splitting are considered spurious and are removed. In the latter case, the gap is closed by snapping the end point to the closest paths and the snapped point is used as a new intersection. After improving the geometry of existing paths, the location of existing junction is updated based on the new geometry of pedestrian paths. Figure 6-12 gives three examples of the task of topology update.

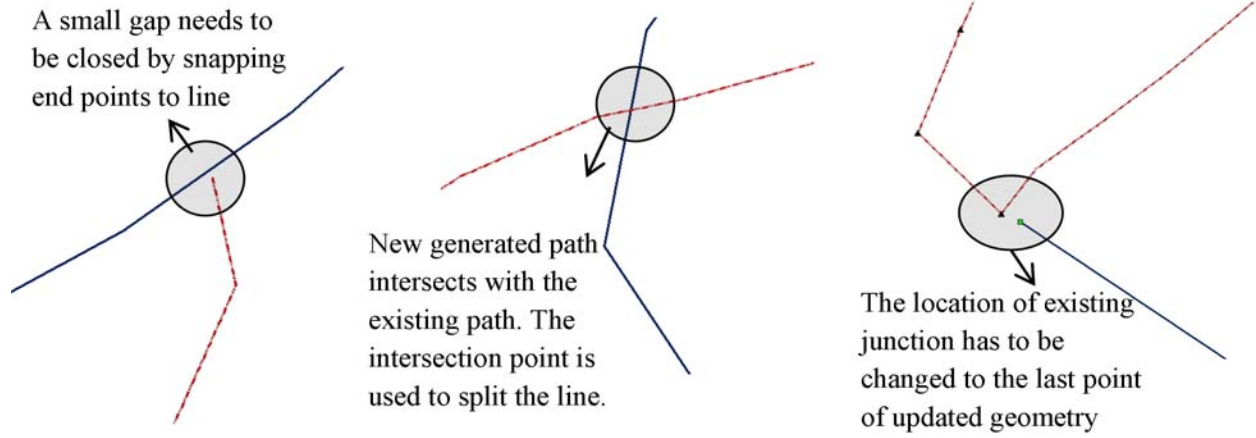


Figure 6-12. Examples of validating network topology

7.0 IMAGE PROCESSING

With the development of digital photogrammetry, computer vision, and pattern recognition, currently several semi-automatic and automatic techniques for analyzing, enhancing, and extracting features from digital images are available. Due to the need for efficient acquisition and update of data for GIS, much research has been on extracting road networks, vegetation areas, and buildings from high-resolution images. In contrast, research on extracting pedestrian networks from imagery is scarce (Walter et al., 2006). Since roads and pedestrian paths are man-made objects and share similar characteristics, existing automatic urban road network extraction techniques are reviewed (Chapter 3) and are considered as a starting point for developing the pedestrian network extraction algorithm. Table 7-1 shows the characteristics of roads and pedestrian path segments.

Table 7-1. Characteristics of roads and pedestrian paths

Characteristics	Road	Pedestrian path segment
Surface	Concrete, Firm and smooth Color: dark gray	Concrete, Firm and smooth Color: light gray
Shape	Line	Line
Width	Constant: 3.96-4.57 m/ lane	Constant: 1.83-7.62 m
Curve	Depend on road type (e.g., highway has less curvature than rural road)	Curve radius should vary between 15.25 – 91.44 m
Context objects	Cars, buildings, trees, pedestrians, sidewalks	Road, building, vegetation, parking lot

In high-resolution images, pedestrian paths appear as small-elongated regions with parallel borders. They generally have smooth and firm surfaces and are usually made of concrete, asphalt, brick, or cobblestone (ADA, 2004). The Federal Highway Administration (FHWA) and ITE recommend a minimum width of 1.83 m, which allows two people to pass comfortably (Center, 2009). Figure 7-1 shows the relationship between the pedestrian network model and context objects in the image.

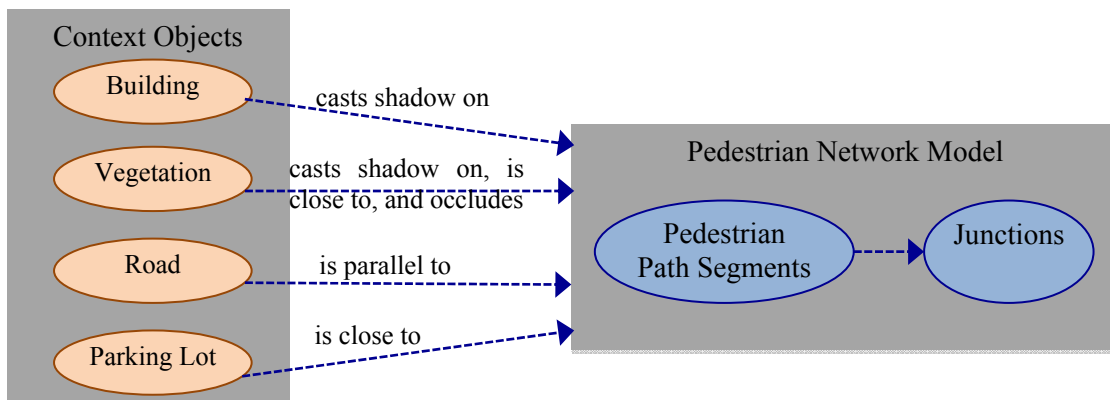


Figure 7-1. A pedestrian network model and context relations

Pedestrian path segments are approximately parallel, connected, or close to context objects including roads, buildings, parking lots, and vegetation areas. The image intensity of pedestrian path areas is not constant because of shadows from trees or buildings, and small objects located on the path such as mailboxes, garbage cans, fire hydrants, or parking meters. A parking lot refers to an outdoor area reserved for off-street parking for multiple cars and it can be considered in two different ways: (1) as a walkable area where pedestrians can walk at random and (2) as an obstacle that precludes pedestrian paths. In this dissertation, the parking lot is considered as an obstacle, not a pedestrian path type because the digital representation of a parking lot is significantly different from the other types described above and it requires a special model and design.

Figure 7-2 shows the steps of the pedestrian network construction using two types of sensors, remotely-sensed imagery and laser imagery.

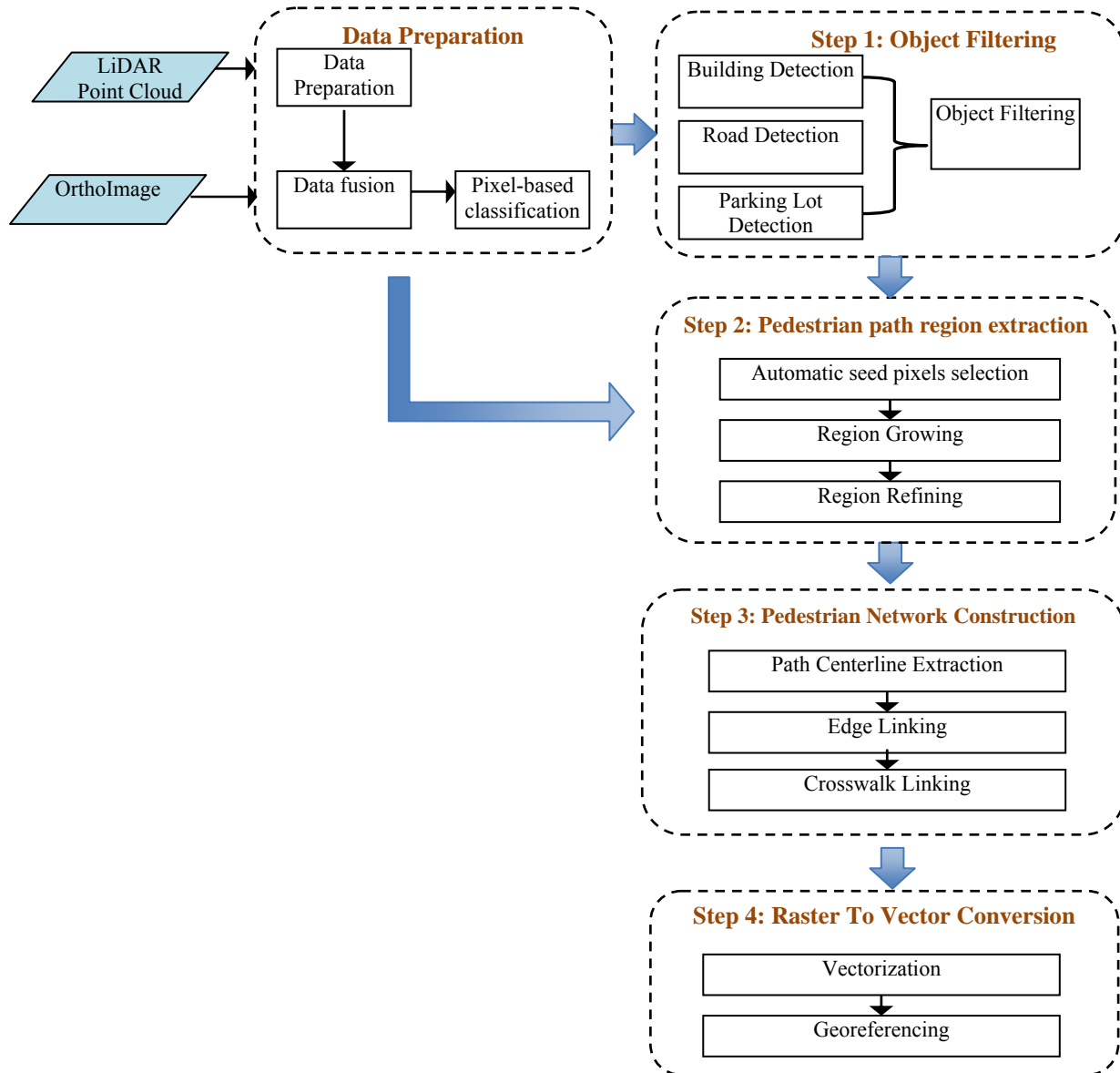


Figure 7-2. Steps of the IP approach

Section 7.1 discusses data sources required in this algorithm. Section 7.2 explains data preparation and Section 7.3 provides details of four steps of network construction: (1) objects

filtering, (2) pedestrian path region extraction, (3) pedestrian network construction, and (4) raster to vector conversion.

7.1 DATA SOURCES

Data required in the image processing approach for constructing pedestrian networks are derived from two sources: remotely-sensed imagery and laser imagery. We chose to utilize these two data sources for two reasons. First, both data sources are widely available and secondly, it has been proven that the 3D information from laser imagery, such as LiDAR point cloud data, is able to improve the analysis of optical images such as high-resolution images for detecting roads and buildings in urban areas (Hinz et al., 2001, Hofmann, 2001, Hu et al., 2004).

7.1.1 Orthoimages

Remotely-sensed images (e.g., aerial photos) are taken from an elevated position such as from an airplane or helicopter and contain measurements in x, y, z coordinates (NRC, 2003). Remotely sensed imagery has been widely used for creating and updating large-scale maps as well as for maintaining up-to-date GIS databases. The resolution of the orthoimages (low-resolution and high-resolution) has impacted on the techniques used to extract objects. High-resolution imagery is required for extracting pedestrian paths because the geometrical properties of pedestrian paths are much clearer in them than the low-resolution imagery. An orthoimage is “remotely-sensed image data in which displacement of features in the image caused by terrain relief and sensor

orientation have been mathematically removed” (PAMAP, 2008). Figure 7-3 shows an example covering an orthoimage of the University of Pittsburgh’s main campus area.



Figure 7-3. Example of orthoimage in the University of Pittsburgh's main campus

7.1.2 LiDAR (Light Detection and Ranging)

Aireborne LiDAR is a remote sensing technology that integrates laser scanner, GPS, and Inertial Navigation System (INS) in order to determine the shape of the ground surface for both natural and man-made features (Ackermann, 1999). The laser scanning technique is shown in **Figure 7-4**.

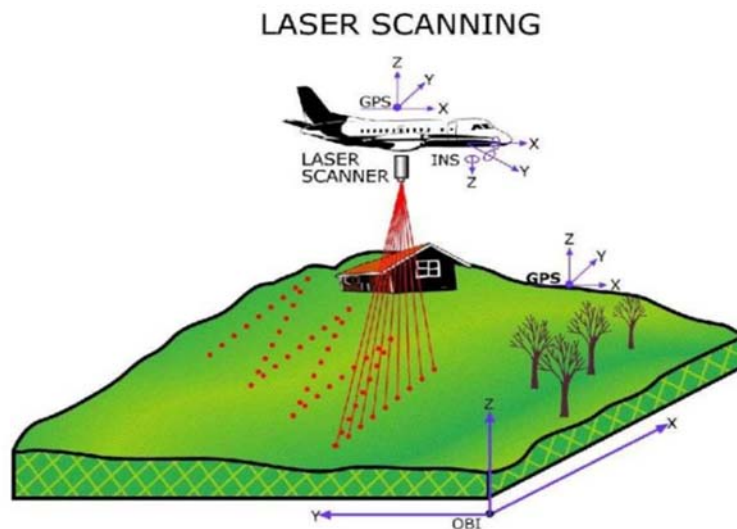


Figure 7-4. The laser scanning technique (Renslow, 2001)

While the aircraft is in flight, the laser transmits a pulse that is reflected off an object or the terrain and returned to the receiver. From a single beam, laser pulses can have multiple reflections that enable detailed modeling of terrain surface. For example, the first return hits the top leaves of the tree and reflect back to the sensor and the last return travels through a gap to hit the ground under the tree. By applying the speed of light, the distance from the sensor to the terrain point is determined by measuring the time delay between the transmitted pulse and return signal. At the same time, the x, y, z positions of antenna and the altitude angles of the aircraft are periodically recorded by the GPS receivers and INS, respectively. Consequently, the system produces abundant 3D information (x, y, z coordinates), called “point cloud” from which most grounds features, such as roads or buildings, are visible. Moreover, the reflective intensity or strength of the reflected laser pulse is commonly collected along with other data. An example of LiDAR point cloud data covering the University of Pittsburgh’s main campus is shown in Figure 7-5.

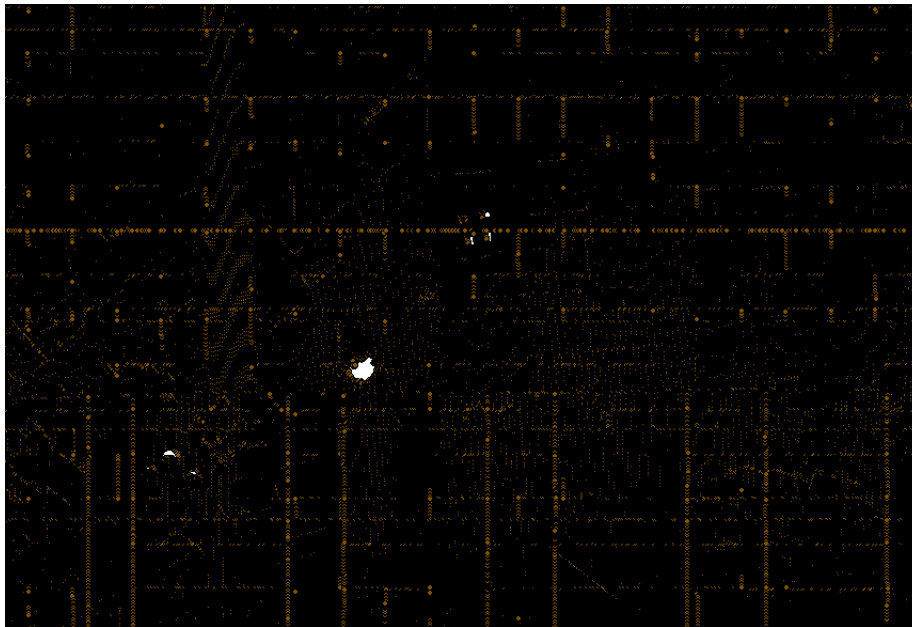


Figure 7-5. Example of LiDAR point cloud in the University of Pittsburgh's main campus

7.2 DATA PREPARATION

Data preparation for image processing involves three tasks. The first task is to create raster-based data from LiDAR point cloud. The four raster-based datasets required for image processing are: (1) Digital Surface Model (DSM), (2) Digital Elevation Model (DEM), (3) Last-return surface, and (4) LiDAR intensity image. DSM represents the surface from the first-return or from which the laser pulse is reflected and typically indicates trees, buildings, and terrain surface. DEM represents height information of the bare ground surface with no objects. Last-return surface represents elevations detected by the LiDAR pulse struck. LiDAR intensity image is a black and white image representing the return strength of the laser pulse that generated the point.

There are two common formats for representing raster surfaces: Triangulated Irregular Network (TIN) and raster grid format. A TIN is a digital structure that uses an irregularly spaced set of points to approximate the terrain surfaces as a series of triangles. Figure 7-6 shows an example of a TIN representing the DSM of the University of Pittsburgh's main campus and Figure 7-7 represents its 3D view. The raster grid format is represented by the origin point, X and Y spacing, and the size of grid. To represent raster-based surface from LiDAR point collections, the raster grid format is chosen because it is a simple way of storing elevation and intensity values. Although TIN representation is able to model the surface more accurate and uses fewer points than the raster grid, determining the elevation of a point is more complicated and requires more computation.

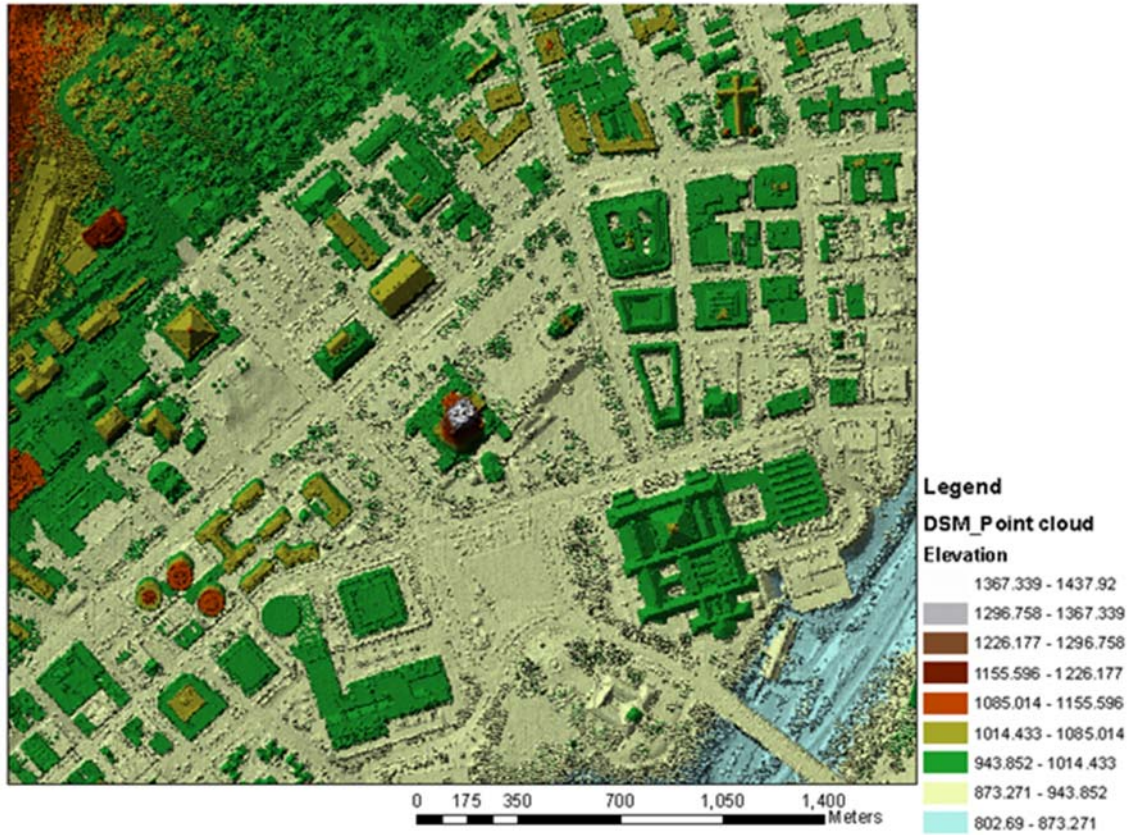


Figure 7-6. An example of TIN representing DSM in the University of Pittsburgh main campus



Figure 7-7. A 3D view of DSM

To produce raster grid data, each point data is resampled into a regular grid with a selected cell size. The nearest neighbor interpolation method is employed to create raster grid data because it is the simplest method and fast, and it preserves edges (e.g., building edges), which are important for huge amount of points representing objects in urban area (Youn, 2006). An example of raster data generated from point clouds using nearest neighbor interpolation is shown in Figure 7-8.

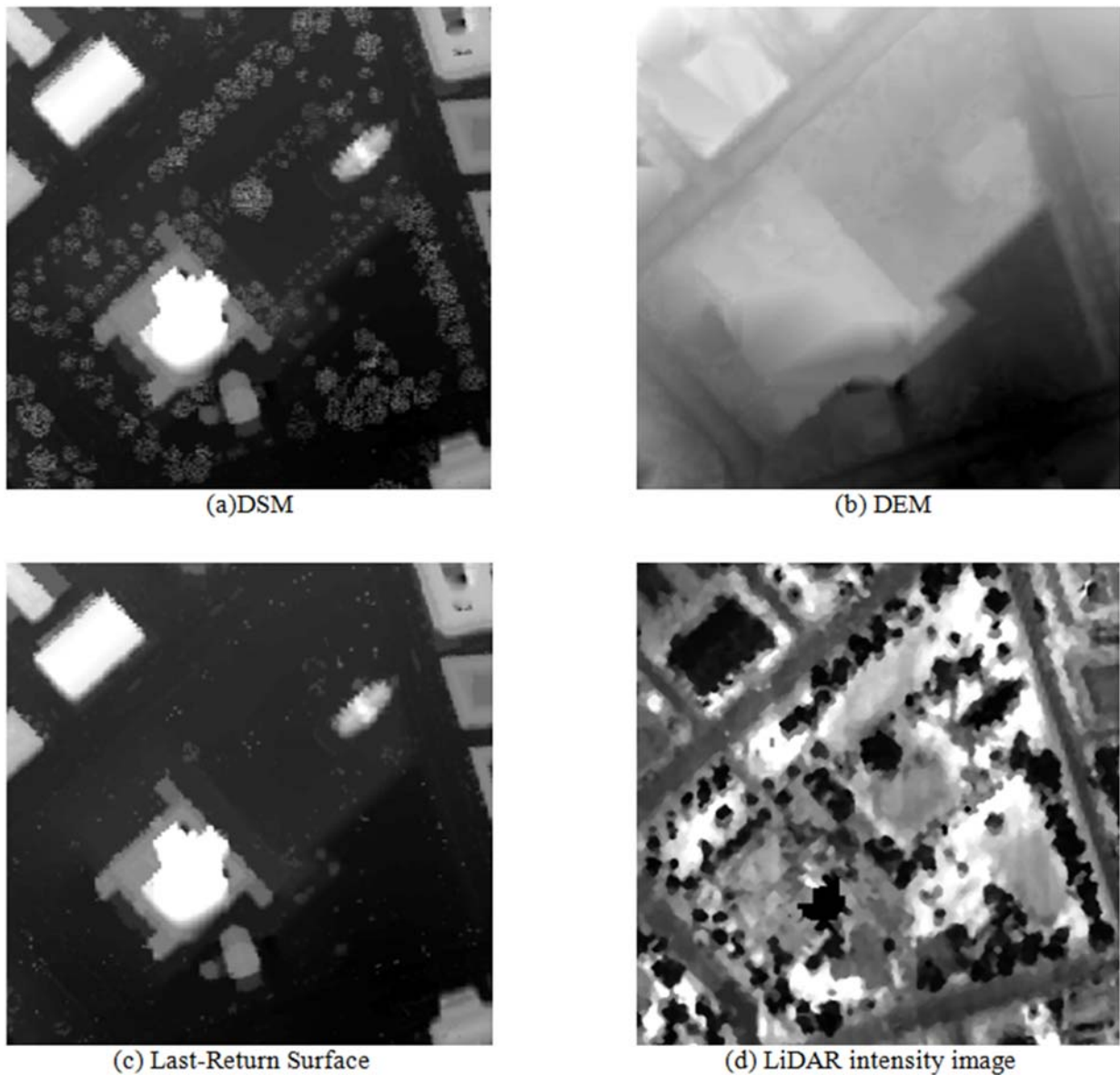


Figure 7-8. Example of DSM, DEM, Last-Return surface, and LiDAR intensity image of the same location

The second task of data preparation (see Figure 7-2) is data fusion. Data fusion integrates information from remotely-sensed images (orthoimage) and laser images (LiDAR). An orthoimage has three color bands, i.e., R (Red), G (Green), B (Blue). The fused data is a 4-band, R, G, B, I (LiDAR intensity), multispectral image that incorporates RGB data with the LiDAR intensity image, after a resampling of points to raster data.

The third task of data preparation (see Figure 7-2) is pixel-based classification. Pixel-based classification refers to the task of extracting information classes using the spectral information from a multiband raster image. The resulting classified image will be used in two subsequent tasks: object filtering (Step1 of network construction) and automatic seed selection (Step 2 of network construction). Two common image classification approaches are supervised classification and unsupervised classification. Supervised classification uses the spectral signature of different classes obtained from training samples to classify an image, while unsupervised classification groups the image into clusters without the training data. Support Vector Machine (SVM), Maximum Likelihood classifier, and Neural Network classifier are common classifier algorithms. Supervised classification using SVM is selected in this dissertation because it has been proven that it can produce a high classification accuracy and outperforms other competing algorithms (Hermes et al., 1999, Song and Civco, 2004). SVM is a classification technique developed by Vapnik and his group at AT&T BELL laboratories (Vapnik, 1995) and is widely used in a variety of applications. The main idea of SVM is to separate classes with a hyperplane surface so as to maximize the margin among them. For more details of SVM refer to Burges (1998).

To perform supervised classification, groups of features need to be specified, in order to collect training samples and create a classifier model. We first identify two groups of features, a

pedestrian paths group including actual pedestrian paths, and a non-pedestrian paths group including other features, which have spectral values different from pedestrian paths. Training samples of two classes are manually collected and evaluated using tools in GIS. An example of training samples is shown in Figure 7-9, where blue polygons represent pedestrian paths group and red polygons represent non-pedestrian paths group.



Figure 7-9. An example of training sample for pedestrian paths and non-pedestrian paths groups

The histogram and statistics are used to compare the distributions of specified classes and to evaluate the training samples. If the training samples represent different classes, their histogram should not overlap. An example of the histogram of R (red), G (green), B (blue), and I (LiDAR intensity) is shown in Figure 7-10 and the statistics of training samples are shown in Table 7-2.

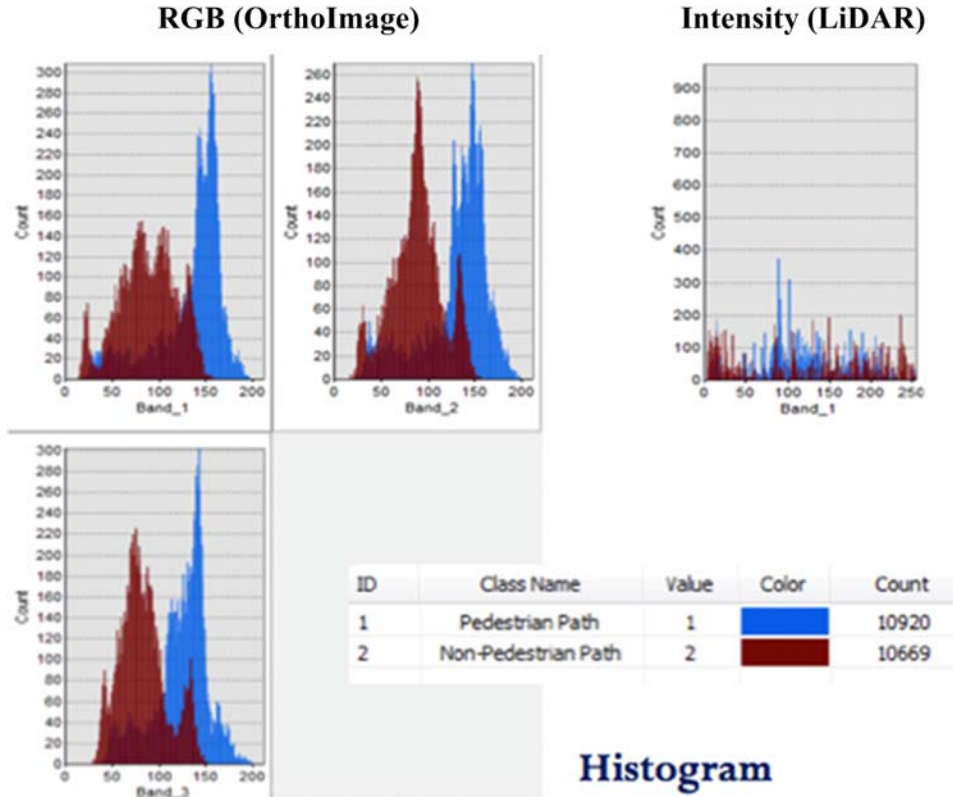


Figure 7-10. The histogram of the training samples

Table 7-2. The statistics of training samples for two groups

Statistics	Pedestrian path group				Non-pedestrian path group			
	R	G	B	I	R	G	B	I
Minimum	46	54	65	5	44	48	60	3
Maximum	227	228	229	255	190	187	182	255
Mean	164.17	160.59	154.39	120.7	118.92	118.70	113.10	135.25
Stdev	35.72	34.65	28.65	56.05	30.37	27.15	24.82	85.98

As seen in the image, the histogram shows that there is significant overlapping between two classes, especially using LiDAR intensity. The standard deviation of LiDAR intensity values for both pedestrian paths group and non-pedestrian paths group are high. This is the reason why we tried to classify classes based on surface material. Four classes, which are concrete, asphalt, brick, and vegetation, are identified. The training samples of these four classes are collected and their histograms are shown in Figure 7-11.

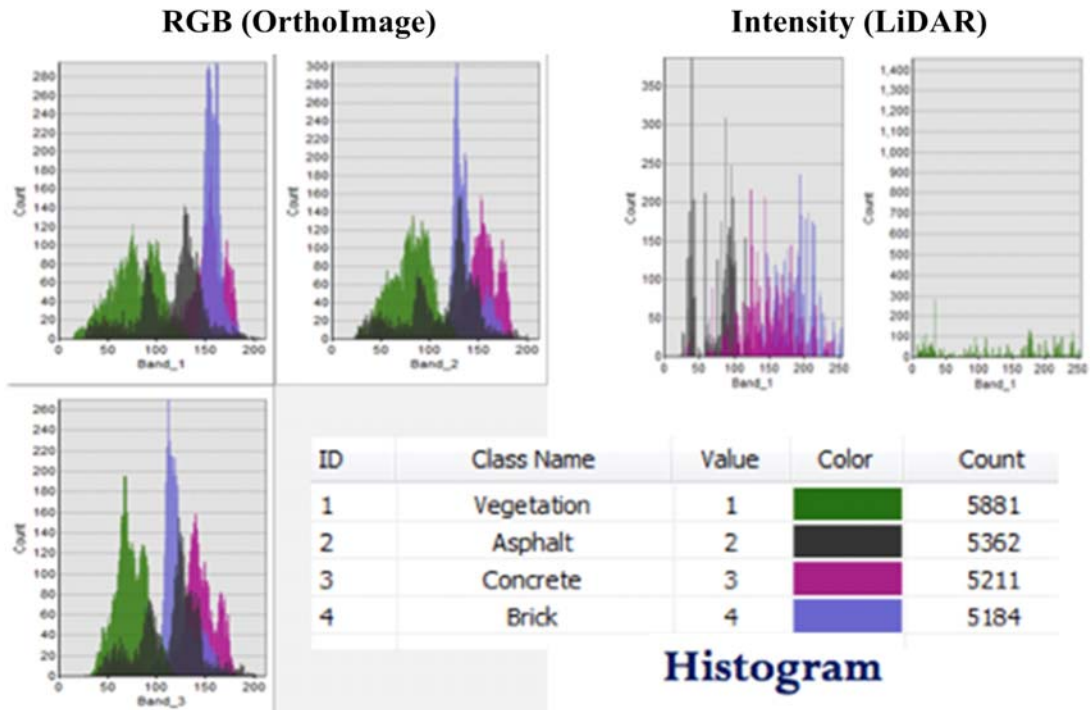


Figure 7-11. Examples of histograms for four classes

Table 7-3. Statistics of training samples for four classes

Groups	Minimum	Maximum	Mean	Stdev
Vegetation				
R	46	157	102.47	20.13
G	55	159	106.10	17.4
B	59	149	99.37	12.86
I	9	255	179.66	90.08
Concrete				
R	53	217	174.08	32.89
G	60	215	174.48	32.58
B	69	212	167.02	28.19
I	21	241	145.62	36.92
Brick				
R	124	218	187.95	7.56
G	101	212	167.47	13.05
B	99	208	153.68	14.63
I	136	255	192.90	28.99
Asphalt				
R	54	235	143.85	33.14
G	54	230	142.74	35.65
B	63	232	143.51	30.21
I	26	120	74.63	26.10

Comparing the histograms and statistics of training data between two classes and four classes, we chose to classify images into four classes because of less overlapping between classes.

To generate a classifier model, we experimented and compared results of SVM using three different image sources: 1-band (I-LiDAR intensity), 3-band (R, G, B), and 4-band (R, G, B, I). To perform supervised classification, the training data were used to generate a classifier model and the resulting model was used to classify the image into predefined classes. The selection of training areas was done in ArcGIS software, which supports a polygon tool for selecting features. The LIBSVM library by Chang and Lin (2011) was employed to implement SVM. The Radial Basis Function (RBF) was selected as a kernel function due to its suitability for classification of images that have nonlinear relationship between class labels and attributes. Two parameters for RBF kernel are C and γ and they were selected by using the 10-fold cross validation and grid search. In 10-fold cross validation, the training data was divided into 10 subsets of equal size, where one subset was used as the testing set and the remaining data were used as the training set. To measure the performance of the classifier model, the cross-validation accuracy, which is the percentage of data that are correctly classified, was used. As recommended by Chang and Lin (2011), various pairs of (C, γ) were tried and the one with the highest cross validation accuracy ($C = 1024$ and $\gamma = 64$) was selected. The classifier model was tested by 10-fold cross validation with three image sources: 1-band (LiDAR intensity), 3-band (RGB), and 4-band (RGBI). The error matrix introduced by Congalton (1991) was employed to represent the classification accuracy. Table 7-4, Table 7-5, and Table 7-6 show the error matrices for the classification results for 1-band, 3-band, and 4-band, respectively. In the error matrix, each column represents the reference data (actual class) and each row represents the instances in a classified class. Three

measurement values including producer’s accuracy, user’s accuracy, and overall accuracy were calculated. Producer’s accuracy corresponds to error of omission indicating the probability of a reference pixel being incorrectly classified. User’s accuracy corresponds to the error of commission (false alarm rate) indicating the probability that a pixel classified actually does not represent that class on the ground. Overall classification accuracy is the proportion of the total number of correct predictions.

Table 7-4. Error matrix for the classification result using 1-band (LiDAR intensity)

Classified class	Reference Data				Total	User’s Accuracy (%)
	Vegetation	Concrete	Brick	Asphalt		
Vegetation	2632	138	428	79	3277	80.32
Concrete	459	2442	458	324	3683	66.30
Brick	1708	1844	4247	0	7799	54.46
Asphalt	940	627	0	4935	6502	75.90
Total	5739	5051	5133	5338	21261	
Producer’s Accuracy (%)	45.86	48.35	82.74	92.45		
Overall classification accuracy = 67.05%						

Table 7-5. Error matrix for the classification result using 3-band (RGB)

Classified class	Reference Data				Total	User’s Accuracy (%)
	Vegetation	Concrete	Brick	Asphalt		
Vegetation	5516	380	2	588	6486	85.04
Concrete	85	3369	301	764	4519	74.55
Brick	2	451	4802	40	5295	90.69
Asphalt	136	851	28	3946	4961	79.54
Total	5739	5051	5133	5338	21261	
Producer’s Accuracy (%)	96.11	66.70	93.55	73.92		
Overall classification accuracy = 82.94%						

Table 7-6. Error matrix for the classification result using 4-band (RGBI)

Classified class	Reference Data				Total	User’s Accuracy (%)
	Vegetation	Concrete	Brick	Asphalt		
Vegetation	5636	154	0	166	5956	94.63
Concrete	50	4423	187	378	5038	87.79
Brick	1	245	4916	0	5162	95.23
Asphalt	52	229	30	4794	5105	93.91
Total	5739	5051	5133	5338	21261	
Producer’s Accuracy (%)	98.21	87.57	95.77	89.81		
Overall classification accuracy = 92.98%						

A comparison of Table 7-4, Table 7-5, and Table 7-6 reveals that, from producer's accuracy, classification using RGBI produced the most accurate result for all classes, except the asphalt class. The asphalt class is most accurate in classification using the LiDAR intensity; however, the resulting rate is not much different from the RGBI (92.45% and 89.81%) rate. From user's accuracy, using RGBI produced the most accurate result for all classes. With this result, the final classifier model was generated using the entire training data set of RGBI and the selected parameters for SVM. This classifier model was employed to classify the images in the study area. Figure 7-12 shows examples of classification results where white areas represent "concrete" class and black areas are background.

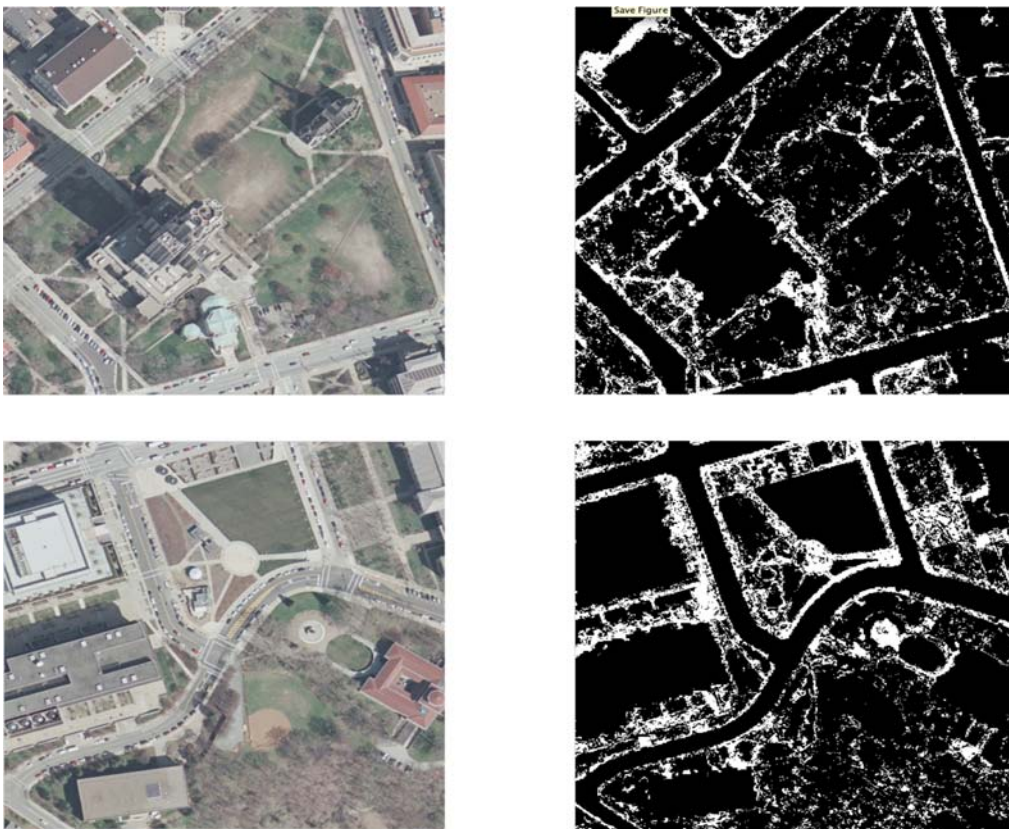


Figure 7-12. Examples of classified class "Concrete" represented by white areas

7.3 NETWORK CONSTRUCTION (IP ALGORITHMS)

As seen in Figure 7-2, the network construction based on image processing approach employs the generated classified raster image to construct pedestrian networks. Four main tasks of the network construction are explained as follows.

7.3.1 Object Filtering

Pedestrian networks often exist in urban areas and are surrounded by objects such as buildings, roads, parking lots, and vegetation areas and might be occluded by trees or shadows. The algorithm first attempts to eliminate those nearby features that are unlikely to represent pedestrian paths before extracting them. Since we focus only on outdoors, buildings, roads, and parking lots are three large potential features in an image that preclude pedestrian paths. The goal of object filtering is to filter building, road, and parking lot pixel out of an image and to produce a binary image containing candidate pedestrian path pixels. There are three separate tasks in this step: building detection, road detection, and parking lot detection. Building and parking lot pixels are detected and marked as obstacles, while road pixels are detected and used in crosswalk linking. Moreover, detected road pixels can alleviate the difficulty of pedestrian path extraction because roads and pedestrian paths have similar shape and intensity. The steps of the object filtering algorithm are illustrated in Figure 7-13.

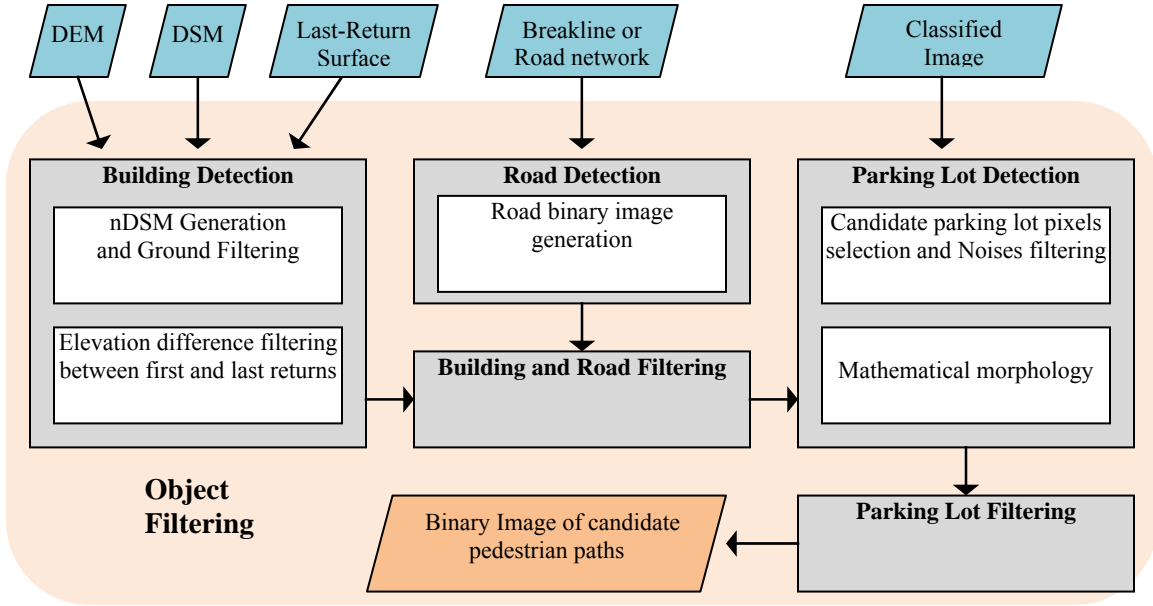


Figure 7-13. Steps of object filtering algorithm

Building detection employs DSM, DEM, and Last-return surface raster images generated from LiDAR point clouds. The ground filtering method (Morgan and Tempfli, 2000, Ekhtari et al., 2008, Meng et al., 2009) is used to separate ground and non-ground pixels. Non-ground pixels that do not represent buildings, such as trees, telephone poles, and vehicles, are removed by using the elevation difference filtering method. The ground filtering method starts by generating normalized DSM (nDSM), where each pixel contains height information aboveground. nDSM is the difference between DSM and DEM. Then the threshold value (σ) for maximum height is set in order to separate the aboveground and ground areas. This can be expressed as:

$$Aboveground(i, j) = \begin{cases} 1(aboveground_pixel), & \text{if } (nDSM \geq \sigma) \\ 0(ground_pixel), & \text{otherwise} \end{cases} \quad (7.1)$$

where $Aboveground(i, j)$ denotes the value for the binary map corresponding to the i^{th} and the j^{th} pixel coordinates.

The ground filtering method can detect most buildings but large size trees and other noises still remain and need further filtering. The most common characteristic used to remove trees from aboveground features is the elevation between the first and last LiDAR returns (Δh). The first return data contains elevations from the first or the only surfaces that the LIDAR pulse struck, whereas the last return contains elevations from the second or last surface that the LIDAR pulse struck. Therefore, Δh can indicate the likelihood of the existence of a penetrable object (e.g., trees) or a non-penetrable object (e.g., buildings). Theoretically, Δh for buildings should be 0 or a small value because laser lights do not penetrate hard (man-made) objects such as building roofs (Meng et al., 2009). On the other hand, a large Δh is a critical indicator of large sized trees. The aboveground features extracted as described above can be refined with the result of tree extraction and expressed as:

$$Building(i, j) = \begin{cases} 1(Building), & \text{if } (aboveground = 1) \text{ and } (tree = 0) \\ 0(Non - Building), & \text{otherwise} \end{cases} \quad (7.2)$$

where $Building(i,j)$ denotes the value for the binary map corresponding to the i^{th} and the j^{th} pixel coordinates.

The pixel is classified as a building feature when it is an aboveground feature and is not a tree feature. Building regions are derived after combining the extracted aboveground and tree features. However, the resultant building regions might still contain small features or holes caused by the ground filtering and the elevation difference filtering. The mathematical morphology operators of dilation and erosion are applied to fill in the holes and remove the small regions, respectively. Figure 7-14 shows the processes of building detection consisting of (a) nDSM, (b) aboveground binary image, (c) tree binary image, and (d) building binary image.

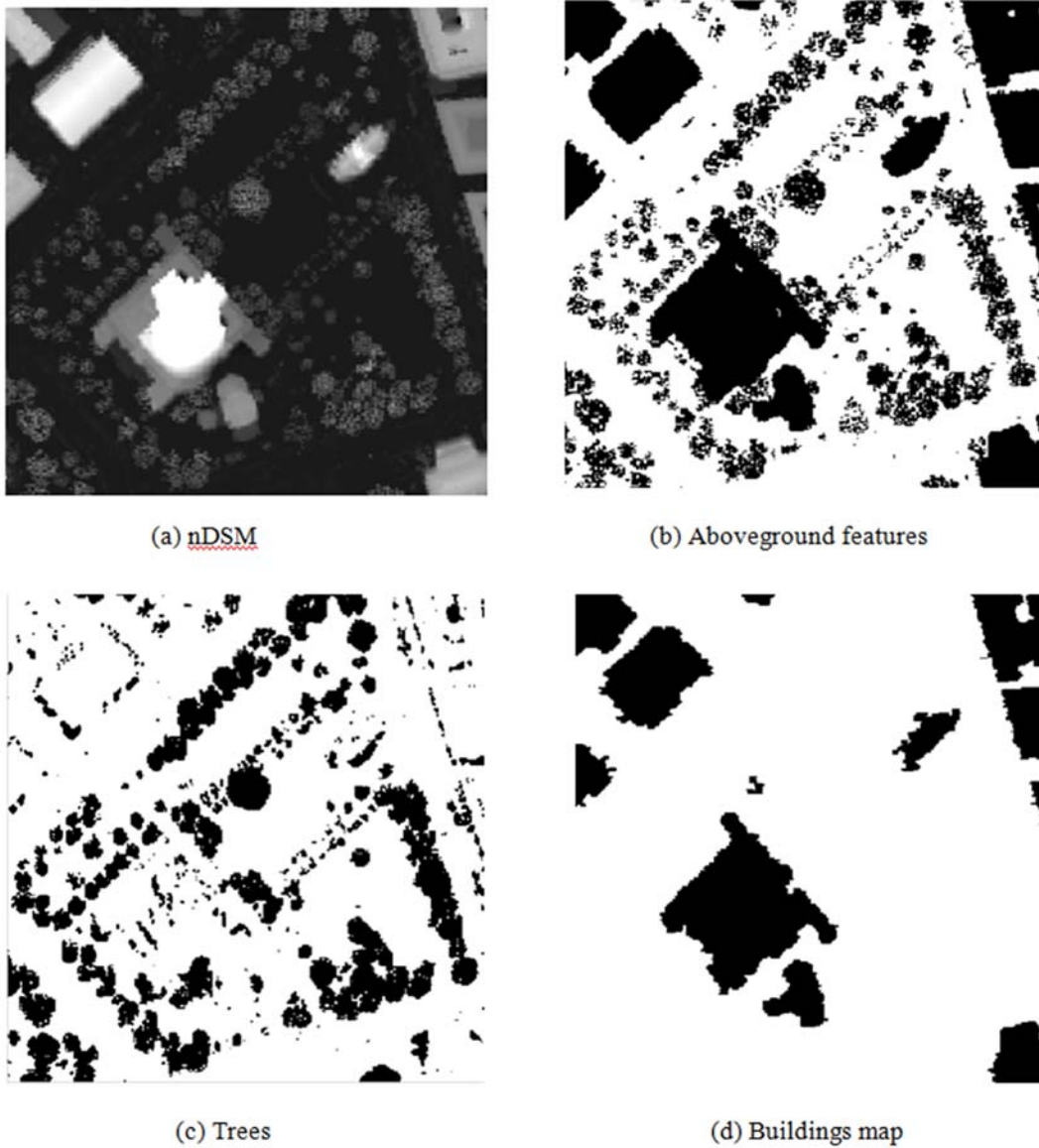


Figure 7-14. Example of building detection result

Road detection can be achieved by using either breakline data or road centerlines. Breaklines are contour enhancing lines that were collected photogrammetrically along both natural and man-made features, such as road edges, bridges, overpasses, shorelines of lakes/ponds/rivers, and railroads. Breaklines are usually one data product from LiDAR and are used in the creation of DEM and contour lines. Breaklines are 3D polylines with elevation values

and each breakline has attributes described with feature type such as paved roads, bridges, lakes and ponds. Breaklines of paved roads and unpaved roads are selected to generate the binary image of road area. The selected breaklines are used to generate the polygon when polyline objects are closed and then the non-polygon area is assigned as the road pixel in the binary image. If the breakline data is not available, another way to indicate the road area is to use the buffering method on existing road centerlines network. The buffer size can be approximated by using a road lane category and direction of travel, as employed in the network buffering approach. The binary image is generated from the road buffer polygon, where “1” represents a road area and “0” represents a non-road area. Figure 7-15 shows an example of (a) breakline and (b) road detection, where black color represents road pixels.

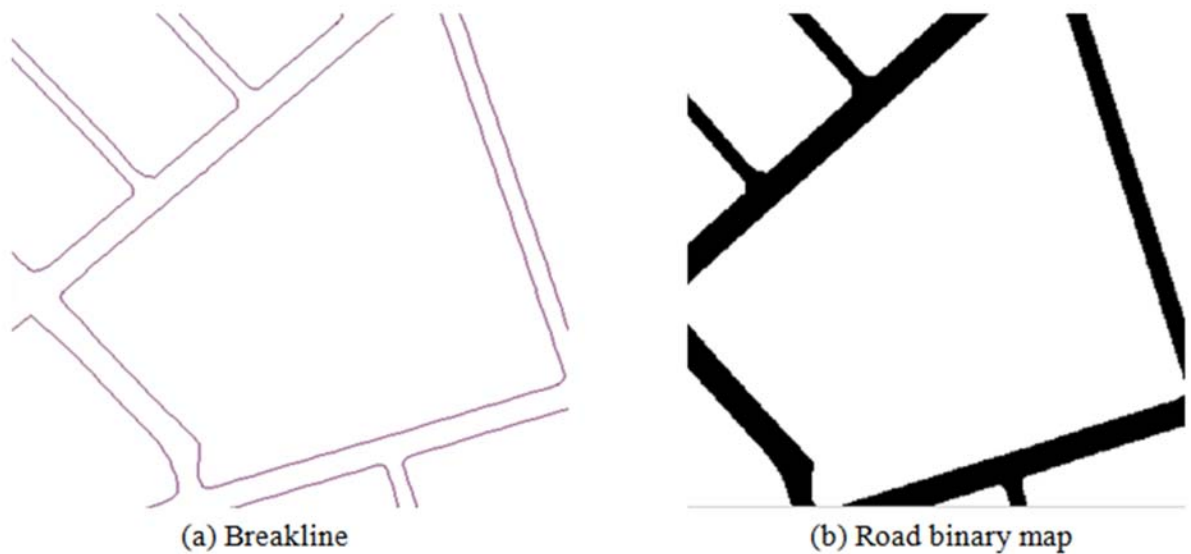


Figure 7-15. An example of road detection result

Once building and road are detected, their pixels are removed and a binary map of non-road ground level is generated, using Equation 7.3. Figure 7-16 shows the derivation of non-road ground level map, where white color represents road-building and black color represents non-road ground level pixels.

$$Non - road_ground_level(i, j) = \begin{cases} 1, & \text{if } (building = 0) \text{ and } (road = 0) \\ 0, & \text{otherwise} \end{cases} \quad (7.3)$$

where non-road ground level (i,j) denotes the value for the binary map corresponding to the i^{th} and the j^{th} pixel coordinates .

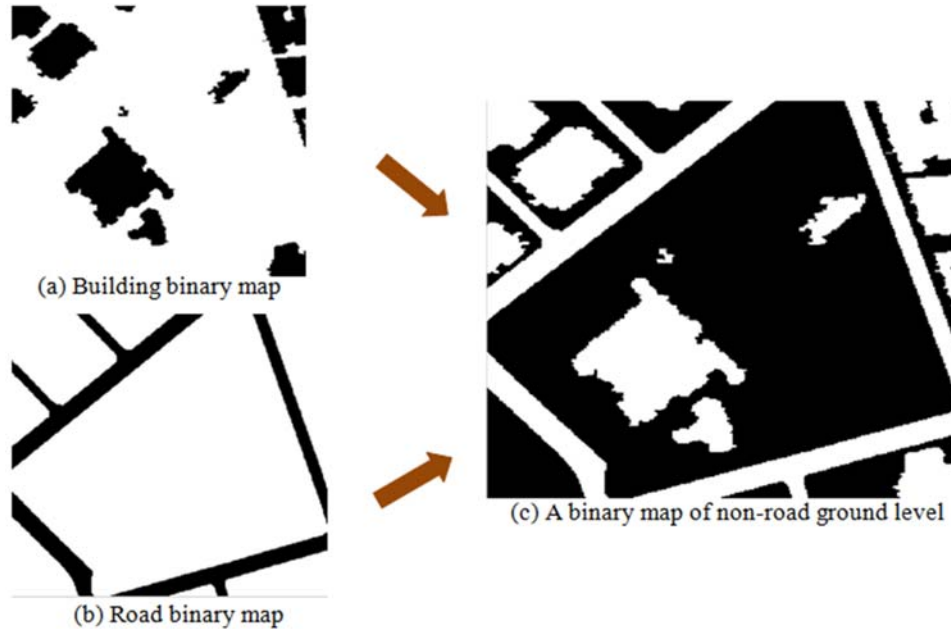


Figure 7-16. Building and road filtering

As mentioned earlier, parking lots are considered as obstacles in this dissertation. Parking lot detection and filtering are described as follows. Parking lot detection employs the classified image and the resultant binary image from building and road filtering processes to extract the pixels representing parking lots. Each pixel of the classified image, derived from pixel-based classification, contains a class label, which can be asphalt, concrete, brick, or vegetation. Detecting parking lots starts by choosing only pixels that are non-road ground level features and have class label of “asphalt”. The class label “asphalt” is selected because parking lots are commonly paved with an asphalt material. Next, the median filter (Lim, 1990), a non-linear operation, is applied to remove randomly occurring white and black pixels, also known as salt and pepper noise. After noise filtering, the mathematical morphological operations are employed

to analyze and distinguish the objects according to shape and size characteristics. The morphological operators of opening and closing are applied using a rectangular shaped structuring element. The opening operator removes small objects from an image while preserving the shape and size of larger objects. The closing operator fills in the region gaps and smoothes the outer edges. Finally, the regions with a minimum number of pixels representing a 2-space parking lot are kept. Figure 7-17b shows the example of candidate parking lot pixels and Figure 7-17c shows the result after noise removal and applying morphological operation. Figure 7-17d shows parking lots in the image.

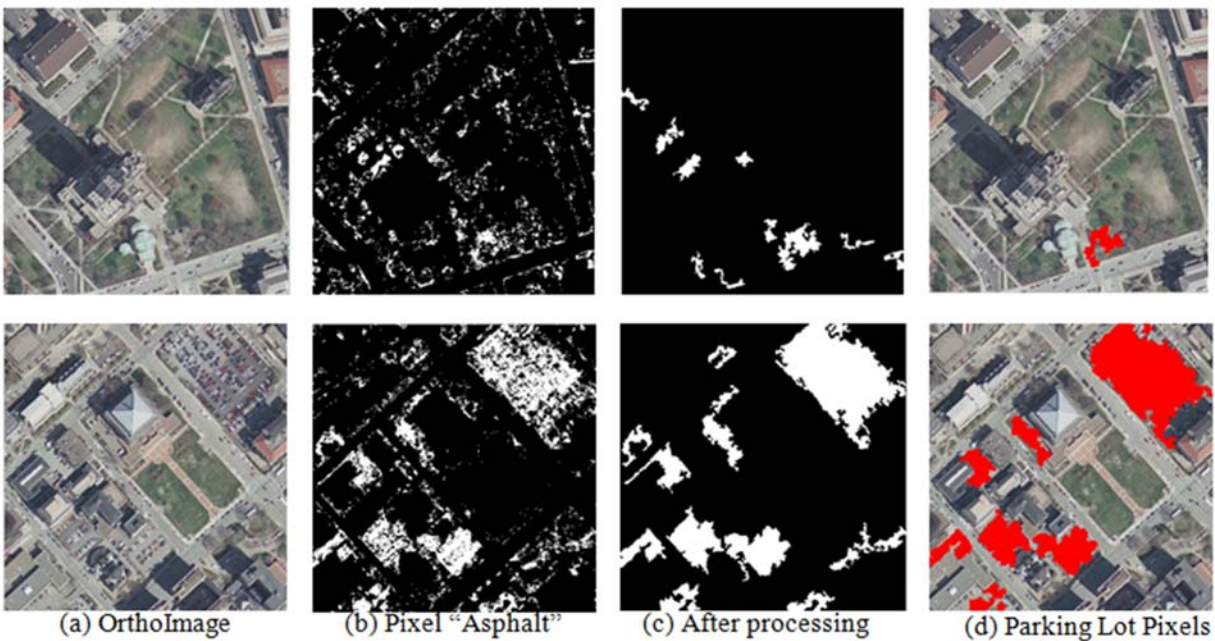


Figure 7-17. Parking lot detection

Once parking lot pixels are determined, the binary map of pedestrian path candidates is obtained from Equation 7.4.

$$pedestrian_path_candidate(i, j) = \begin{cases} 1, & \text{if } (building = 0) \text{ and } (road = 0) \text{ and } (parking = 0) \\ 0, & \text{otherwise} \end{cases} \quad (7.4)$$

where pedestrian path candidate (i,j) denotes the value for the binary map corresponding to the i^{th} and the j^{th} pixel coordinates.

7.3.2 Pedestrian Path Region Extraction

Image segmentation is the process of partitioning a given image into salient objects or regions (e.g., pedestrian path regions representing walking areas). There are three types of segmentation techniques: thresholding, edge-based, and region-based. Thresholding is a simple but effective technique used to separate objects from the image background when the intensity of pixels belonging to the object is substantially different from the intensity of the pixels belonging to the background. In edge-based segmentation, an edge detector is applied to the image to classify each pixel as edge or non-edge and form connected regions. This technique is suitable for images in which the pixel properties change abruptly between different regions. Region-based segmentation aims to find the regions directly by iteratively grouping neighboring pixels that have similar values and splitting groups of pixels, which are dissimilar in value. To segment pedestrian path regions, a hybrid method that combines edge-based and region-based methods was employed to achieve better segmentation because many regions (e.g., vegetation, concrete structure) in remotely-sensed images contain noises, which are not well separated. The pedestrian path region extraction algorithm starts with selecting seed points that are considered to be inside pedestrian path regions. From assigned seeds, regions are grown by merging the neighboring pixels that are likely to represent pedestrian paths under the condition that regions are not grown beyond their edges. Figure 7-18 highlights the algorithm's steps: (1) seed selection, (2) region growing, and (3) region refining. Two required inputs are the binary image representing the pedestrian path candidate map derived from the object filtering step and the pixel spectral information derived from the data fusion.

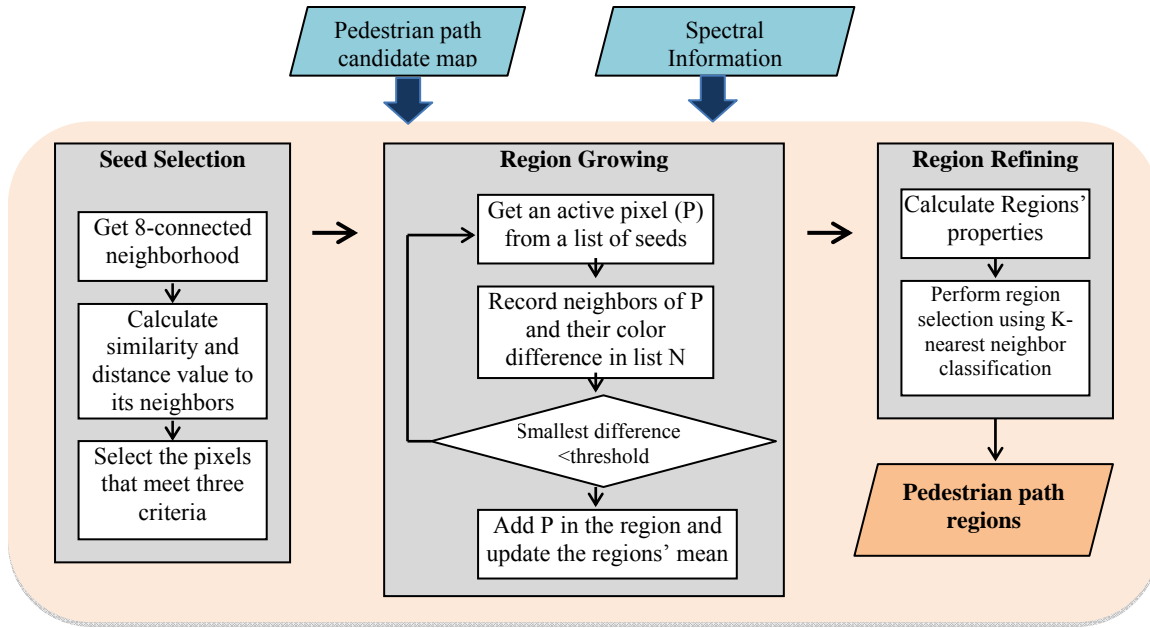


Figure 7-18. Flowchart of pedestrian path area extraction

The goal of the seed selection is to select initial growing pixels or seeds from the image. This step is very important because poorly selected initial pixels may result in incorrect segmentation of an image. In this algorithm, seeds must have: (1) class label (L) “concrete” or “brick”, (2) high color and intensity similarity (S) to neighbor pixels, and (3) low color and intensity difference (D) to neighbor pixels expressed as:

$$Seeds = \begin{cases} True, if (L = 'Concrete' or L = 'Brick') and (S \geq t_1) and (D \leq t_2) \\ False, otherwise \end{cases} \quad (7.5)$$

where t_1 is similarity threshold and t_2 is difference threshold.

The class label concrete and brick are specified since pedestrian path surfaces are most often made of concrete and brick. The second and third criteria are needed to verify that the seeds do not lie on the edge of a region. To calculate the similarity of a pixel to its neighbors, the formula by Frank and Cheng (2005) is applied and explained as follows. Considering eight-connected neighbors, the standard deviations of the 4-band spectral (R, G, B, I) of each pixel are calculated and then summed (Equation 7.6) to calculate the spectral deviation. This spectral

deviation is then normalized by dividing the maximum spectral deviation of all the pixels in the image (σ_{\max}) by the spectral deviation of each individual pixel as illustrated in Equation 7.7. Therefore, the normalized spectral deviation of each pixel falls in the range from 0 to 1. Finally, the similarity value of a pixel to its eight neighbors is derived by subtracting the normalized spectral deviation from 1 as shown in Equation 7.8.

$$\sigma = \sigma_R + \sigma_G + \sigma_B + \sigma_I \quad (7.6)$$

$$\sigma_N = \frac{\sigma}{\sigma_{\max}} \quad (7.7)$$

$$\text{Similarity} = 1 - \sigma_N \quad (7.8)$$

The Euclidean distance formula is used to determine the color and intensity difference of a pixel to its eight neighbors, as shown in Equation 7.9. For each pixel, the maximum difference of eight neighbors is used as the third criteria of seed selection.

$$d_i = \frac{\sqrt{(R - R_i)^2 + (G - G_i)^2 + (B - B_i)^2 + (I - I_i)^2}}{\sqrt{R^2 + G^2 + B^2 + I^2}}, i = 1, 2, \dots, 8 \quad (7.9)$$

Once suitable seeds are identified, the second step, region growing, is performed, in order to obtain homogeneous regions of pedestrian paths in the image. This step incorporates both spatial context and spectral information with the goal of selecting a group of adjacent pixels that have similar spectral information. The process starts by selecting an initial active pixel and comparing its spectral information to the eight neighboring pixels that are candidate pedestrian path pixels, are non-edge pixels, and are not yet allocated to the region. The edge pixels are extracted using the canny edge operator and are excluded from the growing process because they, by definition, indicate a border and not a continuation. The comparison of an active pixel and its neighbor pixels consists of first calculating the difference between its color and intensity value from the neighbors' color and intensity value. This calculated value is then ranked lowest

to highest, stored in list N, and is the basis for choosing the next active pixel. The next active pixel is chosen by looking at the lowest value in list N and comparing it to a predetermined threshold value. If the lowest value is below the threshold then it is added to the region. The process continues in a similar fashion where the pixels in list N are compared with the average color and intensity value determined from the pixels in the region. The region grows until no adjacent pixel is below the predetermined threshold value. When the growth of a region stops, another seed, which does not yet belong to any region, is chosen and the process starts again. This process continues until all pixels are assigned to a region.

The outcome from the region growing process might result in holes, spurious regions, or overgrowing as a result of various noises, non-optimal parameter settings, or inappropriate seed locations. To overcome these problems, the region refining process is applied. The refining process starts by calculating each region's properties including area, eccentricity, and spectral difference (in terms of RGBI). The spectral difference is the difference between a region and the sample pedestrian path region with shadow and no shadow. Area is the actual number of pixels in the region and the eccentricity is the fraction of the distance along the major axis' length at which the focus lies. The eccentricity value is between 0 and 1 where 0 represents a circle and 1 represents a line segment. The mean spectral (R,G,B,I) of each extracted region and sample pedestrian path region both with and without a shadow are computed. The spectral difference between each region and both samples are calculated using the Mahalanobis distance (De Maesschalck et al., 2000) as follows:

$$D(x, y) = \sqrt{(x - y)^T S^{-1} (x - y)} \quad (7.10)$$

Where $x = (\bar{R}, \bar{G}, \bar{B}, \bar{I})$ of a region

$y = (\bar{R}, \bar{G}, \bar{B}, \bar{I})$ of sample region

S is a covariance matrix

Once the properties of all extracted regions are calculated, they are then classified into one of two classes, pedestrian path and non-pedestrian path, based on properties and training samples. The training samples are manually chosen from a set of regions for which the correct classification is known and used to create a region refining model based on the k-Nearest Neighbor algorithm. According to the region refining model, each region is assigned to its closest class and only regions corresponding to the pedestrian path class are kept and used in the following step. Figure 7-19a shows the example results of seed selection, where red dots represent seeds. Figure 7-19b presents three examples of region growing, where white pixels represent the extracted regions. The final result of pedestrian path extraction is shown in blue in Figure 7-19c.

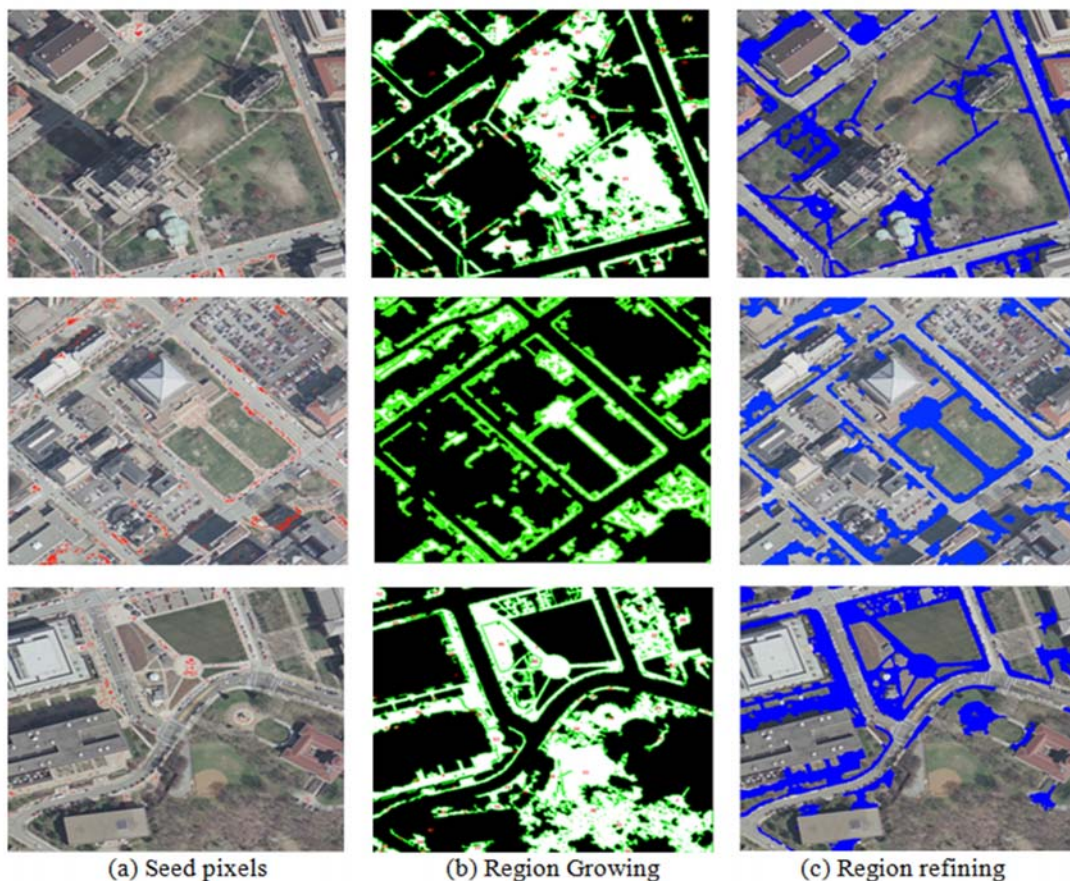


Figure 7-19. Examples of pedestrian path regions extraction

7.3.3 Pedestrian Network Construction

The pedestrian network is generally composed of pedestrian path centerlines and their connections. The pedestrian network construction algorithm first reduces the number of pixels from several (regions) to one (lines) and then closes the remaining gaps through edge linking. The crosswalks, which are one type of pedestrian path, are added in order to complete the pedestrian network.

The pedestrian path centerline extraction is the process of generating the centerline of the extracted pedestrian path regions. The mathematical morphology erosion operator and thinning algorithm are employed to extract centerlines. The erosion operator is used to shrink the pedestrian path regions and the thinning algorithm (Lam et al., 1992) is used to reduce the regions to lines of one pixel wide that approximate their centerlines and preserve the extent and connectivity of the original regions. The erosion operator is applied before the thinning algorithm because the thinning process distorts lines near the intersections and the extent of the distortion depends on the thickness of the regions (Chiang and Knoblock, 2010).

After the pedestrian path centerlines are obtained, there are situations where gaps in lines, caused by shadows or overlap objects in the images, still exist. To deal with this problem, we developed an algorithm to close the gaps by analyzing each end point and extending it to the best linking end points. The edge linking algorithm is illustrated in Figure 7-20.

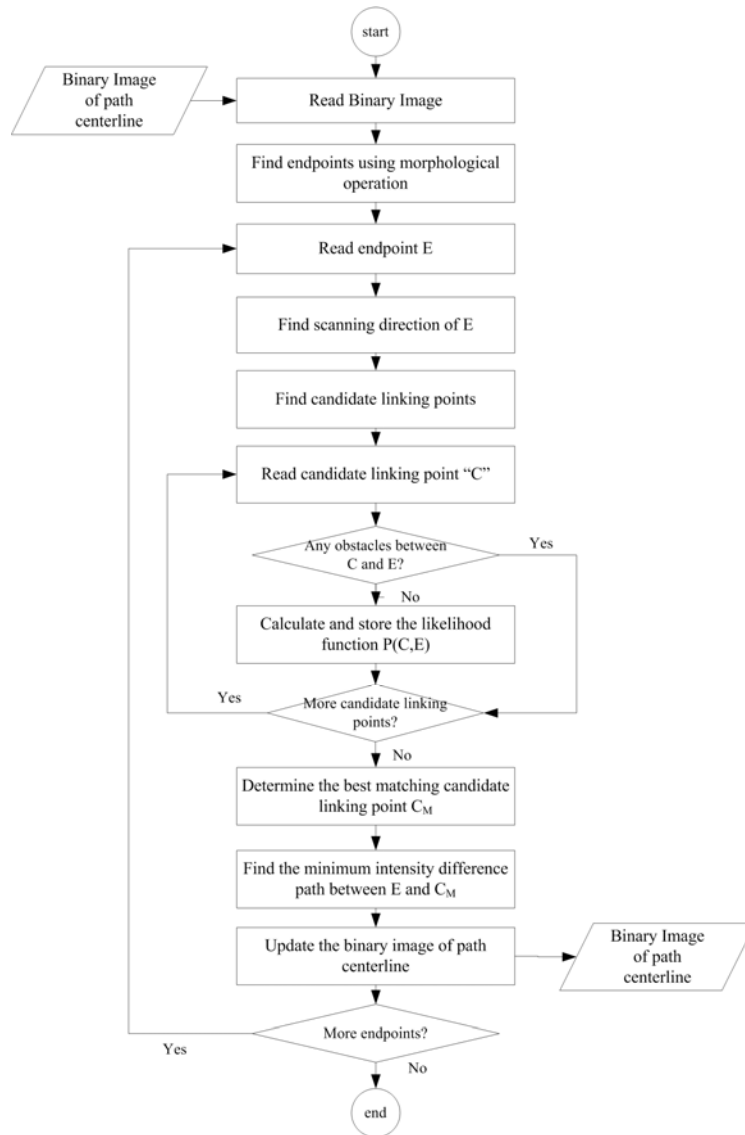


Figure 7-20. Algorithm to link the broken pedestrian path centerlines

The algorithm starts by extracting endpoints of the pedestrian path centerlines using a morphological operation. To efficiently close the gaps between end points, correct pairs for linking need to be identified. However, not every end point requires linking, such as end points close to buildings. To identify pairs of linking, the scanning direction and area for each end point by evaluating the linked pixels that generated it need to be determined. The edge direction template from CAEL (Ghita and Whelan, 2002) is applied in determining scanning direction and area. The scanning direction is identified by the majority of directions derived from last four

edge pixels. Examples of eight scanning directions and areas of an end point are illustrated in Figure 7-21.

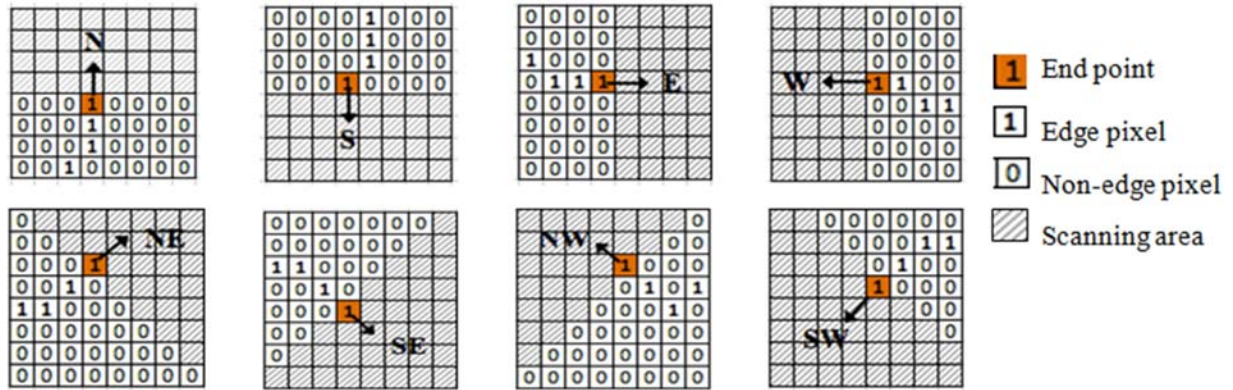


Figure 7-21. Scanning direction and area of an end point

Once the scanning direction is determined, all end points that are located within the scanning area and a maximum gap are considered as candidate linking points. If the list of candidate linking points is empty, it is interpreted that the end point does not require edge linking. In the next step, all candidate linking points are evaluated using the likelihood function (Wang and Zhang, 2008) of two parameters: Euclidean distance and angle between current end point and each candidate linking point:

$$P(C,E) = \frac{1}{|D(C,E) \times \theta(C,E)|} \quad (7.11)$$

where C and E are the current end point and the candidate linking point, respectively; $D(C,E)$ is the number of pixels on a straight line between C and E that is derived by employing the Bresenham algorithm (Bresenham, 1965). However, if the straight line between C and E passes through a building, a road, or a parking lot, C will be eliminated from the candidate list. $\theta(C,E)$ is the angle between C and E used to evaluate how well C matches the edge direction at E. The smaller the $\theta(C,E)$, the more likely the two directions will match. The candidate linking point with the largest $P(C,E)$ is chosen as the best matching point of E. An example of two

candidate linking points and the calculation of a likelihood function is shown in Figure 7-22. From the example, the candidate linking point “A” is chosen as the best match because of its highest likelihood value ($P(C,E)$).

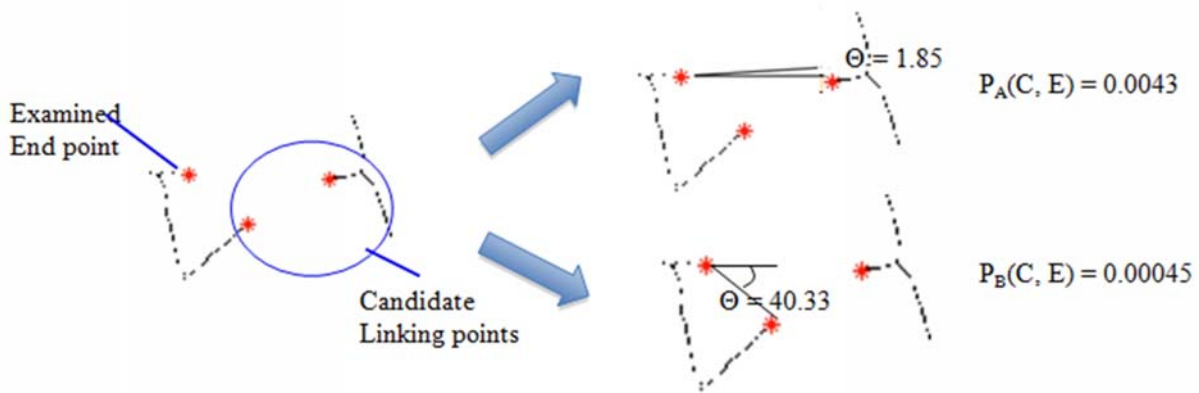


Figure 7-22. An example of candidate linking points and calculation likelihood function

Once pairs of linking end points are identified, the algorithm attempts to determine the missing edge segment between each pair of end points. Most existing edge linking methods use the smallest distance to link between end points but are not suitable for linking the missing pedestrian paths because a straight line path based on the smallest distance might contain pixels that are not pedestrian path types. For this reason, the intensity information is used in determining linking paths. Dijkstra’s algorithm was employed to determine the linking path that has the smallest intensity difference from the current pedestrian path pixels in the image. Four inputs required for Dijkstra’s algorithm are an adjacency matrix, non-negative weight, and two end points. The adjacency matrix represents which nodes of a directed graph are adjacent to each other, where node refers to a pixel in the raster image. Weight of each pixel is the intensity difference between the pixel and other pixels that belong to pedestrian paths in the image. The intensity difference is calculated by using the Mahalanobis distance (Equation 7.10). Two examples of linking paths between two end points using the minimum intensity difference (intensity) and using the minimum distance (distance) are shown in Figure 7-23. As seen in the

figure, the linking paths obtained from using the intensity information covers more pedestrian path pixels than those using the minimum distance do.

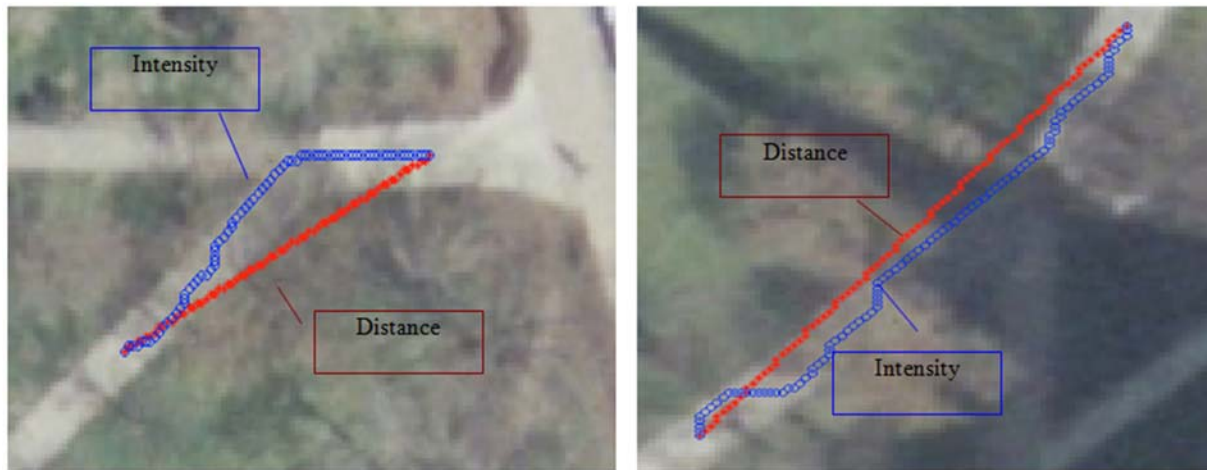


Figure 7-23. Two examples of linking paths between two end points

The last task of pedestrian network construction is crosswalk linking. Crosswalk is a designated point on a road that aims to increase pedestrian safety. In remotely-sensed images, a crosswalk appears as a road marking consisting of several parallel lines in white or yellow on a road. Since the color of road area and crosswalk marking are quite different, it is feasible to extract high-brightness pixels from the road area using the thresholding method. However, some crosswalk markings in remotely-sensed images are not clear because of old pavements, obstruction by vehicles, shadows or trees. Additionally, some crosswalks are unmarked. As a result, we do not extract crosswalk pavement markings from imagery, instead, we add crosswalk links to existing paths at all road intersections, based on the assumption that crosswalks are usually located at every road intersection. The algorithm of crosswalk linking is shown in Figure 7-24.

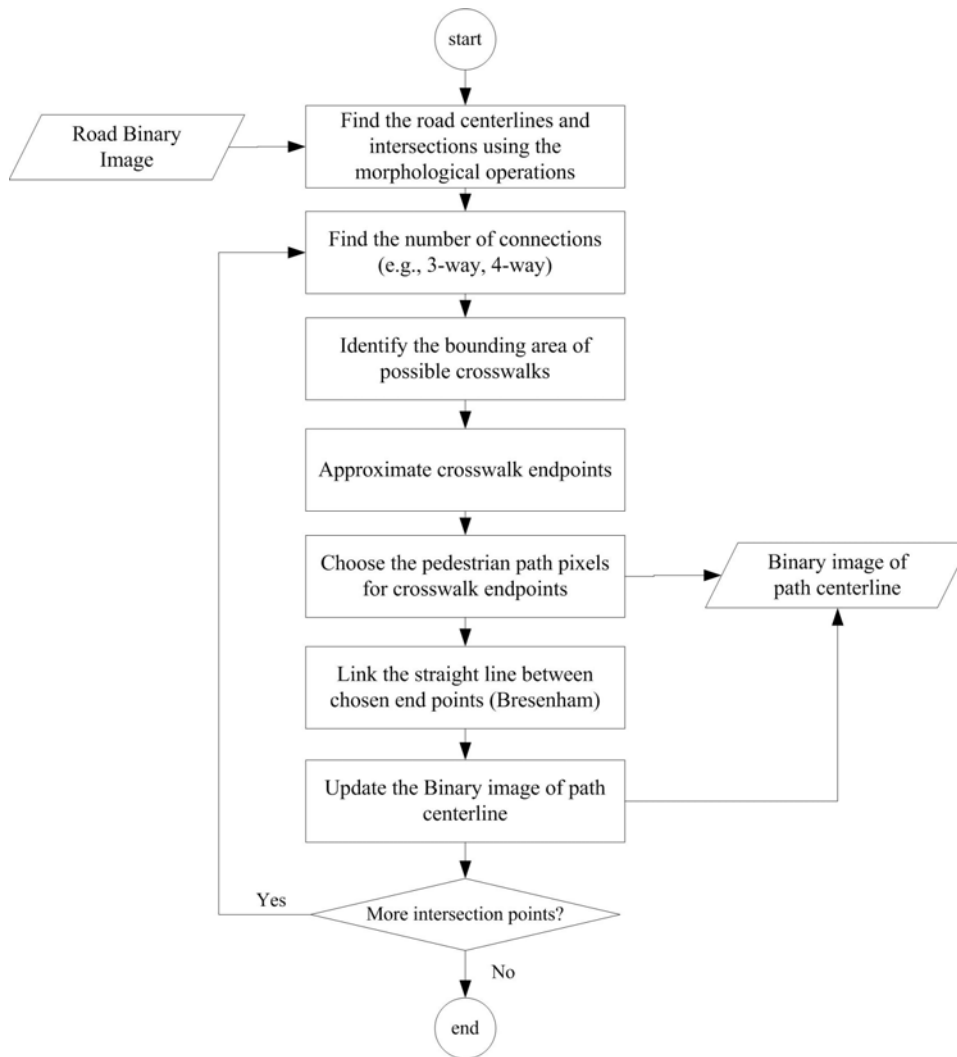
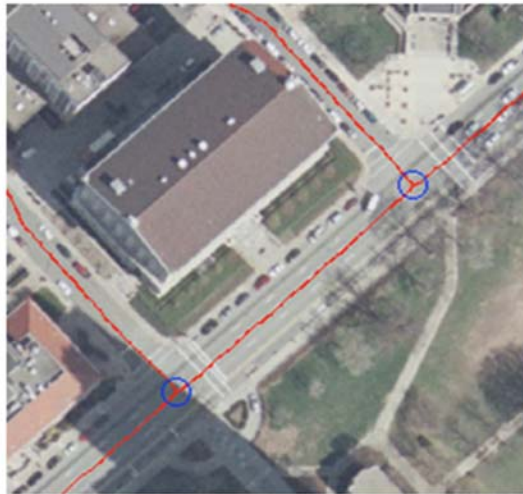


Figure 7-24. Algorithm for crosswalk linking

The crosswalk linking algorithm starts by finding road centerlines and intersections from the road binary image using the mathematical morphology operations. Figure 7-25a shows an example of road centerlines and intersections. At each intersection, we find the number of connections, which are used as the number of crosswalk links (e.g., 3-way intersection determines 3 crosswalk links) and determine the approximate crosswalk endpoints, as shown in Figure 7-25b. The pedestrian path pixels closest to the approximate crosswalk endpoints are selected and used to generate the crosswalk links, as shown in Figure 7-25c and Figure 7-25d.



(a) Road centerlines and intersections



(b) Boundaries of crosswalks and approximated linking points



(c) Pedestrian path pixels in the boundary of crosswalk



(d) Linking path at the crosswalk

Figure 7-25. An example of crosswalk linking

Figure 7-26a shows the pedestrian path centerlines and the endpoints represented by red dots. Once the endpoints are determined, the edge-linking algorithm identifies the missing links between end points. Figure 7-26b shows an example of edge linking. The last task, crosswalk linking, added the crosswalk segments at every intersection of road segments. Figure 7-26c shows the final result of a pedestrian network overlaid on the image.

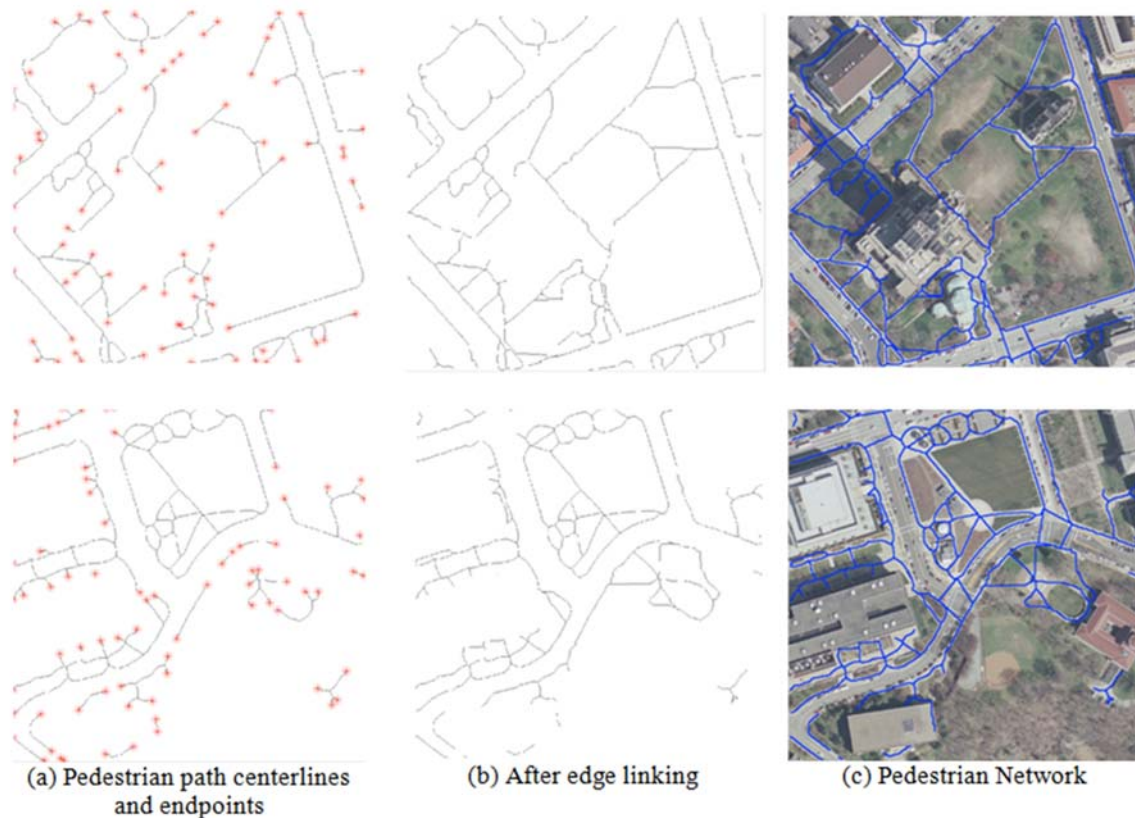


Figure 7-26. Three steps of pedestrian network construction

7.3.4 Raster-To-Vector Conversion

The extracted pedestrian networks are in raster format with all edge pixels stored in the order of screen coordinates. To support navigation systems/services or other GIS applications, the geographic data in vector format is often required. Two processes, vectorization and georeferencing, are performed on the binary raster images, obtained from the previous step. Vectorization is the process of transferring pixels into line vector data and georeferencing is the process of transforming screen coordinates into geographic coordinates.

For vectorization, all pedestrian path pixels must be organized according to the edge they belong to through edge tracing. The steps of edge tracing are described in Figure 7-27.

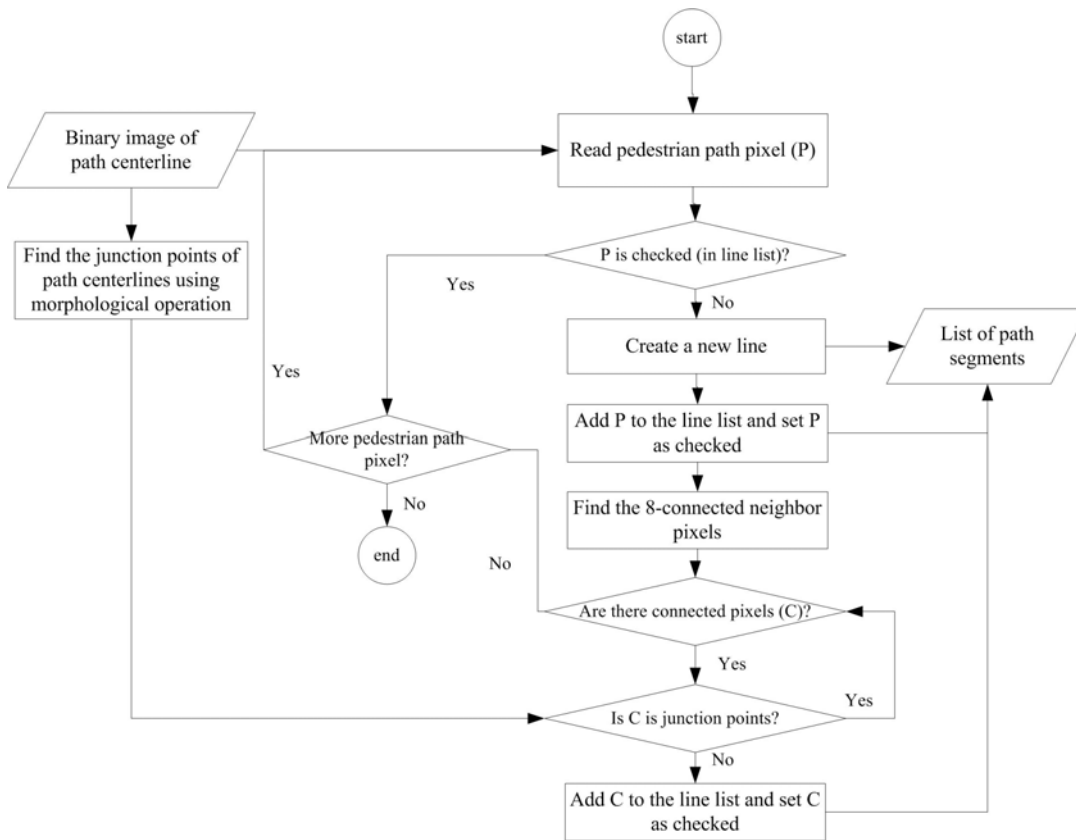


Figure 7-27. Algorithm for edge tracing

After edge tracing, a set of lines containing edge pixels is derived and is used to generate line vector data. The geometry of a line is represented by at least two end points. Other than two end points, the shape points are added to represent the curved line geometry. For this reason, we choose only the necessary edge pixels to represent the geometry of each line by employing the corner detector based on chord-to-point distance accumulation (Awrangjeb and Lu, 2008). Figure 7-28 shows examples of selected edge pixels (green circles) to represent line geometry.

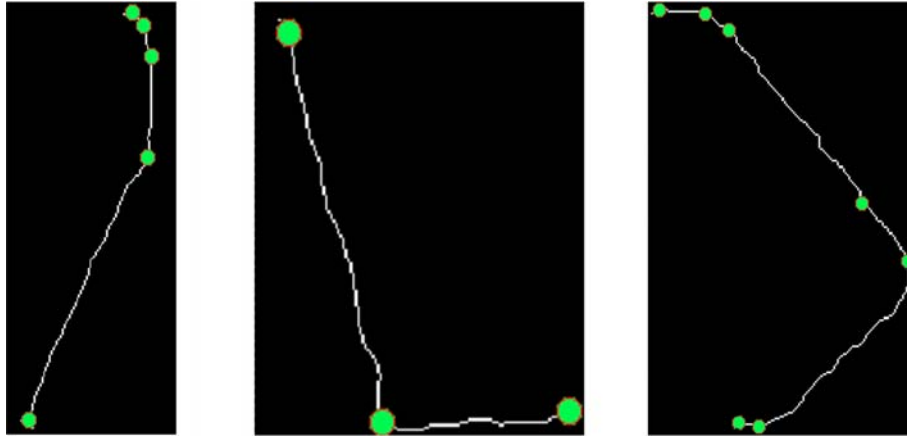


Figure 7-28. Examples of selected edge pixels to represent the geometries of lines

The final task of pedestrian network extraction technique is georeferencing that adds location information (i.e., geographic coordinates) to the extracted pedestrian networks. A spatial referencing matrix that ties the row and column of an image space to coordinate space is created and is used to transform screen coordinates to geographic coordinates, as shown in Figure 7-29.

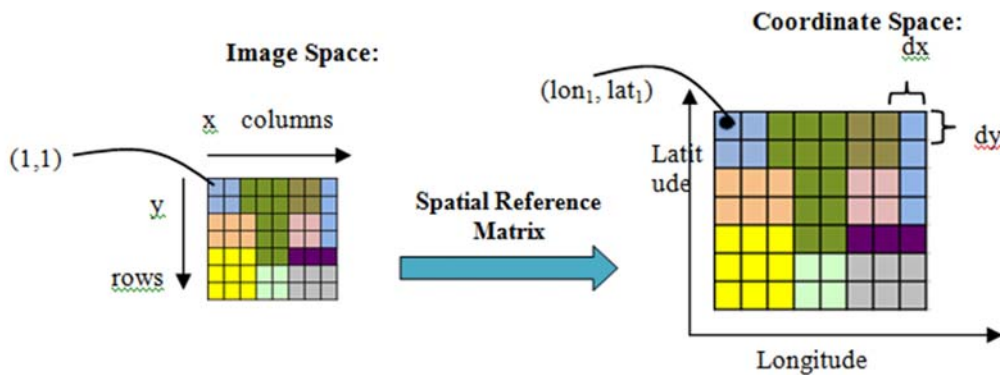


Figure 7-29. Georeferencing image space to coordinate space

The parameters needed to create a spatial referencing matrix are lon_1 , lat_1 , dx , and dy , where lon_1 and lat_1 specify location of the center of the first pixel (1,1) in the image; dx is the difference in longitude between pixels in successive columns; and dy is the difference in latitude between pixels in successive rows. After obtaining all the parameters, the map coordinates (longitude, latitude) of related pixels with screen coordinates (col, row) can be calculated as:

$$[col, row] \longrightarrow [lon_1 + (col - 1) \times dx, lat_1 + (row - 1) \times dy] \quad (7.12)$$

8.0 EVALUATION

This chapter describes the evaluation of the pedestrian network construction based on the three different approaches, network buffering, collaborative mapping, and image processing. In Section 8.1, the evaluation methodology is provided. Section 8.2 details the pedestrian network baseline and the study area for the evaluation. Sections 8.3, 8.4, and 8.5 details the experiment settings and the evaluation results obtained from the three approaches.

8.1 EVALUATION METHODOLOGY

This section describes the evaluation of the constructed pedestrian networks by the network buffering, collaborative mapping, and image processing approaches. The method proposed by Wiedemann (2003) for evaluating automatic road extraction by image processing approach, is adapted for evaluating the constructed pedestrian networks. The method compares the results from each of three approaches with a pedestrian network baseline. The pedestrian network baseline (ground truth) is a high-quality network of pedestrian path segments in an area. Details of creating the baseline are described in Section 8.2.

The evaluation method consists of two steps: (1) comparing the pedestrian network baseline with the constructed pedestrian network through a pedestrian segment matching process and (2) calculating quality measures of evaluation criteria (described in Table 2-4). The purpose

of the first step is to ensure that the generated paths are correct and provide measurement data for the second step. The purpose of the second step is to analyze the matched results in the first step to determine the quality of the generated paths.

The first step, matching, has two similar tasks. The first task begins by using a polygon buffer of a predefined width around the pedestrian network baseline. We have used a buffer width of 1.83 m as it is the recommended minimum width for a sidewalk or walkway according to ITE (Center, 2009). Then, the generated pedestrian path segments are individually compared with the baseline network buffer where the length of each segment that falls within the buffer is recorded. Those generated pedestrian path segments within the buffer are considered as “matched” (True Positive: TP), and those outside the buffer are considered as “unmatched” (False Positive: FP), as shown in Figure 8-1(a). The length of matched generated segments is calculated. Once the first task is complete, the buffering and matching tasks are repeated, only this time the buffer is produced around the generated pedestrian path segments and the pedestrian network baseline are compared with this buffer. The unmatched reference data are denoted as false negative (FN), as depicted in Figure 8-1(b). The length of matched reference segments is calculated from the second task.

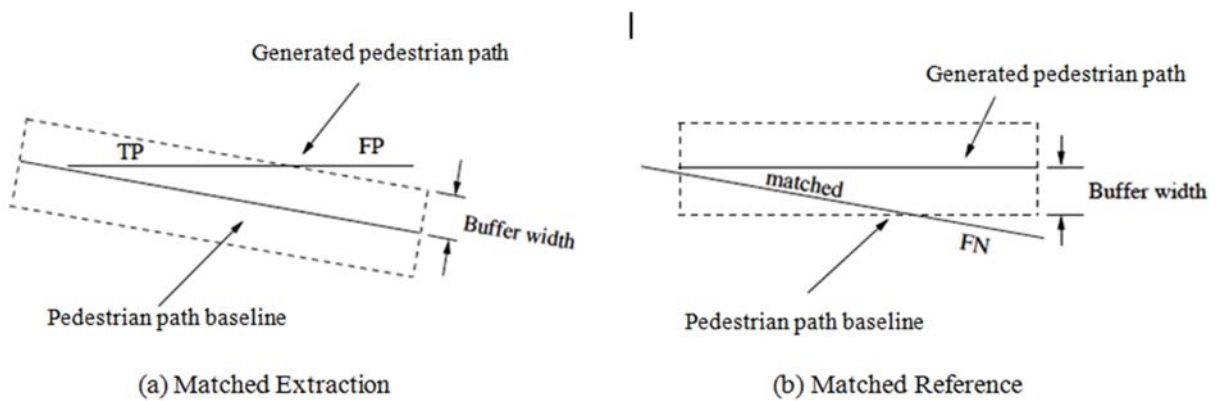


Figure 8-1. Matching principle (adapted from Wiedemann (2003))

Once the matching task is complete, the next step is to calculate quality measures in order to validate the performance of the three approaches. Table 8-1 shows the definition and formula for the evaluation criteria (Wiedemann, 2003).

Table 8-1. Definition and formula for evaluation criteria

Criteria	Formula	Range value	Optimum value
Geometrical completeness: the degree to which pedestrian path features describing the actual pedestrian paths are included in the extracted dataset	$\frac{\text{length_of_match_reference}}{\text{length_of_reference}}$	[0;1]	1
Geometrical correctness: the percentage of the generated pedestrian paths (extraction), which is in accordance with the baseline	$\frac{\text{length_of_matched_extraction}}{\text{length_of_extraction}}$	[0;1]	1
Topological completeness: the presence or absence of connection nodes in a dataset	$\frac{CB^{ref}}{CR}$	[0;1]	1
Topological correctness: the degree to which extracted features represent correct connections	$\frac{CB^{gen}}{CG}$	[0;1]	1

Explanations of the variables in Table 8-1 are as follows. Length of reference refers to the total length of related segments in the reference network, and length of matched reference refers to the total length of matched segments in the reference network. Length of extraction refers to the total length of the generated segments and length of matched extraction refers to the total length of generated segments that are matched with the reference segments. CR is the number of connection points in the reference network and CB^{ref} is the number of points connected in both networks. CG is the number of connection points in the generated network and CB^{gen} is the number of points connected in both networks.

8.2 PEDESTRIAN NETWORK BASELINE AND THE STUDY AREA

The pedestrian network baseline (ground truth) is a high-quality geographic data representing the network of pedestrian path segments in a given area. It will be used as a reference for validating the pedestrian networks generated by the developed algorithms. Since the pedestrian network baseline is not publicly available, conventional methods such as field survey and manual digitization were employed for its generation. A field survey involves collection and preparation of information for a given area and is carried out through field observation and personal familiarity (Shekhar, 2008). Digitization generally refers to a method of manually converting information from analogously produced graphic maps to machine readable vector formats. Although conventional methods require a large amount of manpower and cost, they are able to extract objects of interest with the highest geometrical and topological accuracy. High-resolution imagery, surveyed GPS points, and GIS tools were used to generate a pedestrian network baseline. A 0.6 m resolution natural color orthoimage covering the city of Pittsburgh, Pennsylvania, obtained from the PA DCNR (Department of Conservation and Natural Resources) and U.S. Geological Survey was employed as a backdrop and combined with the field survey. The field survey was performed in the study area using both paper maps and Trimble's GeoExplorere®3 handheld GPS units to verify the collected path features and record building entrances. Editing tools in ArcGIS 10 were used to manually create and edit geometry and topology of the pedestrian network baseline. To measure the accuracy of the baseline, sample ground truth positions (i.e., junctions) in the study area were collected by using Trimble's GeoExplorer®3 handheld GPS units. Data for each ground truth position was collected for five minutes and the positional accuracy of the collected GPS points were improved by taking the Differential GPS (D-GPS) approach and using the Continuously Operating Reference Station

(CORS) data in a post-processing mode. The base station used for performing the differential correction is located at the University of Pittsburgh with 997.79 m as the approximate distance between the base station and the study area. A sample of 30 ground truth positions was collected and the difference between D-GPS points and the digitized points is on average 1.59 m with standard deviation of 0.76 m. Figure 8-2 shows the pedestrian network baseline collected and generated and Table 8-2 describes its characteristics.

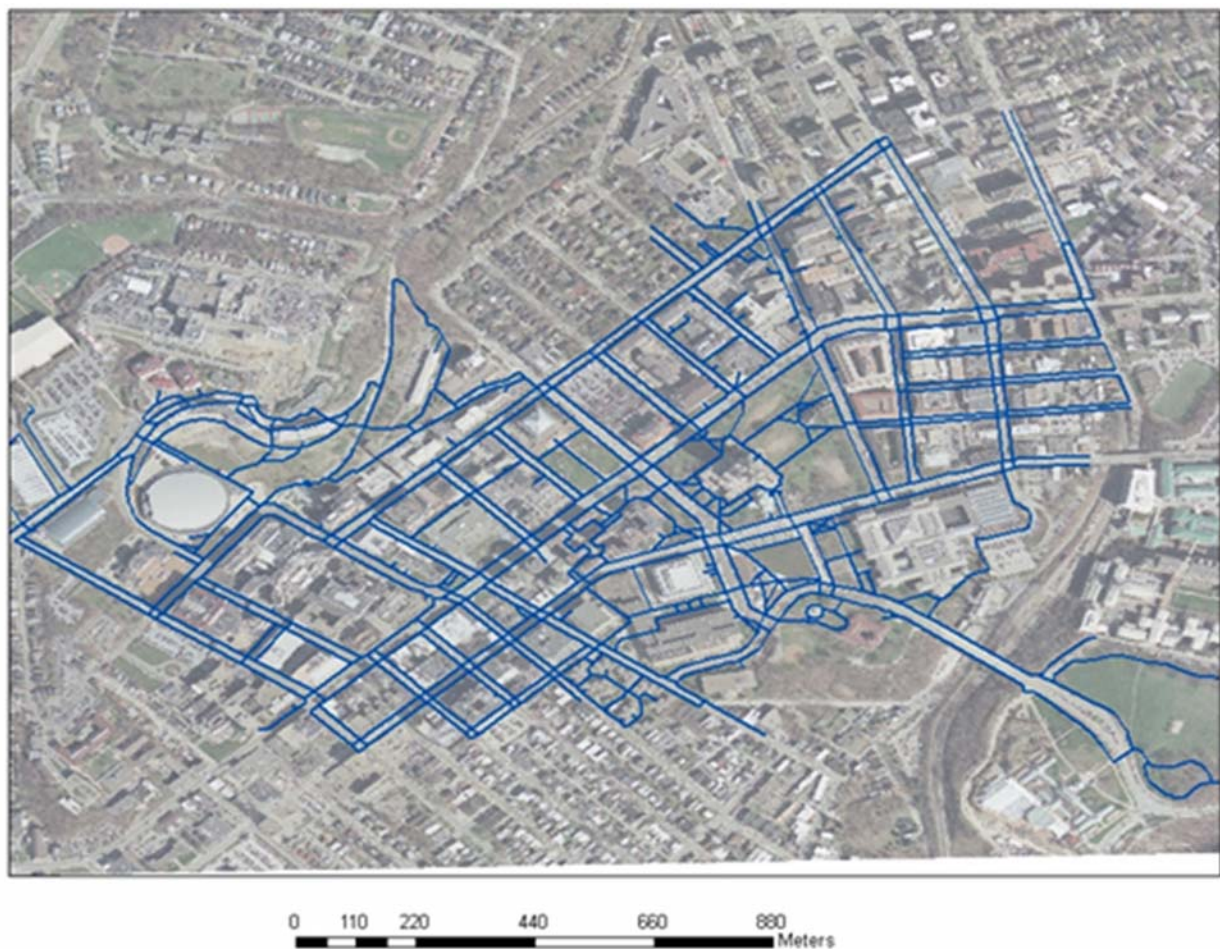


Figure 8-2. The pedestrian network baseline generated by field survey and manual digitization

Table 8-2. The characteristics of pedestrian network baseline

Characteristics	Description		
Area	University of Pittsburgh's main campus Area size: 2,280,000 m ²		
Number of segments	904		
Total pedestrian path length	38468.30 meters		
Scale	1:2400		
Pedestrian path types	# Segments	Total length (m)	Percentage (%)
Sidewalk	398	25158.90	65.40
Crosswalk	198	3241.75	8.43
Building Entrance	83	1150.33	2.99
Footpath	212	8032.17	20.88
Trail	5	846.52	2.20
Pedestrian bridge	2	38.55	0.10
Spatial Reference Information			
Geographic coordinate system	GCS_North_American_1983		
Datum	D_North_American_1983		

The study area is located within the main campus of the University of Pittsburgh, which has a mixture of environment settings, i.e., open sky, moderate or partially blocked, and blocked. Blocked area refers to the area surrounded with high-rise buildings and moderate area refers to the area with mix environment settings of open sky and blocked. The study area is divided into ten tiles each covering approximately 305 m x 305 m on the ground, as illustrated in Figure 8-3. The pedestrian network baseline was also divided into 10 tiles. The environment setting and percentage of pedestrian path types of baseline in each tile are described in Table 8-3. The ten tiles were set up for three experiments with network buffering, collaborative mapping, and image processing approaches.



Figure 8-3. Ten tiles in the study area

Table 8-3. Environment settings and characteristic of 10 tiles

Tile No.	Environment setting	Percentage of pedestrian path types			
		Sidewalk	Crosswalk	Entrance	Footpath
1	Blocked	79.22	12.80	2.45	5.52
2	Blocked	61.94	10.91	2.31	24.85
3	Open Sky	43.41	9.50	3.12	43.97
4	Open Sky	65.69	3.83	2.17	28.31
5	Blocked	51.81	6.38	1.33	40.48
6	Moderate	68.69	7.49	2.41	21.24
7	Open Sky	46.60	4.32	3.46	45.61
8	Blocked	84.18	11.93	0.25	3.63
9	Moderate	73.99	5.16	10.82	10.02
10	Moderate	87.62	12.02	0.36	0

8.3 EVALUATION OF THE NETWORK BUFFERING APPROACH

The data source and parameters used in the network buffering experimentation are explained in Table 8-4.

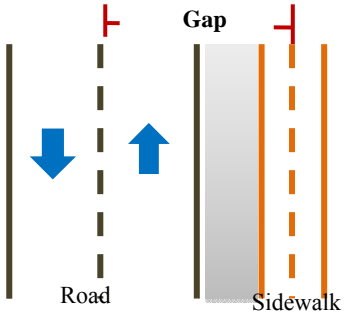
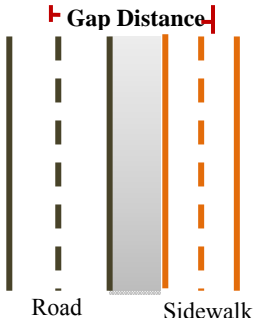
Table 8-4. Parameters for the experimentation (Network buffering)

Data source (Input)	NAVSTREETS
Data preparation	Use road attribute “SPEED_CAT” for road filtering
Network construction	Use road attribute “LANE_CAT” and “DIR_TRAVEL” for estimating gap distance between road and sidewalks (see Table 8-5)
Output	The pedestrian network containing sidewalk and crosswalk features in vector format

NAVSTREETS road networks were employed for the experimentation because they are free for academic research and development, and the data are of high quality. NAVTEQ road networks contain many road attributes describing road characteristics. For the data preparation step, “SPEED_CAT” was used to filter out road segments that were unlikely to have adjacent parallel sidewalks. “SPEED_CAT” classifies road segments based on speed limit. There are 8 speed limit categories where categories 5-8 correspond to a maximum speed of 64 km/h or less and categories 1-4 correspond to a maximum speed of greater than 64 km/h. In this experiment, only roads in the last 4 categories, 5-8, were used for filtering. This is because roads with a speed limit of less than 64 km/h have a high probability of having adjacent sidewalks. To calculate the geometries of sidewalk features, one parameter is gap distance, which was approximated by using road attribute “LANE_CAT” and “DIR_TRAVEL”. Road lane category is determined by number of lanes (“LANE_CAT”) in each direction and direction of travel (“DIR_TRAVEL”) identifies legal travel directions of a road segment (i.e., one-way or two-way). Based on the

standard for minimum road width and sidewalk width, the gap distance along each side of road centerlines was estimated by summation of road width, shoulder width, and sidewalk width for each lane category and direction of travel of a road segment. Examples of gap distance for both one-way and two-way directions are given in Table 8-5.

Table 8-5. Example of gap distance for each direction of travel and number of lanes

Direction of Travel	Figure	Gap distance
Two-way Direction		One lane: Buffer size = $4.267 + 3.048 + (1.829/2) = 8.23$ m.
		Two lanes: Buffer size = $(4.267*2) + 3.048 + (1.829/2) = 12.50$ m.
		Three lanes: Buffer size = $(4.267*3) + 3.048 + (1.829/2) = 16.76$ m.
One-way Direction		One lane: Buffer size = $(4.267/2) + 3.048 + (1.829/2) = 6.1$ m.
		Two lanes: Buffer size = $(4.267*2)/2 + 3.048 + (1.829/2) = 8.23$ m.
		Three lanes: Buffer size = $(4.267*3)/2 + 3.048 + (1.829/2) = 10.36$ m.

It is true that the measurements on real roads and sidewalks may not follow the theoretical values suggested by statutory authorities. In practice, high-resolution satellite images provided by Google Earth and its measurement tools can be used to measure the real road and sidewalk conditions, instead of field test. Thirty samples of two-way roads with one lane for each direction (group 1) and thirty samples of one-way roads with one lane (group 2) were randomly selected and the gap distances between the road centerlines and the sidewalk centerlines were measured. Average and standard deviation of gap distance of group 1 are 7.50 m and 1m, respectively. For group 2, average gap distance is 5.72 m and standard deviation is 0.8 m. Comparing with the

estimated gap distance presented in Table 8-5, the gap difference between the estimated value suggested by authorities and the actual value for group 1 is 0.73 m and for group 2 is 0.38 m, which is a small difference. Since there is no information on real road and sidewalk condition, using the theoretical values as an estimate of the actual value is reasonable.

To implement the algorithm, GeoTools 2.7-M1, an open source Java library that provides a standard source of methods for manipulation of geospatial data (GeoTools, 2009), was used to work with shapefiles, create geometries, perform geometric operations, and manage spatial data. NAVSTREETS road network was divided into ten tiles similar to the study area. Two examples of constructed pedestrian networks through the network buffering approach are shown in Figure 8-4. Blue lines represent road segments and red lines represent sidewalk and crosswalk segments.

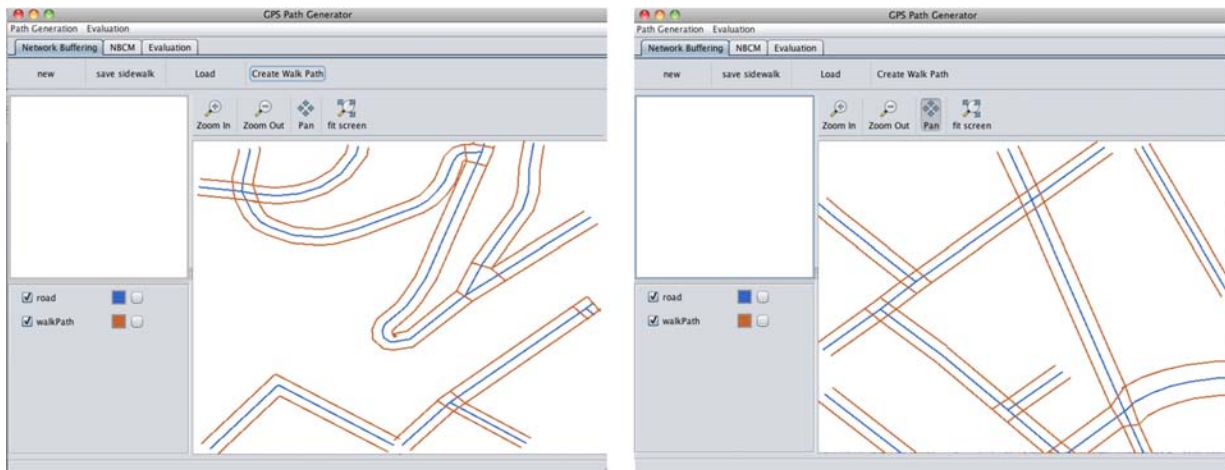


Figure 8-4. Examples of constructed pedestrian networks based on the network buffering approach

To evaluate the performance of the algorithm, a buffer polygon around the pedestrian network baseline was first created and then the matching process between the baseline network segments and the generated path segments was carried out. In the second step of the evaluation, four quality measurements (Table 8-1) were calculated. Figure 8-5 shows an example of

evaluation result. Table 8-6 show the statistics of evaluation results and Table 8-7 shows the results based on environment settings.

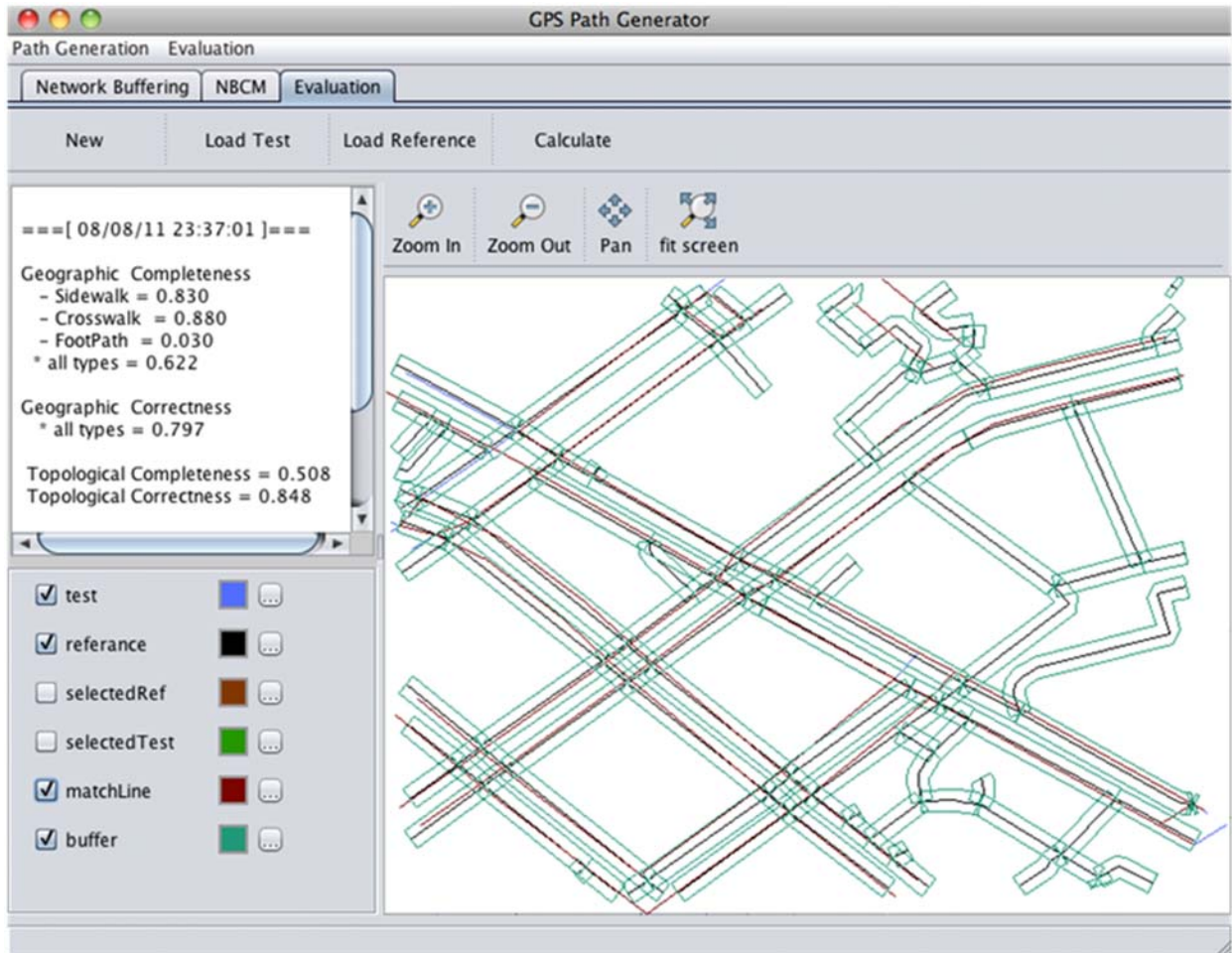


Figure 8-5. Evaluation result of constructed pedestrian network (using network buffering)

Table 8-6. Statistics results of network buffering approach

Tile Number	Path Type	Geometrical Completeness (%)	Geometrical Correctness (%)	Topological Completeness (%)	Topological Correctness (%)
Tile 1	Sidewalk	69.2	49.3	69.3	58.9
	Crosswalk	76.3			
Tile 2	Sidewalk	83.0	79.7	50.8	84.8
	Crosswalk	88.0			
Tile 3	Sidewalk	73.1	72.3	18.4	74.8
	Crosswalk	65.2			
Tile 4	Sidewalk	61.7	56.3	42.4	59.2
	Crosswalk	65.3			
Tile 5	Sidewalk	69.3	45.2	28.4	57.8
	Crosswalk	69.9			

Tile Number	Path Type	Geometrical Completeness (%)	Geometrical Correctness (%)	Topological Completeness (%)	Topological Correctness (%)
Tile 6	Sidewalk	80.0	77.2	39.4	75.2
	Crosswalk	71.3			
Tile 7	Sidewalk	74.0	72.1	21.4	77.9
	Crosswalk	68.1			
Tile 8	Sidewalk	76.2	89.0	63.1	59.2
	Crosswalk	75.0			
Tile 9	Sidewalk	70.2	77.1	35.3	62
	Crosswalk	98.6			
Tile 10	Sidewalk	66.2	69.0	71.3	65.4
	Crosswalk	68.3			
Average	Sidewalk	72.29	68.72	43.98	67.52
	Crosswalk	74.6			

Table 8-7. Statistic results of network buffering approach (Environment setting)

Environment Settings	Path Type	Geometrical Completeness (%)	Geometrical Correctness (%)	Topological Completeness (%)	Topological Correctness (%)
Blocked	Sidewalk	74.43	65.80	52.90	65.18
	Crosswalk	77.30			
Moderate	Sidewalk	72.13	74.43	48.67	67.53
	Crosswalk	79.40			
Open-Sky	Sidewalk	69.60	66.90	27.40	70.63
	Crosswalk	66.20			

Based on the experimental results, the network buffering approach is able to automatically generate the geometries of sidewalk and crosswalk segments and to construct the network. The evaluation results show that the average percentages of geometrical completeness for sidewalk and crosswalk are 72.29% and 74.6%, respectively. The average percentage of geometrical correctness is 68.72%. For quality of pedestrian network, the average values of topological completeness and topological correctness are 43.98% and 67.52%, respectively. The geometrical correctness of Tile 1, Tile 4, and Tile 5 are low because the algorithm generated sidewalk and crosswalk features that do not actually exist. This is because the road attributes used for road selection might contain errors and the areas might not always have sidewalks along

both sides of roads. Figure 8-6 shows an example of a situation where network buffering produces non-existent sidewalks. To verify the existence of sidewalks and crosswalks, combining network buffering with collaborative mapping is a potential approach (see Appendix A).

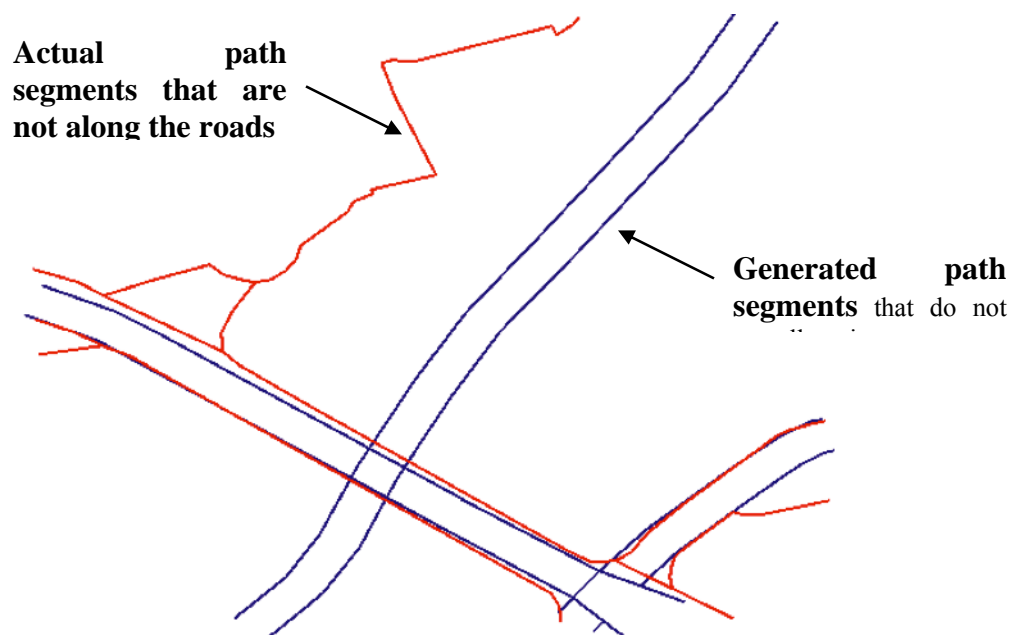


Figure 8-6. Errors from network buffering approach

The topological completeness is low because the algorithm generated only sidewalk and crosswalk features, where the actual network contains other pedestrian path types (see Figure 8-6). For instance, Tile 3 contains 47% of other pedestrian path types (see Table 8-3) that cannot generate by network buffering approach. However, around 68% of the connection points determined by the algorithm are correct. To improve the geometrical and topological completeness, other pedestrian path types that could not be captured by the network buffering approach need to be included. These other pedestrian path types can be captured through other approaches such as collaborative mapping and image processing.

8.4 EVALUATION OF THE COLLABORATIVE MAPPING APPROACH

The data source and parameters used in the collaborative mapping experiment were explained in Table 8-8.

Table 8-8. Data source and parameters used in collaborative mapping

Data source (Input)	Walking GPS traces, Volunteers
Data preparation	GPS data collection with fix interval of 1 s
Network construction	<p>Step 1: Pre-processing HDOP > 0 and HDOP < Average HDOP of a trace Speed > 0 Number of satellites used > 4</p> <p>Step 2: Significant point filtering Minimum number of cluster = $\sqrt{\frac{n}{2}}$ Maximum number of clusters = n/2, (max=50) where n: number of GPS points</p> <p>Step 3: Network construction Distance threshold = 9 m</p>
Output	Pedestrian network in vector format

As part of this research, we searched for but could not find sharing walking GPS traces from existing LBSN web sites (e.g., OSM) in the study area. We emulated a collaborative mapping environment by employing the Social Navigation Network (SoNavNet) prototype (Karimi et al., 2009, Kasemsuppakorn and Karimi, 2009a). The prototype has been developed in the Geoinformatics Laboratory of the School of Information Sciences at the University of Pittsburgh for locating, tracking, and sharing navigation related information (Karimi et al., 2009). Ten members of the Geoinformatics Laboratory participated in collecting data by using Android-based phone and the data logger QStarZ BT-Q1000ex. This data logger features A-GPS and is Wide Area Augmentation System (WAAS)-enabled. An update interval of 1 s was

selected. A total of 60 walking GPS traces in the testing area were collected and the average number of GPS points per trace was about 650 points. Figure 8-7 shows the collected walking traces in the study area.



Figure 8-7. GPS points of walking GPS traces in the study area

The algorithm was implemented using Java, Matlab 2010, and GeoTools 2.7-M1. Each of the raw GPS traces was first filtered through the pre-processing step of the algorithm. GPS points were filtered out and excluded from the experiment based on such criteria as number of satellites used (less than 4 or not), walking speed derived from GPS points (equal to 0 or not), and HDOP value (equal to 0 and greater than average HDOP for all GPS points in a trace or not). Duplicate GPS points were also removed. After pre-processing, approximately 7.3% of raw GPS points were filtered as outliers. To measure the effect of pre-processing, five sample GPS traces and measured were randomly selected and the deviation between each GPS point and the corresponding baseline before and after pre-processing was measured. Of the five sample traces,

compared to the GPS points before pre-processing, the average deviation between GPS points and baseline after pre-processing was reduced around 18%.

Next, significant points on each filtered trace were extracted using the chain coding and PAM clustering techniques. The 12-direction chain code was applied to select candidate significant points representing straight, curved-shape paths and turning angles. Of the 60 traces, about 37% of the filtered GPS points were selected as candidate significant points and were kept for further processing. An important parameter in the subsequent significant filtering process is number of clusters for PAM. Since the optimal number of clusters is unknown, a range of clusters is bounded by a minimum number of clusters derived from the rule of thumb $\sqrt{\frac{n}{2}}$, where n is the number of data points and the maximum number of clusters is $n/2$. The set of clusters with the highest silhouette value was selected. From the experiment, the average silhouette widths were between 0.6 and 0.7, which is considered a reasonable clustering structure (Kaufman and Rousseeuw, 1990). After applying PAM, the significant points on each trace (approximately 20% of candidate significant points) were kept. The average running time for PAM is about 7.5 seconds for each trace.

Once the significant points on a trace were extracted, they were used as input to construct pedestrian network. The new significant points were compared with the existing network data and were employed to generate a new path or merged with the existing paths in order to improve path's geometry. The distance threshold for merging was set to 9 m, based on the accuracy of the GPS Standard Positioning System (SPS) (InsideGNSS, 2008). Each GPS trace was processed one at a time and was incrementally added to and updated the already constructed pedestrian network. Figure 8-8 illustrates the constructed pedestrian network with different number of GPS traces.

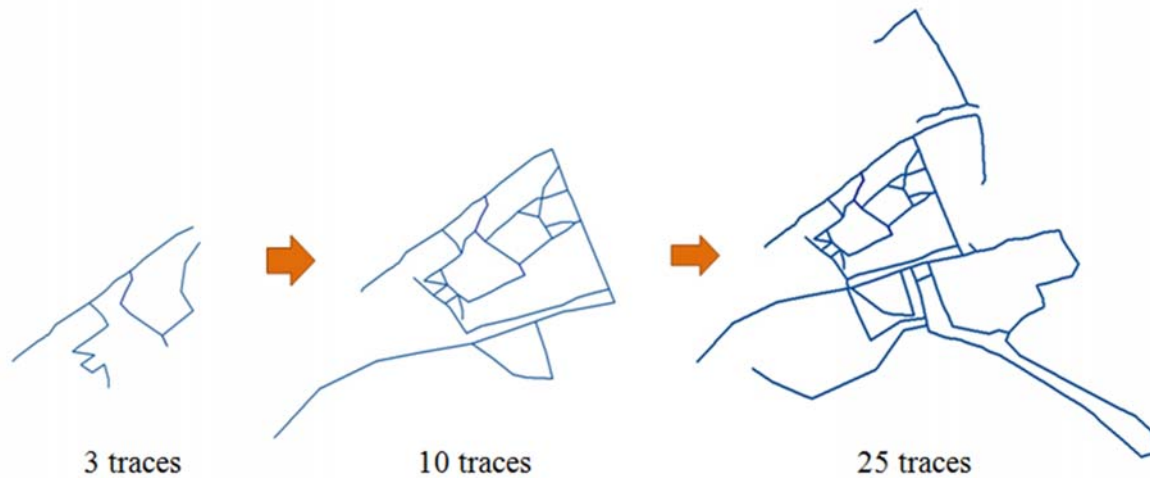


Figure 8-8. Constructed pedestrian networks with different number of traces

Using all 60 GPS traces, the constructed pedestrian network consists of 115 segments. The constructed pedestrian network was overlaid on a high-resolution image, as shown in Figure 8-9. In addition to sidewalks and crosswalks, the constructed pedestrian networks using the collected GPS points include other path types.

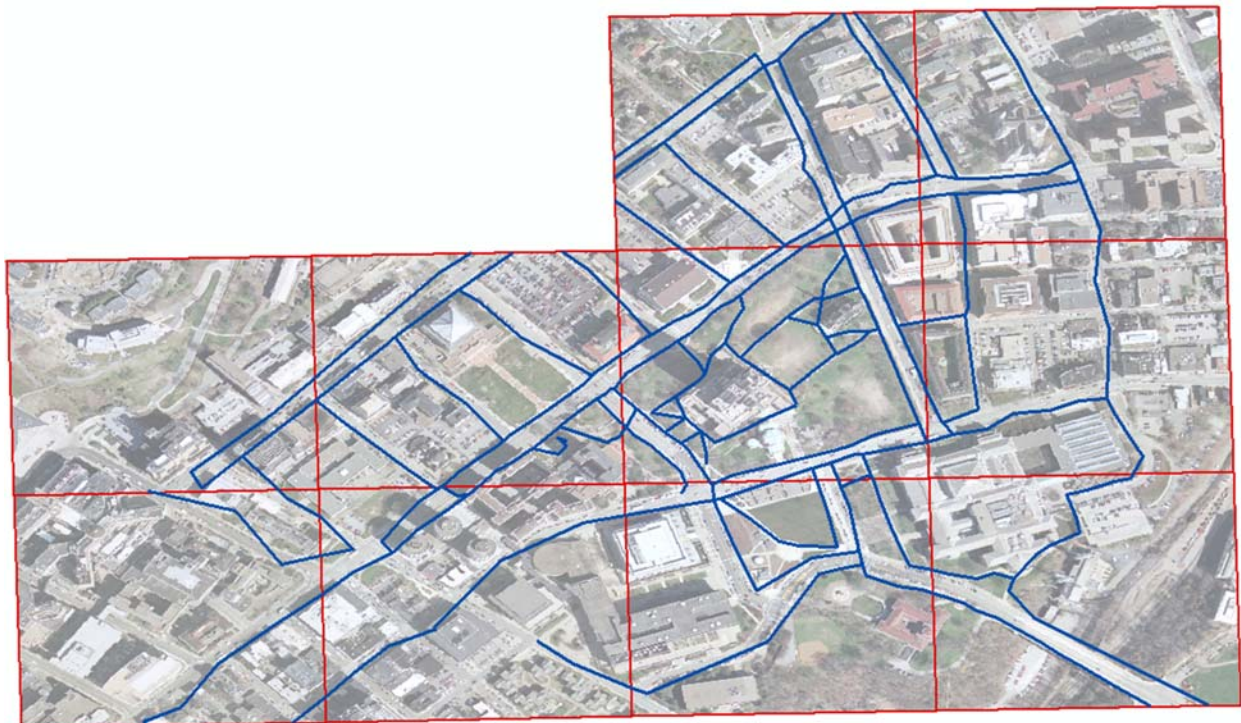


Figure 8-9. Constructed pedestrian networks in 10 tiles of the study area

To measure the performance of the algorithm, the constructed pedestrian network was matched against the pedestrian network baseline and quality measures were calculated. A summary of the evaluation process is shown in Figure 8-10. Since available walking GPS traces do not completely cover the study area, geometrical completeness and topological completeness were not reported in this evaluation. Table 8-9 shows the statistics of evaluation results of ten tiles. We calculated the average values of geometrical correctness and topological correctness for the generated pedestrian paths within the open-sky, moderate and blocked areas (Figure 8-3 and Table 8-3); the results are shown in Table 8-10.

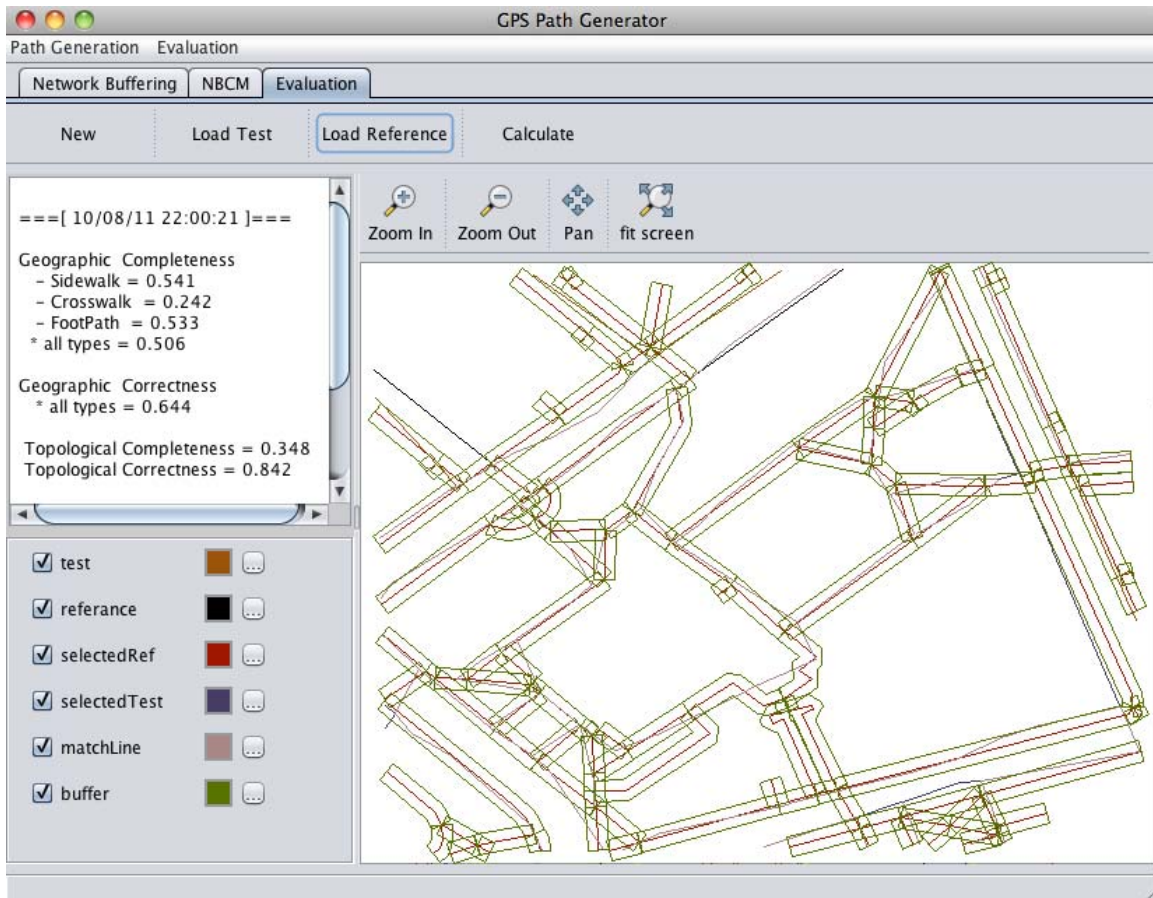


Figure 8-10. An example of evaluation process (Collaborative Mapping)

Table 8-9. Statistics results of collaborative mapping approach

Tile No	Geometrical Correctness (%)	Topological Correctness (%)
Tile 1	42.3	67.4
Tile 2	47.3	63.4
Tile 3	71.5	81.8
Tile 4	74.6	83.0
Tile 5	43.5	75.1
Tile 6	55.2	85.3
Tile 7	64.4	84.2
Tile 8	50.9	70.2
Tile 9	64.2	75.3
Tile 10	61.6	83.3
Average	57.55	76.9

Table 8-10. Statistics results of Collaborative Mapping approach (Environment setting)

Environment settings	Geometrical correctness (%)	Topological correctness (%)
Blocked	46.0	69.03
Moderate	60.33	81.3
Open-Sky	70.17	83.0

The evaluation result shows that the average geometrical correctness is 57.55%, the topological correctness is 76.9%, and the average RMSE for all generated pedestrian paths is 2.25 m. As expected, the quality of the constructed pedestrian network depends heavily on the quality of GPS traces; the constructed paths in the blocked area have low geometrical and topological accuracies. Figure 8-11 shows the generated path segments using collected GPS traces in the blocked area (left) and in the open sky area (right). As seen in the figure, the geometrical accuracies of generated paths in the open sky area are better than those in the blocked area (using the same number of traces).

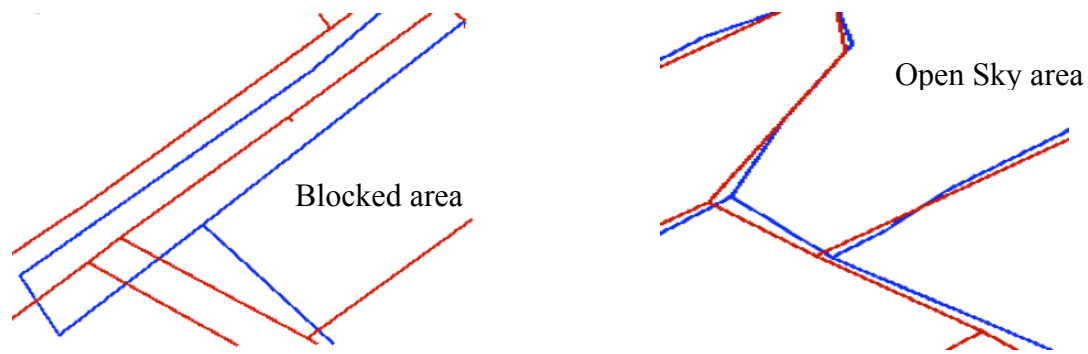


Figure 8-11. The generated path segments in the blocked and open sky area

The evaluation result also shows that the number of GPS traces and the geometrical accuracy of generated pedestrian paths are positively correlated. In the experiment, the geometrical correctness is low (57.55%) because approximately 50% of the pedestrian path segments generated were from 1-2 GPS traces. Of the 30 generated segments using five GPS traces, the average increase in geometrical accuracy is 6.86%.

8.5 EVALUATION OF THE IMAGE PROCESSING APPROACH

For evaluation of the image processing approach, orthoimagery and LiDAR point cloud data, provided by PAMAP were employed. PAMAP (2011) is a program of the federal government that provides publicly available mapping for the state of Pennsylvania. The LiDAR point cloud data was collected with a 1.4 m average point spacing and the natural color orthoimage was produced at 0.61 m resolution. Both data sets were captured in spring 2006 and organized into tiles, with no overlap. Each tile represents 3.048 m x 3.048 m on the ground and is referenced using the NAD83 Pennsylvania State Plane South Coordinate System. Details of the two data sources are provided in Table 8-11.

Table 8-11. Details of Orthoimage and LiDAR point cloud

	Orthoimage	LiDAR point cloud
Year	2006	2006-2008
Created By	PA Department of Conservation and Natural Resources, Bureau of Topographic and Geologic Survey	PA Department of Conservation and Natural Resources, Bureau of Topographic and Geologic Survey
Data Components	R,G,B	x,y,z, intensity, class, echo number, echo type, flight line no.
Resolution/ Average of Point Spacing	0.6 m (2-foot) pixel resolution	1.4-m. (2-m. maximum) point spacing
Vertical Accuracy	N/A	18.5-cm. (open area) and 37 cm. (forested areas) RMSE.
Horizontal Accuracy	1.46 m or less	1.52 m or less
Datum	NAD83 horizontal datum, Ellipsoid GRS80, NAVD88 vertical datum, and Geoid03	NAD83 horizontal datum, Ellipsoid GRS80, NAVD88 vertical datum, and Geoid03
Coordinate System	NAD_1983_Stateplane_Pennsylvania	NAD_1983_Stateplane_Pennsylvania

Raster images used in the construction algorithm were split into ten tiles (same configuration as the study area) of 1000 x 1000 pixels with each pixel approximately covering 0.305 m by 0.305 m on the ground. Let R represent the raster image, which is divided into n small tiles R_1, R_2, \dots, R_n such that $\sum_{i=1}^n R_i = R$ and $R_i \cap R_j$ is a null set for all i and j (where $i \neq j$).

The example of splitting raster image is shown in Figure 8-12.

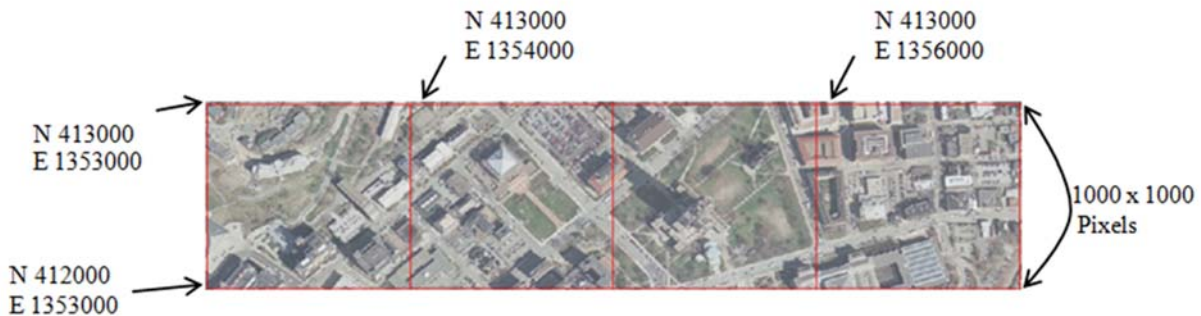


Figure 8-12. An example of splitting orthoimage

For the experimentation, four parameters were used in the algorithm. The first two parameters are minimum building height and tree height thresholds, which were used in the object filtering step. The threshold value of 3 m, (suggested by Tao and Yasuoka (2002)), was set for both heights. The last two parameters, employed in seed selection and region growing, are similarity spectral threshold value and maximum distance. From the experiment, the threshold values of 0.95 and 0.05 were set for the third and fourth parameters, respectively. For the pedestrian network centerline extraction, the mathematical morphology erosion operator and the thinning algorithm by Lam, et al., (1992) were employed to reduce several-pixel wide regions (derived from the previous step) to one-pixel wide lines. The 3 x 3 rectangle-shaped structuring element was used for the erosion operation and the results, after applying the thinning algorithm, were improved by removing spur pixels (small areas). In the last step, raster-to-vector conversion, the set of pixels representing the generated pedestrian network were obtained from edge tracing and pedestrian path pixels selection. Then the set of pixels was converted to line vector data. To deliver the final product, the location information (i.e., longitude and latitude) was added to the line vector data, which are registered to the GCS_North_American_1983.

To measure the performance of the algorithm, the constructed pedestrian network using ten images was compared with the pedestrian network baseline in the same area. Once the matching between the two networks was complete, the quality measures of four evaluation criteria were calculated. Figure 8-13 shows the evaluation process and Table 8-12 shows the statistic results of 10 tiles. We calculated the average values of geometrical correctness and topological correctness for the generated pedestrian paths within the open-sky, moderate, and blocked areas (Figure 8-3 and Table 8-3); the results are shown in Table 8-13.

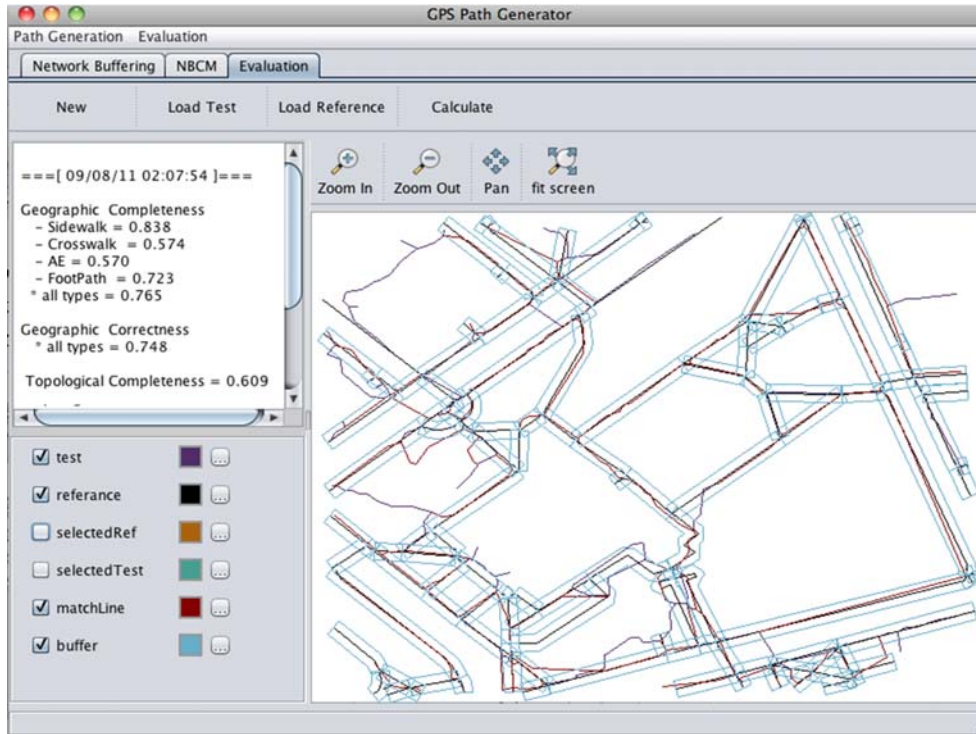


Figure 8-13. The evaluation process (image processing)

Table 8-12. Statistics results of image processing approach

Tile Number	Path Type	Geometrical Completeness (%)	Geometrical Correctness (%)	Topological Completeness (%)	Topological Correctness (%)
Tile 1	Sidewalk	73.1	68.5	61.2	48.3
	Crosswalk	54.3			
	Entrance	63.2			
	Footpath	54.8			
Tile 2	Sidewalk	60.1	69.2	75.1	51.3
	Crosswalk	44.2			
	Entrance	32.2			
	Footpath	59.4			
Tile 3	Sidewalk	70.1	76.4	84.8	72.3
	Crosswalk	54.9			
	Entrance	38.3			
	Footpath	65.2			
Tile 4	Sidewalk	68.2	79.7	69.8	53.9
	Crosswalk	78.4			
	Entrance	53.9			
	Footpath	77.8			
Tile 5	Sidewalk	65.2	64.2	74.2	43.9
	Crosswalk	45.4			
	Entrance	53.3			
	Footpath	69.2			

Tile Number	Path Type	Geometrical Completeness (%)	Geometrical Correctness (%)	Topological Completeness (%)	Topological Correctness (%)
Tile 6	Sidewalk	79.1	63.4	65.3	44.1
	Crosswalk	67.2			
	Entrance	38.3			
	Footpath	57.2			
Tile 7	Sidewalk	83.8	74.8	60.9	48.3
	Crosswalk	57.4			
	Entrance	57.0			
	Footpath	72.3			
Tile 8	Sidewalk	42.1	51.2	59.1	40.9
	Crosswalk	28.9			
	Entrance	77.3			
	Footpath	82.8			
Tile 9	Sidewalk	74.7	66.2	80.1	48.3
	Crosswalk	59.9			
	Entrance	41.2			
	Footpath	67.2			
Tile 10	Sidewalk	63.9	55.8	75.1	57.2
	Crosswalk	67.2			
	Entrance	55.3			
	Footpath	66.7			
Average	Sidewalk	68.03	66.94	70.56	50.85
	Crosswalk	55.78			
	Entrance	51.00			
	Footpath	67.26			

Table 8-13. Statistics results of image processing approach (Environment settings)

Environment Settings	Path Type	Geometrical Completeness (%)	Geometrical correctness (%)	Topological Completeness (%)	Topological Correctness (%)
Blocked	Sidewalk	60.13	63.28	67.4	46.1
	Crosswalk	43.20			
	Entrance	56.50			
	Footpath	66.55			
Moderate	Sidewalk	72.57	61.8	73.5	49.87
	Crosswalk	64.77			
	Entrance	44.93			
	Footpath	63.70			
Open Sky	Sidewalk	74.03	76.97	71.83	58.17
	Crosswalk	63.57			
	Entrance	49.73			
	Footpath	71.77			

The evaluation result of the extracted pedestrian networks in Table 8-12 shows that the algorithm is able to automatically extract four types of pedestrian paths: sidewalk, crosswalk, entrance, and footpath. The average values of geometrical completeness are 68.03%, 55.78%, 51%, and 67.26% for sidewalk, crosswalk, entrance, and footpath, respectively. The extracted data do not exactly match the baseline for the following reasons: (1) missing crosswalks at non-intersection locations (2) generating non-existent crosswalks, (3) creating geometric errors through the thinning algorithm, (4) creating errors through refining regions and edge linking, and (5) creating errors through the extraction of geospatial objects in complex scenes (e.g., dense buildings, shadows, and trees). Figure 8-14 shows examples of errors from shadows and geometric distortion. The extracted data from each image tile has different values for all evaluation criteria because of differences between images such as shadows, number of buildings, and parking lots. The average values of geometrical correctness (66.94%) and topological correctness (50.85%) are low because the algorithm generated spurious pedestrian paths through image misclassification.

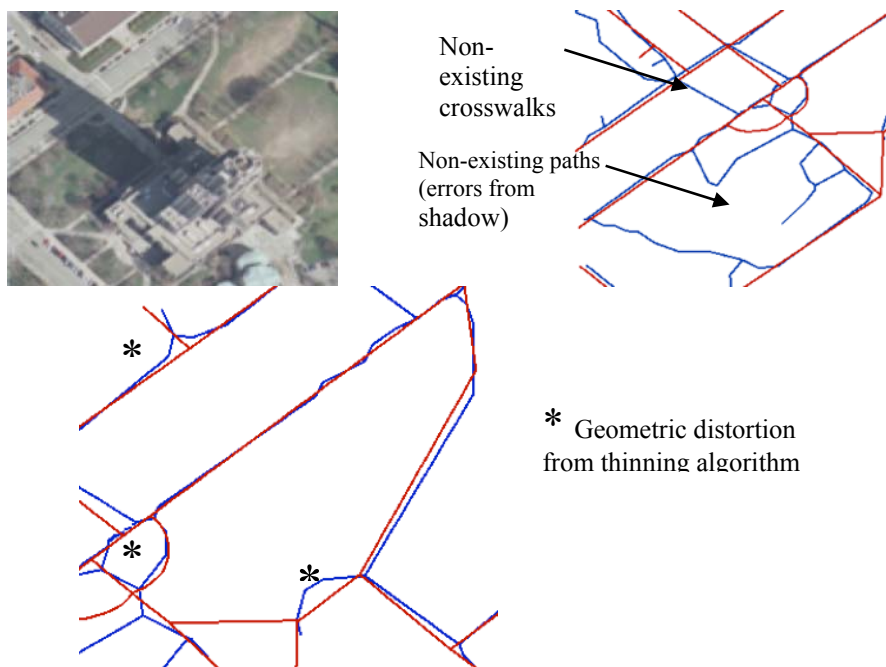


Figure 8-14. Errors from image processing approach

8.6 EVALUATION DISCUSSION

This section discusses the summary results obtained from evaluating the three approaches. In the study area, the percentage distribution of pedestrian path types in the network is shown in Figure 8-15. This chart shows three main pedestrian path types that constitute the bulk of a pedestrian network (e.g., 94.71% in the study area) which are sidewalks, crosswalks, and footpaths.

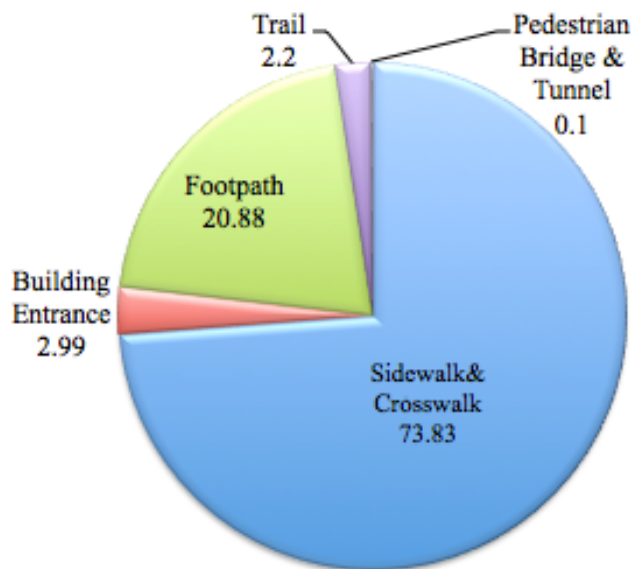


Figure 8-15. Percentage distribution of pedestrian path types

The experimental results indicate that all three approaches are able to collect five pedestrian path types. **Figure 8-16** illustrates the proportion of each path type collected by each approach in the study area. The network buffering approach can generate only sidewalks and crosswalks, while the collaborative mapping and image processing approaches are able to generate all types, except pedestrian bridge and tunnel. The collaborative mapping approach employs collected GPS traces, which cannot differentiate between a pedestrian bridge (a grade separated crossing that is typically at a high elevation above the ground) and other path types because the elevation data computed by GPS devices are not highly accurate. Moreover, given

that GPS receivers usually lose satellite signals while travelling in tunnels or indoor areas, pedestrian tunnels are not collected by this approach as well. The current algorithm based on the image processing approach in this dissertation does not extract pedestrian bridges and tunnels for the following reasons: (1) pedestrian tunnels are usually masked by other objects in high-resolution satellite and LiDAR images, (2) pedestrian bridges collected by using a threshold on height information of LiDAR data are not highly corrected, (3) the percentage of both pedestrian path types (i.e., pedestrian bridges and tunnels) in a pedestrian network is small. However, we believe that other unexplored image sources (e.g., Google Street View, city map) and advanced image processing techniques may have potential to extract pedestrian bridges and tunnels, while their collection by the other two approaches is impossible.

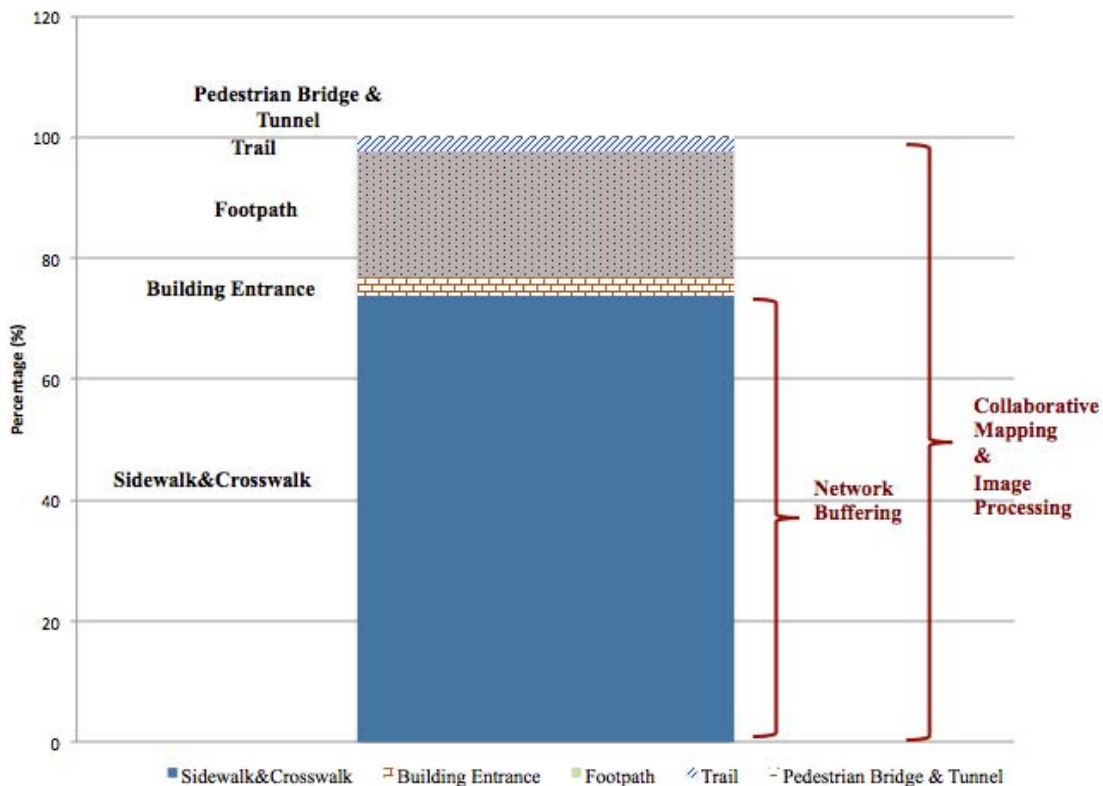
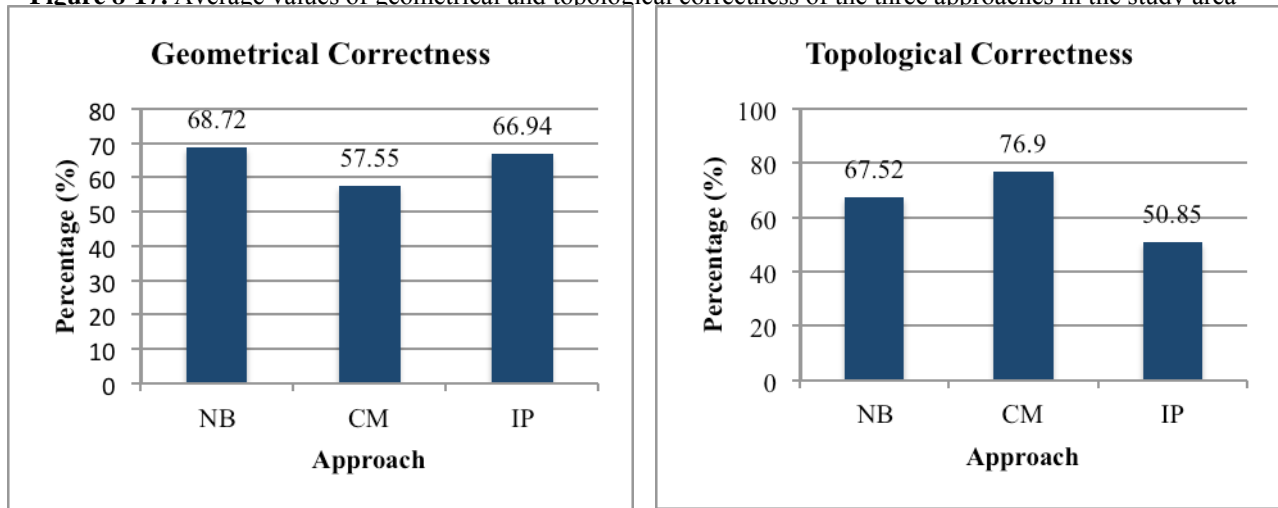


Figure 8-16. Pedestrian Path types and the three approaches

Considering the performances of the three approaches, the average percentage values of the geometrical and topological correctness of generated pedestrian path segments are shown in Figure 8-17. Based on the experimental results, the average value of geometrical correctness from the network buffering approach is higher than the other two approaches, even though network buffering generates only sidewalks and crosswalks. Nevertheless, in the collaborative mapping approach, the geometrical correctness is improved by increasing the number of repeated traces on a segment (e.g., five traces on a segment in the experiment resulted in 6.86% geometrical correctness improvement). The results obtained through the collaborative mapping approach could be used to verify the generated paths from the network buffering approach and to generate other pedestrian path types. For the topological correctness, the collaborative mapping approach has the best performance on topological correctness as it generates only existing pedestrian path segments.

Figure 8-17. Average values of geometrical and topological correctness of the three approaches in the study area



A single approach is unable to generate a complete network consisting of all pedestrian path types in a given area. However, by leveraging the advantages of each approach, it is possible to develop a method to construct a complete network; by “complete network”, a pedestrian network that represents real-world pedestrian paths containing all the seven pedestrian

path types is meant. We analyzed the results obtained from the three approaches and determined the approach with the highest geometrical completeness for each pedestrian path type, see Figure 8-18. In this figure, sidewalks and crosswalks are generated most accurately with the network buffering approach, while building entrances, footpaths, and trails are best collected through the image processing approach. The remaining uncovered segments, or gaps, could be filled in by the collaborative mapping approach since the missing segments can be collected by GPS devices. Furthermore the generated segments can be validated by using walking GPS traces. As can be seen in the figure, no single approach achieves 100% completeness. However, it is possible to achieve 100% completeness by integrating different approaches. Nevertheless, none of the current version of the three approaches can generate pedestrian bridges or tunnels.

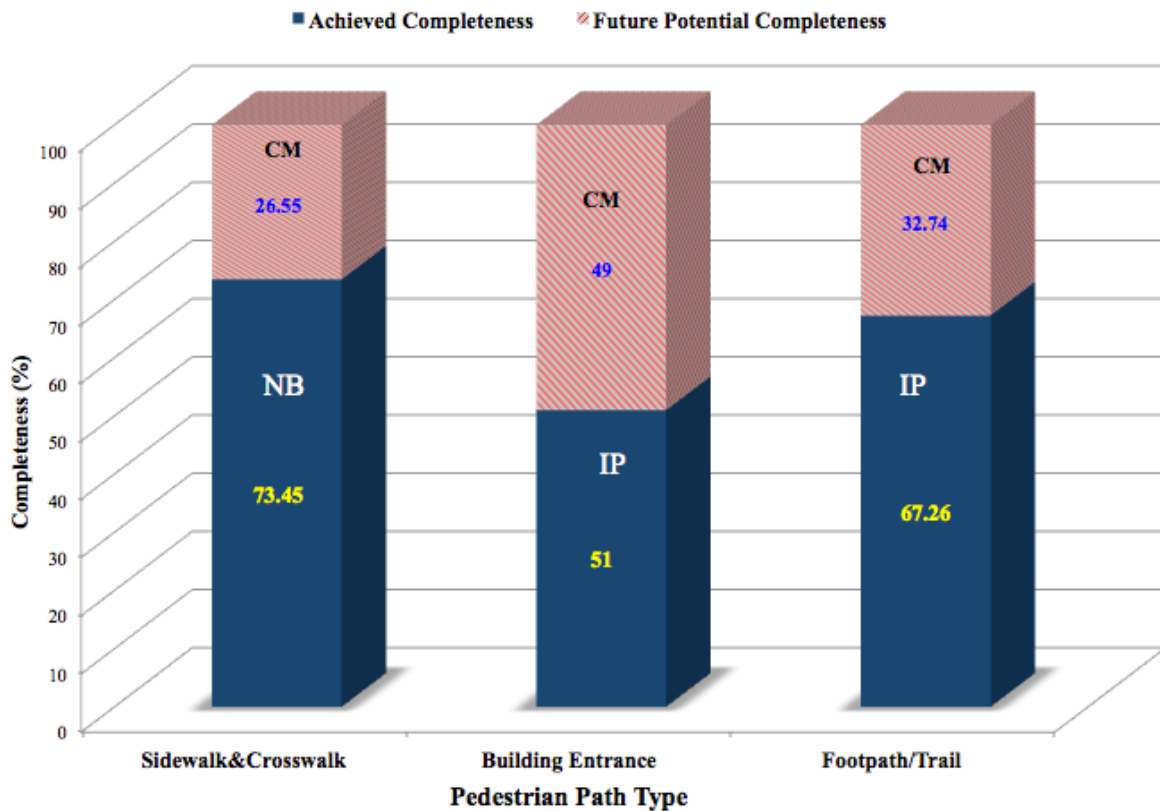


Figure 8-18. Completeness percentages of pedestrian path types and the recommended approaches

9.0 RECOMMENDATION

One objective in this dissertation is to recommend a methodology for constructing pedestrian networks for a given set of requirements and resources, including application requirements and available data sources. This chapter starts by comparing the three pedestrian network construction approaches in terms of development complexity and performance. The chapter closes with a recommendation methodology of choosing appropriate approaches for constructing pedestrian networks.

Table 9-1 compares the development complexity of the three approaches presented in this dissertation by examining required data sources, data acquisition cost, data preparation tasks and effort, and network construction tasks and effort.

Table 9-1. Comparison of development complexity of the three approaches

Approaches	Data Sources	Data Cost	Data Availability	Data Preparation Tasks	Data Preparation Effort (days)	Network Construction Tasks	Network Construction Effort (days)
Network Buffering	Road Network	Inexpensive	High	Road attribute selection for approximating sidewalk locations	2	<ul style="list-style-type: none"> • Pedestrian network construction 	21
Collaborative Mapping	Walking GPS Traces	Free	Sparse	GPS traces collection in a given area	20	<ul style="list-style-type: none"> • Pre-processing • Significant point filtering • Pedestrian network construction 	2 14 21

Approaches	Data Sources	Data Cost	Data Availability	Data Preparation Tasks	Data Preparation Effort (days)	Network Construction Tasks	Network Construction Effort (days)
Image Processing	Orthoimages and LiDAR Point Clouds	Inexpensive / varies	Medium (Urban Areas)	Data noises removing and raster data generation	7	• Data fusion	7
						• Pixel-based classification	14
						• Object filtering	30
						• Pedestrian path area extraction	30
						• Pedestrian network construction	60
						• Raster-to-vector conversion	7

In Table 9-1, *Data Sources* refers to the data required for each approach and *Data Cost* indicates the estimated money cost for acquiring the listed data source. *Data Availability* indicates accessibility to data source and completeness of data given an area. The network buffering approach requires existing road networks, which vary in price but generally inexpensive and widely available. Even though several free road networks are available (e.g., TIGER line data in the U.S.), the data cost for this approach is not considered as free. This is because specific attributes on road segments (e.g., road types, number of lanes), which are not generally available in free databases, are required for the network buffering approach in order to generate accurate pedestrian networks. The collaborative mapping approach requires publicly-shared walking GPS traces, which are expected to become widely available due to proliferation of GPS-enabled mobile devices. GPS traces are considered as the free data source because it assumes the data are shared with others through public collaborative mapping websites and available for download. The image processing approach requires orthoimages and LiDAR point clouds, which are relatively abundant in urban areas within the U.S. and can be acquired from private and public sources for varying prices but generally at a nominal cost. Overall, the easiest to obtain and most abundant data source is road networks and the most affordable is GPS traces.

Data Preparation Tasks and *Data Preparation Effort* refer to the steps and efforts for processing raw data required for each approach. The *Data Preparation Tasks* column summarizes the individual tasks in the refinement process. Since the collaborative mapping approach uses GPS traces, which are currently very sparse, the GPS traces collected in this research are listed as a task in the data preparation of the collaborative mapping approach. The *Data Preparation Effort* column is a rough estimate number of days for a person based on the author's experience with each task and is useful as a relative measure. The *Data Preparation Tasks* of these approaches require manual intervention and cannot be performed in a completely automatic fashion. For example, the network buffering approach requires a human to understand and select road attributes for network construction but takes the least amount of time when compared to the other approaches. The collaborative mapping approach requires volunteers to collect GPS traces in a given area, which significantly depends on the geographic extent. The image processing approach involves the creation of a raster-grid surface from LiDAR point cloud data. Overall, the data preparation for the network buffering approach is the quickest. The collaborative mapping data collection is the most labor intensive and time consuming, since the the average human walking distance a day is around 2,400 m in general (Frank et al., 2004). However, it should be noted that the image processing approach requires knowledge of raster data processing and geospatial tools.

The *Network Construction Tasks* column summarizes the tasks needed to implement an application to build a pedestrian network and the *Network Construction Effort* column lists the estimated number of days for developing such an application, based on the author's experience and is useful as a relative measure. Of the three approaches, the network buffering approach is

the simplest to implement and the image processing approach the most complex requiring a series of steps.

To compare the performance of the three approaches, Table 9-2 provides an analysis of running time and quality measures of the four evaluation criteria.

Table 9-2. Comparison of evaluation results

Approach	Tasks	Average Running Time (Sec)	Result				
			Path Type	Geometrical Completeness (%)	Geometrical Correctness (%)	Topological Completeness (%)	Topological Correctness (%)
Network Buffering	Pedestrian network construction	1.63	Sidewalk	72.29	68.72	43.98	67.52
			Crosswalk	74.60			
Collaborative Mapping	<ul style="list-style-type: none"> • Pre-processing • Significant point filtering • Pedestrian network construction 	1.26	Sidewalk	-	57.55	-	76.9
		7.5	Crosswalk	-			
		14.24	Entrance	-			
			Footpath	-			
Image Processing	<ul style="list-style-type: none"> • Data fusion • Pixel-based classification • Object filtering • Pedestrian path area extraction • Pedestrian network construction • Raster-to-vector conversion 	0.8	Sidewalk	68.03	66.94	70.56	50.85
		62.33	Crosswalk	55.78			
		2.23	Entrance	51.00			
		717.74	Footpath	67.26			
		50.34					
		12.33					

In each approach, the average running time of the listed tasks are reported. All approaches are tested for ten tiles (305 x 305 m²) in the study area and are run under the same computing environment (Intel i7 2.7 GHz Processor with 4 GB of memory). The result shows that the network buffering approach is the fastest (1.63 s) whereas the image processing approach is the most computationally intensive. This is because image processing deals with raster data, which is relatively large comparing to the vector data. In addition, extracting information from images requires several tasks, which must be performed in a sequence. As

shown in Table 9-2, the most expensive task of the image processing approach is pedestrian path area extraction, which employs a region-based segmentation technique.

Before discussing the quality of a pedestrian network constructed by each approach, the assumptions for implementing each approach are outlined as follows. The assumptions for the network buffering approach are: (1) sidewalks exist along both sides of selected roads and (2) crosswalks are located at every intersection. The assumptions for the collaborative mapping approach are: (1) there are always volunteers to collect data, (2) volunteers have GPS-enabled mobile devices, and (3) volunteers walk along the pedestrian path segments. The assumptions for the image processing approach are: (1) LiDAR data, with the same resolution and same collection year with the high-resolution orthoimage are available, (2) crosswalks are located at every intersection, (3) pedestrian path areas are mostly made up of concrete, and (4) parking lot areas are mostly made up of asphalt.

Qualities of the constructed pedestrian networks from the three approaches are described in Table 9-2. All four quality measures, shown in Table 9-2, were derived from the average value of each measure criterion of ten study areas (details in Chapter 8). The results show that the network buffering approach can generate only sidewalks and crosswalks, while the other two approaches are able to generate other pedestrian path types, such as footpath and building entrance (depending on the available data). Network buffering generated more than 70% completeness of sidewalks and crosswalks and around 68.72% of generated sidewalks and crosswalks are correct. This is because network buffering generates non-existent sidewalks and crosswalks in some areas, due to the assumption that all roads have parallel sidewalks on both sides. The topological completeness of the constructed pedestrian networks from the network buffering approach is low (43.98%) because the constructed network is incomplete; other

pedestrian path types are missing. For collaborative mapping, the percentages of geometrical and topological completeness of the results are not reported because this approach depends on the availability of walking GPS traces, which are currently incomplete for the study area. Regarding correctness, the collaborative mapping approach is able to determine the geometries of pedestrian path segments accurately from multiple GPS traces. The higher the number of repeated GPS traces on a single path segment, the higher the percentage of geometrical correctness. As reported in Chapter 8, the average geometrical correctness increases 6.86% by using five repeated GPS traces. The topological correctness of the collaborative mapping approach is high because walking GPS traces only models pedestrian path segments that exist in the real world. The image processing approach provides a moderate level (50-70%) of quality measurements mainly due to noises (e.g., shadows) in the image and errors from the algorithms, such as pedestrian path centerline extraction. The percentage of geometrical correctness is approximately 66.94% because there are geometric distortions due to the thinning algorithm and the errors from edge linking. Moreover, the approach generates spurious pedestrian path segments from image classification.

Comparing the generated sidewalks and crosswalks across the three approaches, the network buffering approach provides better result than the other two approaches due to noises in collected GPS points and in images. Table 9-3 shows a comparison of geometrical and topological correctness between the three approaches in three environment settings. The collaborative mapping and image processing approaches perform well in open sky areas because of high accuracy of collected GPS points and less shadow areas as well as less tall buildings in the images. On the other hand, environment settings have minor impact on the network buffering approach.

Table 9-3. Comparison of evaluation results based on three environment settings

Environment Setting	Network buffering		Collaborative Mapping		Image Processing	
	Geometrical Correctness (%)	Topological Correctness (%)	Geometrical Correctness (%)	Topological Correctness (%)	Geometrical Correctness (%)	Topological Correctness (%)
Blocked	65.80	65.18	46.00	69.03	63.28	46.10
Moderate	74.30	67.53	60.33	81.30	61.80	49.87
Open Sky	66.90	70.63	70.17	83.00	76.97	58.17

The evaluation results and the analysis of quality result of the three approaches reveal that each approach has its own advantages and disadvantages. The advantages of the network buffering approach are that it is very fast and able to automatically construct pedestrian networks in a wide area. Nevertheless, it does not cover the off-road pedestrian path segments and it might create nonexistent segments. The advantage of the collaborative mapping approach is that it is able to generate along the road and off-road pedestrian path segments. However, its data collection is labor intensive and the quality of generated segments is dependent on the GPS accuracy. The advantages of the image processing approach are that it is able to automatically construct pedestrian networks in a wide area and the results include along the road and off-road pedestrian path segments. Nevertheless, the approach is complex, takes long computation time, and might not be able to generate accurate results.

The following section provides the explanation of a methodology for recommending suitable approaches for constructing pedestrian networks of a given location according to the required output pedestrian path type, available data sources, time constraint, cost constraint, and environment settings. Time constraint refers to the amount of time available to complete construction of a pedestrian network. Time constraint is categorized into three groups: short time constraint (less than 1 month), medium time constraint (between 1-3 months), and long time constraint (greater than 3 months). Cost constraint refers to the budgeted amount available for

acquiring data sources for constructing pedestrian networks. Since the quality of constructed pedestrian networks varies based on the provided data sources and network construction approaches, the network quality is categorized into three levels: good, acceptable, and no guarantee. As described in the evaluation chapter (Chapter 8), the quality measures are ranged between 0 and 1, where 1 is the best value. The pedestrian network quality is considered “good” if the quality measure values are greater than 0.7 (70%), “acceptable” if the quality measure values are between 0.5 (50%) and 0.69 (69%), and if the quality measures are below 0.5, the approach cannot guarantee the quality of the results. Since there is no standard to evaluate the level of network quality obtained from automatic construction approaches, the range of each quality level is set based on the claims in the literatures related to automatic road network extraction.

Figure 9-1 shows the criteria for recommending the network buffering approach and the expected quality of constructed pedestrian networks. The network buffering approach is suitable for constructing a pedestrian network, containing only sidewalks and crosswalks, in a short time constraint. Two requirements to employ network buffering approach are: (1) road networks are available in a given location and (2) cost for road networks is affordable. The quality of the constructed pedestrian network is heavily dependent on quality of the underlying road network. In fact, without a road network this approach cannot be used at all. If the road network does not exist for the given area, other approaches would be more suitable. Another criteria to examine quality of this approach are up- to-dateness of the data, accuracy of the data, and scale of the data. The more up to date a road network is, the more closely the data models the real world. It is recommended that the road network data considered in the network buffering approach be less than five years old. Likewise, the more accurate the road network, the more accurate the

generated pedestrian network will be. The recommendation for the scale and accuracy of a road network for urban areas is 1:5000 with a RMSE less than 1.25 m according to the American Society for Photogrammetry and Remote Sensing (ASPRS, 1989). If any of these criteria are not satisfied, then the quality of the generated pedestrian path will most likely be poor.

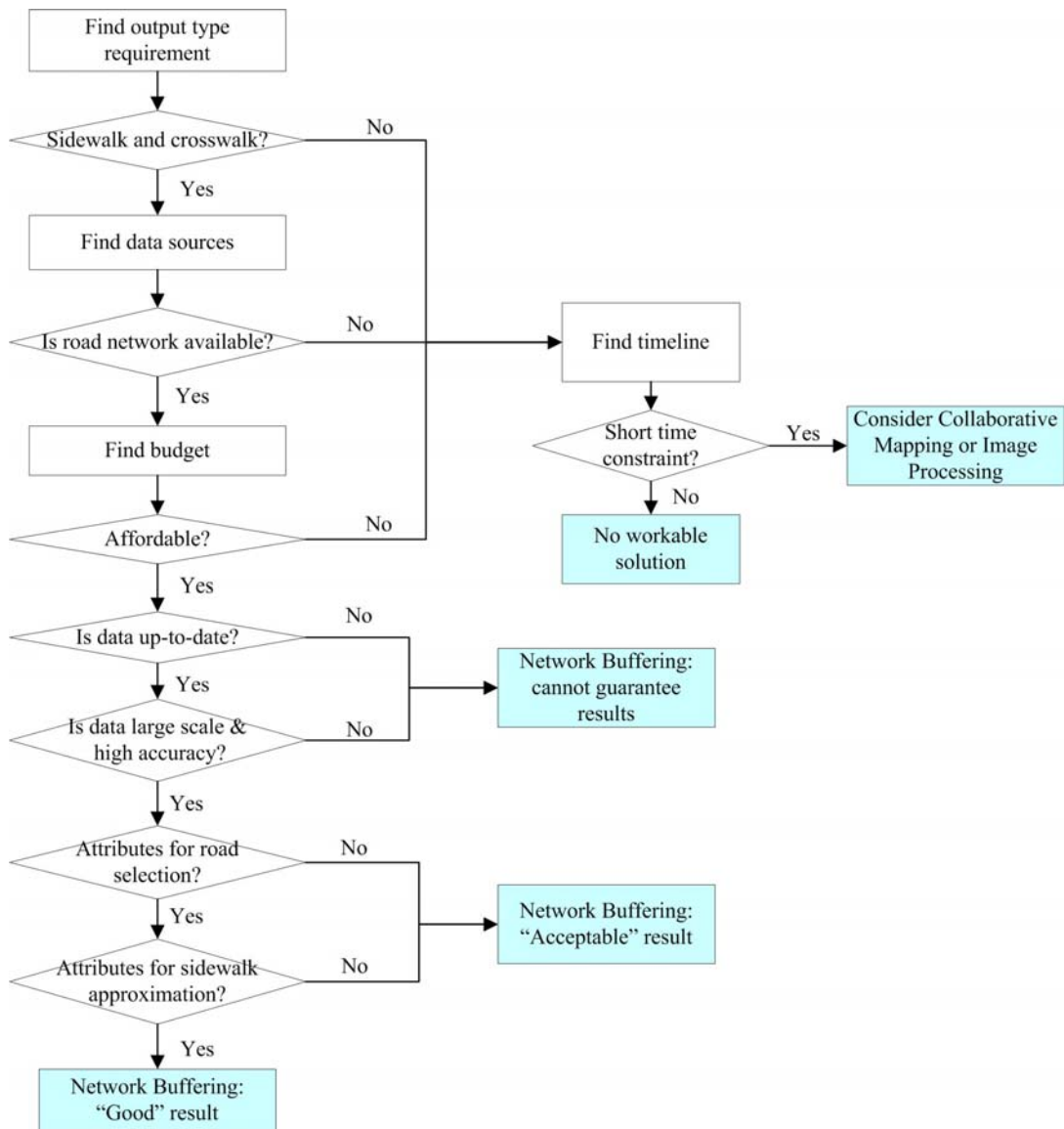


Figure 9-1. The criteria and quality result of the network buffering approach

The final set of criteria to examine for the road network buffering approach are road network attributes, e.g., road width and road type, for each segment. The network buffering approach uses these attributes to more accurately estimate sidewalk locations. Other road

network attributes recommended are number of lanes and road direction (e.g., one-way or two-way). Without these attributes the network buffering approach must assume a fixed distance from the road network to determine sidewalk and crosswalk locations and will most likely produce acceptable results.

Figure 9-2 shows the criteria for recommending collaborative mapping approach and expected quality of constructed pedestrian networks.

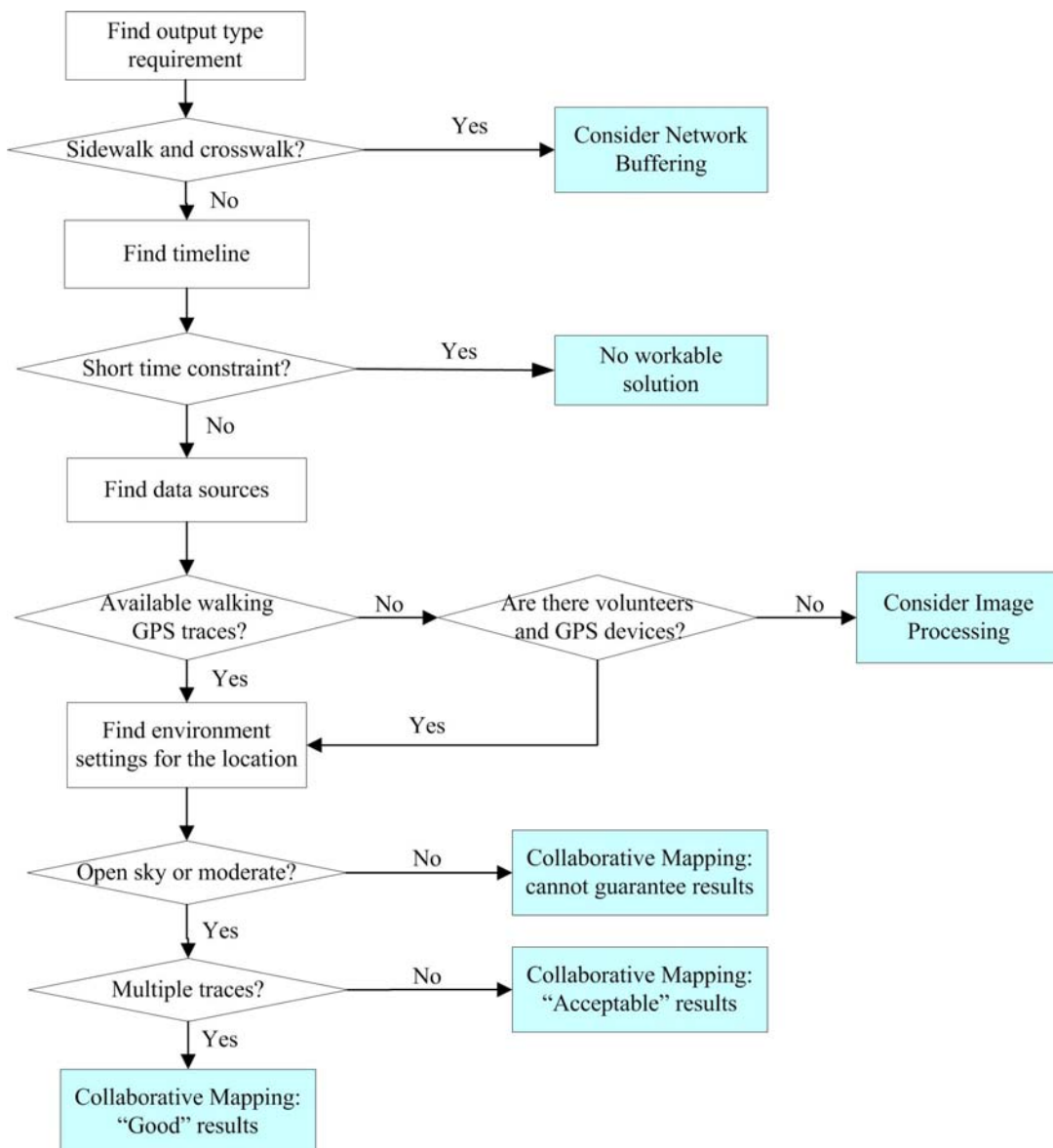


Figure 9-2. The criteria and quality result of the collaborative mapping approach

The collaborative mapping approach is suitable for constructing pedestrian networks containing not only sidewalks and crosswalks, but also other pedestrian path types. To employ this approach, the amount of time requiring to complete data preparation and network construction task is grouped into the medium time constraint. The quality of the constructed pedestrian networks by the collaborative mapping approach is heavily dependent on available walking GPS traces and GPS accuracy. Before collecting GPS traces in a particular area, it is recommended to search various websites (e.g., OSM, Wikimapia) for existing GPS traces in the geographic area of interest. If no GPS traces exist, volunteers with GPS devices or GPS-enabled mobile phones are needed. Accuracy of available GPS traces is a factor affecting quality of the constructed network. GPS accuracy is potentially degraded when collected data along pedestrian paths next to high-rise buildings (i.e., blocked area). In order to produce higher quality pedestrian networks, using multiple traces for a single pedestrian path is recommended. Multiple traces can help lower GPS uncertainty where one GPS trace does not provide enough information to accurately determine the pedestrian path.

Figure 9-3 shows the criteria for recommending the image processing approach and the expected quality of constructed pedestrian networks. Similar to the collaborative mapping approach, the image processing approach is suitable for constructing pedestrian networks containing not only sidewalks and crosswalks, but also other pedestrian path types. Three requirements to employ the image processing approach are: (1) image sources are available in a given location, (2) costs for images are affordable, and (3) there is flexible time constraint.

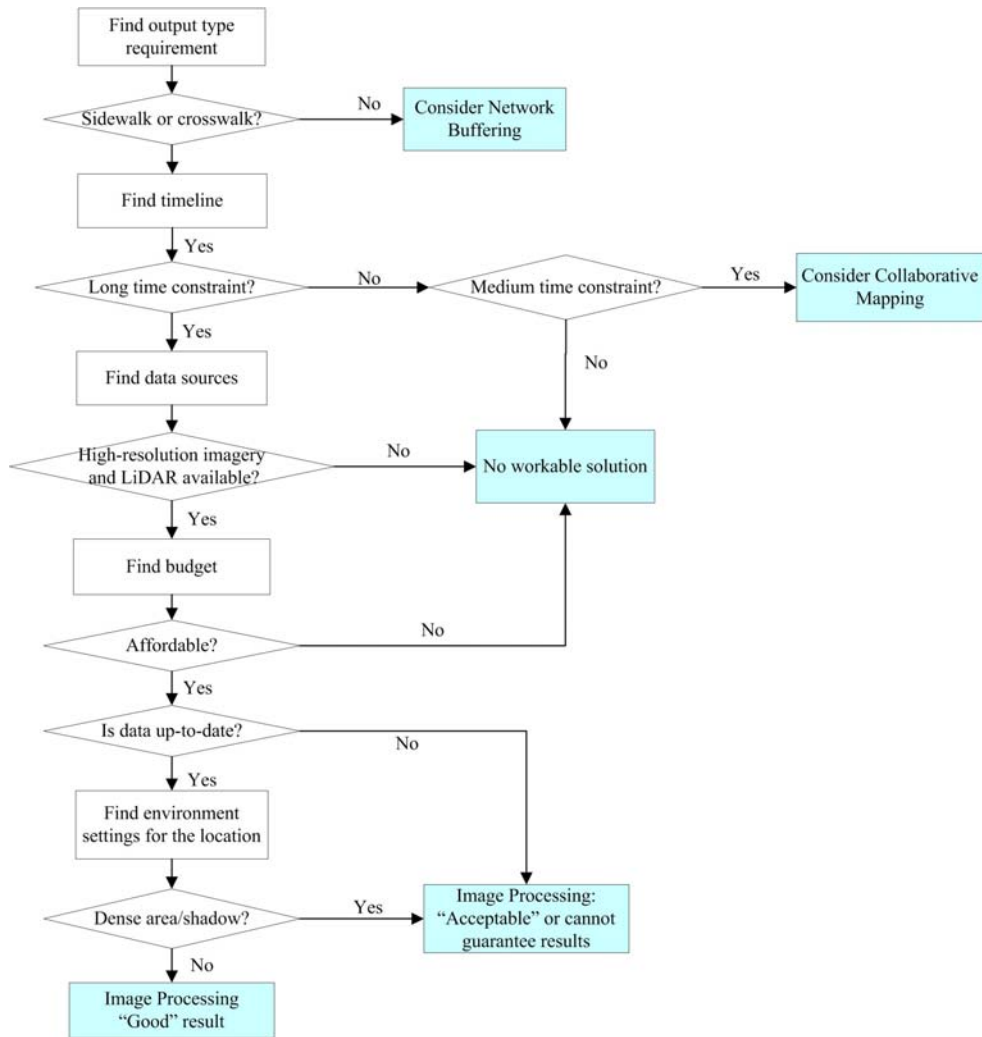


Figure 9-3. The criteria and quality result of the image processing approach

The image processing approach requires a significant amount of time to complete the processes of data preparation and network construction because of the complexity of algorithms involved. Quality of the constructed networks by the image processing approach is heavily dependent on the underlying orthoimages and LiDAR point clouds. The first criterion to examine is resolution of satellite images. Images with resolutions of 0.5 m or better are recommended. Therefore, if high-resolution imagery for a particular area is unavailable, the other approaches may be more suitable. Based on the results of the experiments, 3D information can assist feature extraction and improve results obtained by satellite images alone. For fusion of LiDAR and

satellite imageries, it is recommended that the data be up to date and images be captured from the same period of time for consistency. Another major influence on network extraction is the prevalence of shadow areas caused by trees or buildings in satellite imagery. To obtain good results in areas with many tall buildings, additional image processing algorithms are needed.

In general, sidewalks and crosswalks are two main pedestrian path types in urban areas (e.g., 73.83% of the pedestrian network are sidewalks and crosswalks in the study area). Clearly, no single approach can produce accurate and complete results. In projects where all three approaches are considered, it is suggested to construct pedestrian networks using the network buffering approach first and then to use the other two approaches to incrementally generate complete pedestrian networks. The advantage of collaborative mapping and image processing approaches is that they are able to generate other pedestrian path types (e.g., footpath).

10.0 CONCLUSIONS AND FUTURE RESEARCH

10.1 CONCLUSIONS

A pedestrian network is an essential resource in a variety of applications, especially in pedestrian navigation systems and urban planning projects. Pedestrian networks can be used as base maps for several tasks including route calculation for navigation systems, survey data entry (pedestrian facilities), and walkability index calculations (e.g., Link Node Ratio, Intersection Density) for urban planning projects. However, there is currently a lack of approaches and techniques for automatically constructing pedestrian networks. This dissertation was focused on the problem of automatically generating pedestrian networks and examined various techniques for their automatic construction. The dissertation first defined seven pedestrian path types and their relation to the pedestrian network data model. Three pedestrian network construction approaches, network buffering, collaborative mapping, and image processing, were presented, explored, and evaluated against a pedestrian network baseline in the University of Pittsburgh's main campus. The final result from each of the three approaches was the constructed pedestrian network containing the geometries and topologies of pedestrian path segments. In all three approaches, data inputs were prepared manually and pedestrian networks were constructed automatically. Based on the results, several conclusions can be drawn as discussed below.

The network buffering approach requires a suitable road network database in a given area as input and is able to generate only sidewalks and crosswalks, as they generally exist along roads. The approach is simple and fast, and creates good quality sidewalks and crosswalks with up-to-date and high quality road networks that contain the required attributes. The limitations of this approach are: (a) it cannot generate all pedestrian path types (i.e., footpath, trail, pedestrian bridge, and pedestrian tunnel) and (b) it may produce nonexistent pedestrian path segments.

The collaborative mapping approach requires walking GPS traces in a desired area as an input and is able to generate five pedestrian path types: sidewalk, crosswalk, footpath, trail, and building entrance. The approach cannot detect pedestrian bridges and pedestrian tunnels because the elevation data collected on pedestrian bridges by GPS devices are not of high quality and GPS signals are obscured in tunnels. The results show that the number of repeated GPS traces on the same path and the geometrical correctness of the constructed pedestrian networks are positively correlated. The percentages of geometrical and topological completeness are heavily dependent on available GPS traces. The advantages of this approach are: (a) it generates actual pedestrian path segments and (b) it is able to collect the pedestrian path types that other approaches (e.g., network buffering) cannot generate. Its limitations are: (1) the process of GPS data collection is time consuming and labor intensive and (2) GPS data are of low quality in the urban canyons.

The image processing approach utilizes satellite imagery and laser imagery to extract pedestrian path segments and construct pedestrian networks. The approach is able to extract five pedestrian path types: sidewalk, crosswalk, footpath, trail, and building entrance. The current implementation of the approach does not extract pedestrian bridges, tunnels, or stairs due to the limitation of the data sources (e.g., pedestrian tunnels are not captured in the images). From the

experiments, the pixel-based classification results showed that the satellite/laser fusion provided better results than either satellite or laser alone. The approach can automatically extract pedestrian networks, but does not perform well with images that contain shadows or dense objects.

In summary, this dissertation presents and discusses the concept of pedestrian network model and the three approaches for automatically constructing pedestrian networks. The results of the experiments indicate that these three approaches, while differing in complexity and outcome, are viable for automatically constructing pedestrian networks. However, no single approach can generate complete pedestrian networks. An alternative is to complement each approach by the others as the advantages of one approach can be used to offset the disadvantages of the other approaches. For instance, network buffering only generates pedestrian paths along roads, whereas collaborative mapping and image processing are able to generate pedestrian paths in other areas. Therefore, considering multi approaches could improve the performance of pedestrian network construction. One recommendation is to first use the network buffering approach to automatically generate sidewalks and crosswalks (two main pedestrian path types in urban areas) and then to include additional pedestrian path segments (those not captured by the network buffering) through the collaborative mapping and/or image processing approaches. With the current implementations of the three approaches, pedestrian bridges and tunnels are not collected; however, these two types are a very small percentage of pedestrian networks.

10.2 FUTURE RESEARCH

Future research should address the three main tasks of pedestrian network map generation: pedestrian network data model analysis, pedestrian network construction, and pedestrian network database design.

Firstly, a pedestrian network data model can represent objects either in 2D or in 3D. The pedestrian network data model employed in this dissertation is a 2D data model representing pedestrian networks as points and lines. However, points and lines do not represent some pedestrian areas well, such as parking lots or free walking areas. Future research should extend the current pedestrian network data model in order to represent geometries of walking areas and how to incorporate them into pedestrian networks.

Modern city footpath designs include many kinds of interchanges (e.g., stairs, pedestrian bridges, pedestrian tunnels, and walking areas between buildings) making 2D data models inappropriate to represent such 3D objects, especially in large-scale maps. Future research should address designing and building 3D pedestrian network data models and spatial operations in 3D pedestrian networks.

Secondly, future research on pedestrian network construction can be carried out in two directions: (1) improving the developed algorithms and (2) investigating and developing new approaches. The findings in this dissertation revealed that the three developed approaches are practical for automatically constructing pedestrian networks. However, future research is needed to improve the developed algorithms (e.g., network buffering algorithms and collaborative mapping algorithms) in order to generate more accurate results. Additionally, the experimental results revealed that there is no single approach that can generate complete pedestrian networks. Combinations of the three approaches to generate complete pedestrian networks should be

investigated. The feasibility of combining network buffering with collaborative mapping is discussed in Appendix A. Future work will need to compare the performance of an integrated approach and a single approach, in terms of geometrical and topological completeness.

Currently, several collaborative mapping projects allow people to contribute their travelled GPS traces; however, the map generation process still requires manual work. Future work could integrate the network construction algorithm presented in this dissertation with existing collaborative mapping projects (e.g., OpenStreetMap).

New data sources and new approaches for pedestrian network construction are other topics of future research. With today's advanced technologies, many valuable datasets are unexplored. Examples of new data sources are Synthetic Aperture Radar (SAR) imagery and Google Street View. SAR, an active microwave instrument, produces high-resolution imagery of the Earth's surface in all weather. Google Street View supports 360-degree panorama images in wide areas. Such new data sources could be used to extract pedestrian networks, especially Google street view that provides close-up images and makes it possible to detect pedestrian bridges and tunnels. Similar to data sources, several techniques, such as snakes or optimization techniques, could be explored.

Lastly, future research should explore pedestrian network databases. One area for exploration is 3D database design for pedestrian networks. Research in this area should focus on ways to efficiently store, visualize, and manipulate complex geometrical models. Along with the database design, automatic attribute extraction techniques on pedestrian path segments, e.g., to support pedestrian navigation systems/services, are needed. Examples of attributes are distance, width, surface type, surface condition, stairs, and slope. Research could also be focused on connecting pedestrian networks with other existing transportation networks, such as road

networks, hallway networks, public transportation networks, subway networks, and sky train networks, in order to support universal/multimode navigation services.

APPENDIX A

VERIFICATION: SIDEWALKS AND CROSSWALKS USING GPS TRACES

The experimental results of the network buffering approach reveal that the approach may generate non-existing sidewalk and crosswalk features. The existence of sidewalks and crosswalks generated from the network buffering can be verified by using GPS traces collected from the collaborative mapping approach. A verification algorithm and an experiment are provided in the proceeding sections. Furthermore, combining different approaches to improve the completeness and accuracy of generated pedestrian networks is explored.

A.1 VERIFICATION ALGORITHM

This section discusses the algorithm to verify the existence of sidewalks and crosswalk using walking GPS traces. Figure A-1 shows the flowchart of the verification algorithm.

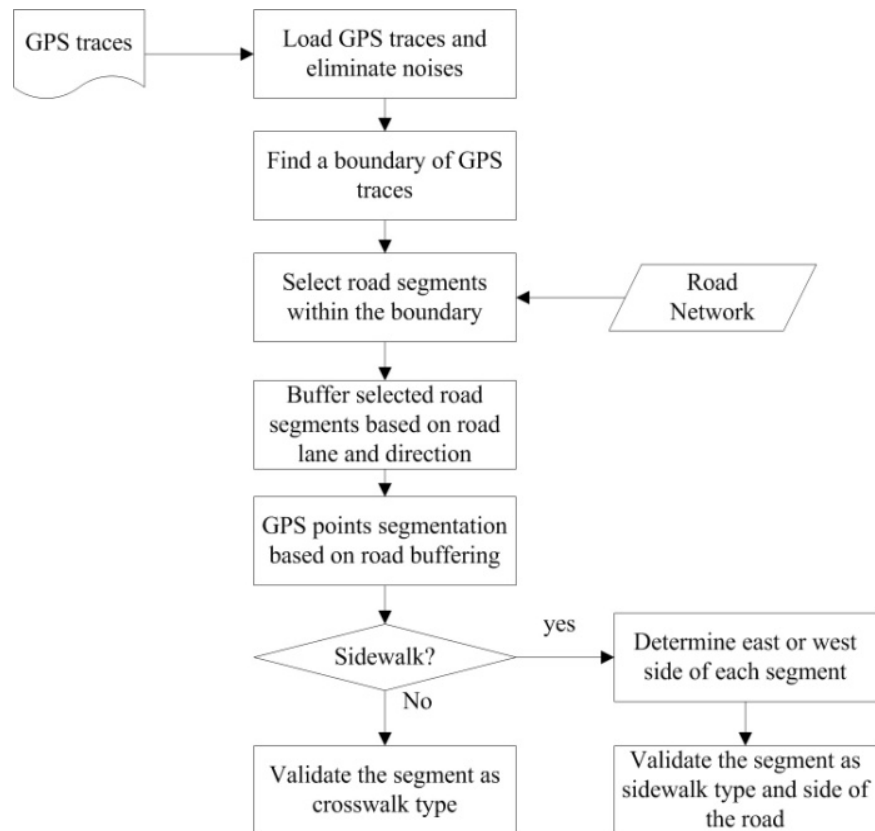


Figure A-1. Flowchart of verification of sidewalks and crosswalks using GPS traces

The algorithm starts by loading GPS traces and eliminate outliers caused by GPS errors and the TTFF problem. After filtering GPS traces, the road segments within the boundary of the filtered GPS traces are selected, in order to reduce the number processed road segments. Then, the selected road segments are buffered using a road lane category and road direction as the buffer size. After buffering selected road segments, the filtered GPS points are clustered using the geometry relationship “within”. GPS points are grouped into the same segment if their coordinates are within the same buffer geometry. An example of GPS point segmentation is illustrated in Figure A-2.

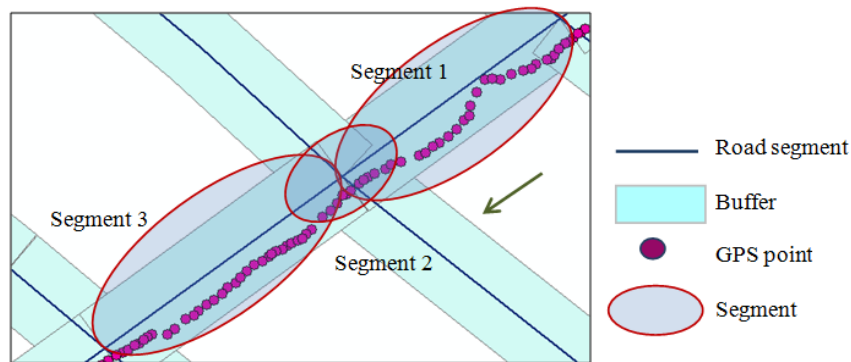


Figure A-2. An example of GPS point segmentation

The next task is to determine whether or not the segment crosses the road and the side of the road on which the segment is. To achieve this task, we first determine the geographic relationship between the road segment and associated GPS points using the bearing and geographical distance. Between successive GPS points, the bearing is calculated by using the great circle navigation formula (Williams, 2008) and the geographical distance is calculated by using the haversine formula (Sinnot, 1984). A segment is classified as a “sidewalk” when the average bearing between successive points is closely parallel to the bearing of a particular road segment. Moreover, the total distance between successive points in a segment should be close to the length of a road segment in order to be considered as a sidewalk segment, otherwise, these GPS points are considered as noise. A segment is identified as a “crosswalk” when the average bearing between successive points is nearly perpendicular to the bearing of the road segment.

To determine the east or west side of a road segment, the linear regression model is employed and the pseudocode of the side determination is illustrated in Figure A-3.

```

Side determination
Get the coordinate  $(x_1, y_1)$  of the beginning point of a road segment
Get the coordinate  $(x_2, y_2)$  of the end point of a road segment
Get the coordinate  $(x_3, y_3)$  of a GPS point
Case road segment of
  Vertical line  $((x_2 - x_1) == 0)$ :
    If  $(x_3 < x_2)$  then a GPS point lies to the west of the road
    Else if  $(x_3 > x_2)$  then a GPS point lies to the east of the road
    Else a GPS point lies on the road
    End if
  HeadingNorth  $(m > 0)$ :
    If  $(y_3 > m * x_3 + b)$  then a GPS point lies to the west of the road
    Else if  $(y_3 < m * x_3 + b)$  then a GPS point lies to the east of the road
    Else a GPS point lies on the road
    End if
  HeadingSouth  $(m < 0)$ :
    If  $(y_3 < m * x_3 + b)$  then a GPS point lies to the west of the road
    Else if  $(y_3 > m * x_3 + b)$  then a GPS point lies to the east of the road
    Else a GPS point lies on the road
    End if
  Horizontal line  $(m=0)$ :
    If  $(y_3 > y_2)$  then a GPS point lies to the west of the road
    Else if  $(y_3 < y_2)$  then a GPS point lies to the east of the road
    Else a GPS point lies on the road
    End if
End Case

```

Figure A-3. Pseudocode of side determination

In practice, the coordinates of two end points of each road segment in the road network are used. One point (x_1, y_1) is considered as the start and the other (x_2, y_2) as the end point. There are four possible cases of road segment alignment. The first is vertical line which uses the longitude of a GPS point to determine the side. A GPS point lies to the west when the longitude of a GPS point is less than the longitude of either the start or the end point, otherwise it lies to the east. For other three cases, the slope and intercept of each road segment are calculated in order to generate a line equation, using the linear regression model. The heading of each road segment is indicated by the latitude of each coordinate. The second case, the heading of a road segment points to north ($m > 0$), if the latitude of the start point is less than the latitude of the end point, otherwise ($m < 0$), it points to south (the third case). The side of a GPS point lies to the west of a road, when the heading of a road segment points to north and the latitude of a GPS point (y_3) is greater than the calculated latitude from the line equation. If the heading of a road segment points to south, a GPS point lies to the east of a road when the latitude of a GPS point (y_3) is greater than the calculated latitude from the line equation. The last case, horizontal line, uses the latitude of a GPS point to determine the

side of the segment. A GPS point lies to the west when the latitude of a GPS point is greater than the latitude of either the start or end point, otherwise it lies to the east.

To illustrate the process of determining side of a road segment, two examples are given. The first example is a straight road segment that is composed of two points, as shown in Figure A-4 (left) and the second example is a curved line that is composed of seven points, as shown in Figure A-4 (right). A GPS point (within the circle) in the first example is determined to be on the west side of the road segment because the slope of a line is greater than zero and the calculated latitude is less than the latitude of this GPS point. On the other hand, a GPS point (within the circle) in the second example is determined to be on the east side of the road segment. Using only one GPS point along a road segment is not sufficient to determine the actual side of the road segment. To reduce biases in determining side of a road segment to which every GPS point belongs, the probability of being east or west is calculated. The final result is determined by majority of GPS points.

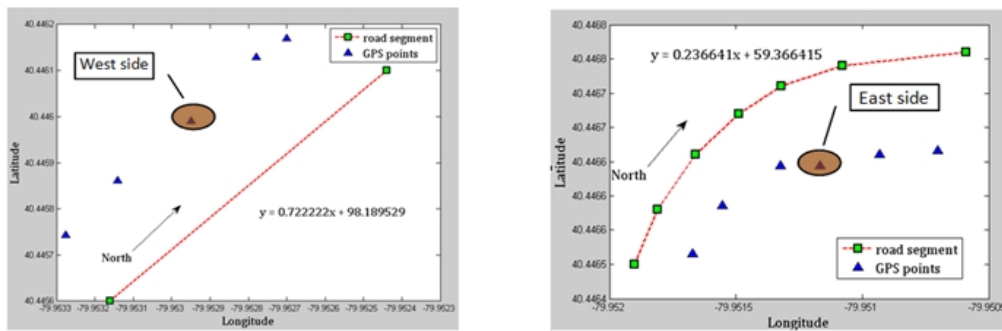


Figure A-4. Examples of establishing sides of a road segment

A.2 EXPERIMENT

The goal of this experiment is to demonstrate the possibility of using walking GPS point to verify the existence of actual sidewalks and crosswalks. Three metrics were used to evaluate the algorithm: (1) accuracy of distinguishing between sidewalks and crosswalks, (2) success rate of sidewalk/ crosswalk determination, and (3) accuracy of determining side of the road for sidewalk segments.

A.2.1 Test Data

The testing environment was confined within the University of Pittsburgh's main campus which includes both high-rise buildings and open sky environments. Ten GPS traces (with fixed interval of 1 s) along sidewalks and crosswalks were collected and treated as separate inputs to the algorithm and experimented one at a time. Number of GPS points, number of sidewalk segments, crosswalk segments and total length of each actual walking path were collected, in order to validate the performance of the algorithm. The characteristics of the ten GPS traces used in the experiment are shown in the Table A-1.

Table A-1. GPS traces used in the experiment

Trip #	# GPS points	Actual Walking Paths			
		# segments	# sidewalks	#crosswalks	Total Length (m)
1	992	32	24	8	1,486.90
2	325	22	13	9	1,234.00
3	282	20	14	6	1,244.50
4	1,264	73	44	29	3,019.10
5	1,247	68	45	23	3,159.60
6	767	37	28	9	2,395.50
7	1,127	42	30	12	2,784.50
8	1,311	49	37	12	3,121.70
9	1,307	56	41	15	3,756.40
10	881	28	20	8	1,704.10

A.2.2 Experimental results

The purposes of this experiment were to measure the accuracy of the algorithm in classifying path type, sidewalk and crosswalk, and to examine the accuracy of the algorithm in identifying the correct side of the road for each sidewalk segment. Inputs to this experiment included ten GPS traces and the road network of the testing area. The result from the algorithm was the segments of pedestrian path type along with road segment number and the side of the road. This result was compared against actual pedestrian paths travelled (identified from data collectors after trips). The number of actual sidewalks and crosswalks travelled and those generated by the algorithm in each trip were reported. For comparison, the numbers of correctly identified sidewalks (S_c), crosswalks (C_c), and side of sidewalks (SS_c) were calculated. Three evaluation parameters to validate the performance of the algorithm are accuracy of path type identification (A_p), success rate of sidewalk/ crosswalk determination (SR), and accuracy of side identification (A_s). A_p , SR, and A_s values range from 0 to 1, with 1 being highest. A_p , SR, and A_s are calculated as follows:

$$A_p = (S_c + C_c) / \text{number of generated sidewalk and crosswalk segments} \quad (\text{A.1})$$

$$\text{SR} = (S_c + C_c) / \text{actual number of travelled sidewalks and crosswalks} \quad (\text{A.2})$$

$$A_s = SS_c / \text{number of generated sidewalk segments} \quad (\text{A.3})$$

A_p was calculated by dividing the number of correctly identified sidewalks and crosswalks by the number of generated segments (sidewalk and crosswalk segments) by the algorithm. SR was calculated by dividing the number of correctly identified sidewalks and crosswalks by the actual number of travelled segments for both sidewalks and crosswalks. A_s

was calculated by dividing the number of correctly identified sides by the number of generated sidewalk segments by the algorithm. Table A-2 shows the result.

Table A-2. Results of three evaluation metrics

Trip #	# actual travelled sidewalk	# actual travelled crosswalk	# generated sidewalk	# generated crosswalk	S_c	C_c	SS_c	A_p	SR	A_s
Trip 1	24	8	19	10	18	7	18	0.862	0.781	0.947
Trip 2	13	9	11	9	10	9	10	0.95	0.864	0.909
Trip 3	14	6	11	8	11	1	4	0.632	0.600	0.364
Trip 4	44	29	41	28	39	18	30	0.826	0.781	0.732
Trip 5	45	23	40	23	39	23	39	0.984	0.912	0.975
Trip 6	28	9	25	8	22	8	21	0.909	0.811	0.840
Trip 7	30	12	30	10	28	7	20	0.875	0.833	0.667
Trip 8	37	12	35	15	31	14	30	0.9	0.918	0.857
Trip 9	41	15	34	13	31	12	30	0.915	0.768	0.882
Trip 10	20	8	21	9	19	5	19	0.8	0.857	0.905
Average value								0.865	0.812	0.808

The average accuracy of path type identification, success rate of sidewalk/crosswalk determination, and accuracy of side identification are 0.865, 0.812, and 0.808, respectively. The results from most trips are near optimum (greater than 85%), which means that the algorithm is able to determine pedestrian path type and side of the road segments from collected walking GPS traces. However, the algorithm performed poorly around high-rise buildings and narrow road areas as it identified wrong walking sides (e.g., Trip3 and Trip7).

BIBLIOGRAPHY

- AASHTO 2005. A policy on Design Standards.
- ACKERMANN, F. 1999. Airborne laser scanning-present status and future expectations. *ISPRS Journal of Photogrammetry & Remote Sensing*, 54, 64-67.
- ADA 2004. Americans with disabilities act and architectural barriers act accessibility guidelines. United States Access Board.
- AMBLER, S. W. 2005. *The Elements of UML 2.0 Style*, Cambridge University Press.
- ARIKAWA, M., KONOMI, S. & OHNISHI, K. 2007. Navitime: Supporting Pedestrian Navigation in the Real World. *Journal of Urban Computing*, 21-29.
- ASPRS 1989. ASPRS Accuracy Standards for Large-Scale Maps. *Photogrammetric Engineering and Remote Sensing*, 55, 1068-1070.
- AWRANGJEB, M. & LU, G. 2008. Robust Image Corner Detection Based on the Chord-to-Point Distance Accumulation Technique. *IEEE Transactions on Multimedia*, 10, 1059-1072.
- BEALE, L., FIELD, K., BRIGGS, D., PICTON, P. & MATTHEWS, H. 2006. Mapping for Wheelchair Users: Route Navigation in Urban Spaces. *The Cartographic journal*, 43, 68-81.
- BING. 2011. *Bing Map* [Online]. Available: <http://www.bing.com/maps/>.
- BRESENHAM, J. E. 1965. Algorithm for computer control of a digital plotter. *Journal of IBM Systems*, 4, 25-30.
- BRUNTRUP, R., EDELKAMP, S., JABBER, S. & SCHOLZ, B. Incremental Map Generation with GPS Traces. 8th International IEEE Conference on Intelligent Transportation Systems, 2005 Vienna, Austria. 413-418.
- BUREAU, U. S. C. 2011. *TIGER/Line* [Online]. Available: <http://www.census.gov/geo/www/tiger/>.
- BURGES, C. J. C. 1998. A Tutorial on Support Vector Machines for Pattern Recognition. *Data Mining and Knowledge Discovery*, 2, 121-167.
- CAO, L. & KRUMM, J. From GPS Traces to a Routable Road Map. the 17th ACM SIGSPATIAL International Conference on Advances in Geographic Information Systems, 2009 Seattle, Washington 3-12.
- CASTRO, M., IGLESIAS, L., RODRIGUEZ-SOLANO, R. & SANCHEZ, J. A. 2006. Geometric modelling of highways using global positioning system (GPS) data and spline approximation. *Transportation Research Part C: Emerging Technologies*, 14, 233-243.
- CENTER, P. A. B. I. 2009. *Sidewalks and Walkways* [Online]. Available: <http://www.walkinginfo.org/engineering/roadway-sidewalks.cfm> [Accessed August 16 2009].

- CHANG, C.-C. & LIN, C.-J. 2011. LIBSVM: A library for support vector machines, . *ACM Transactions on Intelligent Systems and Technology*, 2, 1-27.
- CHANG, K.-T. 2010. *Introduction to Geographic Information Systems*, McGraw Hill.
- CHEN, C. & CHENG, Y. Roads Digital Map Generation with Multi-track GPS Data. 2008 International Workshop on Geoscience and Remote Sensing, 2008. 508-511.
- CHIANG, Y.-Y. & KNOBLOCK, C. A. 2010. Extracting Road Vector Data from Raster Maps. *Lecture Notes in Computer Science*, 6020, 93-105.
- CHIN, G. K. W., NIEL, K. P. V., GILES-CORTI, B. & KNUIMAN, M. 2008. Accessibility and connectivity in physically activity studies: The impact of missing pedestrian data. *Journal of Preventive Medicine*, 46, 41-45.
- CHRISMAN, N. R. The role of quality information in the long-term functioning of a geographic information system. AutoCarto, 1983 Ottawa, ON. 303-312.
- CHRISMAN, N. R. 1991. *The error component in spatial data*, Longman, New York.
- CLIFTON, K. J., SMITH, A. D. L. & RODRIGUEZ, D. 2007. The development and testing of an audit for the pedestrian environment. *Journal of Landscape and Urban Planning*, 80, 95-110.
- CLODE, S., ROTTENSTEINER, F., KOOTSOOKOS, P. & ZELNIKER, E. 2007. Detection and Vectorization of Roads from LiDAR Data. *Photogrammetric Engineering & Remote Sensing*, 73, 517-535.
- CONGALTON, R. G. 1991. A Review of Assessing the Accuracy of Classifications of Remotely Sensed Data. *Remote Sensing of Environment*, 37, 35-46.
- DAVIES, J. J., BERESFORD, A. R. & HOPPER, A. 2006. Scalable, Distributed, Real-Time Map Generation. *IEEE Pervasive Computing*, 5, 47-54.
- DE MAESSCHALCK, R., JOUAN-RIMBAUD, D. & MASSART, D. L. 2000. The Mahalanobis distance. *Chemometrics and Intelligent Laboratory Systems*, 50, 1-18.
- DONG, Z.-B., SONG, G.-J., XIE, K.-Q. & WANG, J.-Y. 2009. An Experimental Study of Large-Scale Mobile Social Network. *18th International World Wide Web Conference (WWW2009)*. Madrid, Spain.
- EDELKAMP, S. & SCHRODLL, S. 2003. Route Planning and Map Inference with Global Positioning Traces. *Computer Science in Perspective*, 128-151.
- EKHTARI, N., SAHEBI, M. R., ZOEJ, M. J. V. & MOHAMMADZADEH, A. 2008. Automatic Building Detection from LiDAR Point Cloud Data. *International Archives of Photogrammetry and Remote Sensing*, XXXVII, 473-477.
- EKPENYONG, F., PALMER-BROWN, D. & BRIMICOMBE, A. 2009. Extracting road information from recorded GPS data using snap-drift neural network. *Journal of Neurocomputing*, 73, 23-46.
- ELIAS, B. Pedestrian Navigation-Creating a tailored geodatabase for routing. 4th workshop on positioning, navigation and communication (WPNC'07), 2007 Hannover, Germany. IEEE, 41-47.
- FATHI, A. & JRUMM, J. 2010. Detecting Road Intersections from GPS Traces. In: FABRIKANT, S., REICHENBACHER, T., VAN KREVELD, M. & SCHLIEDER, C. (eds.) *Lecture Notes in Computer Science*. Springer Berlin / Heidelberg.
- FRANK, L. D., ANDRESEN, M. A. & SCHMID, T. L. 2004. Obesity Relationships with Community Design, Physical Activity, and Time Spent in Cars. *American Journal of Preventive Medicine*, 27, 89-96.

- FRANK Y, S. & CHENG, S. 2005. Automatic seeded region growing for color image segmentation. *Image and Vision Computing*, 23, 877-886.
- FREEMAN, H. 1974. Computer Processing of line-drawing images. *Computing Surveys*, 6, 57-97.
- GAISBAUER, C. & FRANK, A. U. Wayfinding Model for Pedestrian Navigation. 11th International Conference on Geographic Information Science 2008 University of Girona, Spain. 1-9.
- GEOTOOLS. 2009. *GeoTools: User Guide* [Online]. Available: <http://geotools.org/> [Accessed June 15 2009].
- GHITA, O. & WHELAN, P. F. 2002. Computational approach for edge linking. *Journal of Electronic Imaging*, 11, 479-485.
- GILLAVRY, E. M. 2006. Collaborative Mapping and GIS: An alternative Geographic Information Framework. In: S.BALRAM & S.DRAGICEVIC (eds.) *Collaborative Geographic Information Systems*. IGI Publishing.
- GOODCHILD, M. F. 2007. Citizens as sensors: the world of volunteered geography. *GeoJournal*, 69, 211-221.
- GOOGLE. 2010. *Google maps* [Online]. Available: <http://maps.google.com/maps?hl=en&tab=wl>.
- GUO, T., IWAMURA, K. & KOGA, M. 2007. Towards High Accuracy Road Maps Generation from Massive GPS Traces Data. *IEEE International Geoscience and Remote Sensing Symposium (IGRASS 2007)*, 667-670.
- HAKLEY, M. & WEBER, P. 2008. OpenStreetMap: User-Generated Street Maps. *IEEE Pervasive Computing*, 7, 12-18.
- HAMPE, M. & ELIAS, B. 2003. Integrating topographic information and landmarks for mobile navigation.
- HANDY, S., BOARNET, M. G., EWING, R. & KILLINGWORTH, R. E. 2002. How the built environment affects physical activity: views from urban planning. *American Journal of preventive Medicine*, 23, 64-73.
- HANDY, S., BUTLER, K. & PATERSON, R. G. 2003. Planning for Street Connectivity - Getting from Here to There. In: ASSOCIATION, A. P. (ed.). Chicago.
- HELAL, A., MOORE, S. E. & RAMACHANDRAN, B. 2001. Drishti: An Integrated Navigation System for Visually Impaired and Disabled. *5th International Symposium on Wearable computers*. Zurich, Switzerland.
- HERMES, L., FRIEAUFF, D., PUZICHA, J. & BUHMANN, J. M. Support Vector Machines for Land Usage Classification in Landsat TM Imagery. *IEEE International Geoscience and Remote Sensing Symposium (IGARSS)*, 1999 Hamburg. 348-350.
- HINZ, S. & BAUMGARTNER, A. 2003. Automatic extraction of urban road networks from multi-view aerial imagery. *ISPRS Journal of Photogrammetric*, 58, 83-98.
- HINZ, S., BAUMGARTNER, A., MAYER, H., WIEDEMANN, C. & EBNER, H. 2001. Road extraction focussing on urban areas. In: BALTSAVIAS, E., GRUEN, A. & VAN GOOL, L. (eds.) *Automatic Extraction of Man-Made Objects from Aerial and Space Images (III)*. Rotterdam: Balkema Publishers.
- HOFMANN, P. 2001. Detecting buildings and roads from IKONOS data using additional elevation information. *GIS*, 6, 28-33.

- HOLDEN, W. 2009. *Advertising to Fuel Mobile Social Networking Growth as UGC Revenues Reach \$7.3bn by 2013* [Online]. Juniper Research Ltd. Available: <http://juniperresearch.com/shop/viewpressrelease.php?pr=108> [Accessed August 4 2009].
- HOLONE, H., MISUND, G. & HOLMSTEDT, H. Users Are Doing It For Themselves: Pedestrian Navigation With User Generated Content. *International Conference On Next Generation Mobile Applications, Services and Technologies (NGMAST '07)*, 2007 Cardiff, UK.: IEEE, 91-99.
- HU, X., TAO, C. V. & HU, Y. 2004. Automatic Road Extraction From Dense Urban Area by Integrated Processing of High Resolution Imagery and LIDAR Data. *IAPRSIS XXXV-B3*, 288 - 292.
- HUMPEL, N., OWEN, N. & LESLIE, E. 2002. Environment factors associated with adults' participation in physical activity: a review. *American Journal of preventive Medicine*, 22, 188-199.
- INSIDEGNSS 2008. New GPS Standard Positioning System (SPS) Performance Standard. 10.
- KARIMANZIRA, D., P.OTTO & WERNSTEDT, J. 2006. Application of Machine Learning Methods to Route Planning and Navigation for Disabled people. *The 25th IASTED International Conference Lanzarote*. Canary islands, Spain.
- KARIMI, H. A. & LIU, S. 2004. Developing an Automated Procedure for Extraction of Road Data from High-Resolution Satellite Images for Geospatial Information Systems. *Journal of Transportation Engineering*, 130, 621-631.
- KARIMI, H. A., ZIMMERMAN, B., OZCELIK, A. & ROONGPIBOONSOPIT, D. 2009. SoNavNet: A Framework for Social Navigation Networks. *International Workshop on Location Based Social Networks (LBSN'09)*. Seattle, WA.
- KASEMSUPPAKORN, P. & KARIMI, H. A. 2008. Data Requirements and a Spatial Database for Personalized Wheelchair Navigation *2nd International Convention on Rehabilitation Engineering & Assistive Technology*. Bangkok, Thailand.
- KASEMSUPPAKORN, P. & KARIMI, H. A. 2009a. Pedestrian Network Data Collection through Location-Based Social Networks. *The 5th International Conference on Collaborative Computing: Networking, Applications and Worksharing* Washington D.C., USA: IEEE.
- KASEMSUPPAKORN, P. & KARIMI, H. A. 2009b. Personalised routing for wheelchair navigation. *Journal of Location Based Services*, 3, 24-54.
- KAUFMAN, L. & ROUSSEEUW, P. J. 1987. Clustering by means of medoids. In: DODGE, Y. (ed.) *Statistical Data Analysis based on the L1 Norm*. Elsevier/ North-Holland Amsterdam.
- KAUFMAN, L. & ROUSSEEUW, P. J. 1990. *Finding Groups in Data: An Introduction to Cluster Analysis*, John Wiley and Sons Inc.
- KOTHURI, R., GODFRIND, A. & BEINAT, E. 2007. *Pro Oracle Spatial for Oracle Database 11g*, APress.
- LAM, L., LEE, S.-W. & SUEN, C. Y. 1992. Thinning methodologies-a comprehensive survey. *Pattern Analysis and Machine Intelligence, IEEE Transactions*, 14, 869-885.
- LEE, Y. & CHO, S.-B. 2007. Extracting Meaningful Contexts from Mobile Life Log In: YIN, H., TINO, P., CORCHADO, E., BYRNE, W. & YAO, X. (eds.) *Lecture Notes in Computer Science*. Springer Berlin / Heidelberg.

- LESLIE, E., COFFEE, N., FRANK, L., OWEN, N., BAUMAN, A. & HUGO, G. 2007. Walkability of local communities: Using geographic information systems to objectively assess relevant environment attributes. *Journal of Health & Place*, 13, 111-122.
- LIM, J. S. 1990. *Two-Dimensional Signal and Image Processing*, Englewood Cliffs, NJ, Prentice Hall,.
- LO, C. P. & YEUNG, A. K. W. 2006. *Concepts and techniques of geogrphic information systems*, Pearson Prentice Hall
- MAPQUEST. 2011. *MapQuest* [Online]. Available: <http://www.mapquest.com/>.
- MAYERHOFER, B., PRESSEL, B. & WIESER, M. 2008. ODILIA: A Mobility Concept for the Visually Impaired. In: MIESENBERGER, K., KLAUS, J., ZAGLER, W. & KARSHMER, A. (eds.) *Computers Helping People with Special Needs*. Springer.
- MENG, X., WANG, L. & CURRIT, N. 2009. Morphology-based building detection from airborne Lidar data. *Photogrammetric Engineering & Remote Sensing* 75, 437-442.
- MORGAN, M. & TEMPFLI, K. 2000. Automatic Building Extraction from Airborne Laser Scanning Data. *International Archives of Photogrammetry and Remote Sensing*, 33, 616-623.
- MURUGESAN, S. 2007. Understanding Web 2.0. *IT Professional*, 9, 34-41.
- NAVTEQ. 2010. *NAVTEQ* [Online]. Available: <http://www.navteq.com/>.
- NIEHOEFER, B., BURDA, R., WIETFIELD, C., BAUER, F. & LUEERT, O. GPS Community Map Generation for Enhanced Routing Methods based on Trace-Collection by Mobile Phones. the 1st International Conference on Advances in Satellite and Space Communications (SPACOMM), 2009 Colmar. 156-161.
- NOKIA. 2008. *Nokia Maps 2.0* [Online]. Available: <http://betalabs.nokia.com/betas/view/nokia-maps-20>.
- NRC 2003. NCHRP Report 506: Quality and Accuracy of Positional Data in Transportaion. Washington, D.C.: Transportation Research Board.
- OCHIENG, W. Y., QUDDUS, M. A. & NOLAND, R. B. 2003. Map-Matching in Complex Urban Road Networks. *Brazilian Journal of Cartography*, 55, 1-18.
- OGC. 2003. *OpenGIS Reference Model* [Online]. Available: http://portal.opengeospatial.org/files/?artifact_id=3836.
- OSM. 2010. *Public GPS Traces* [Online]. Available: <http://www.openstreetmap.org/traces>.
- PAMAP. 2008. *PAMAP Program Cycle 1 High Resolution Orthoimage 2003 - 2006* [Online]. Available: http://www.pasda.psu.edu/uci/MetadataDisplay.aspx?entry=PASDA&file=PAMAP_cycle1.xml&dataset=77.
- PAMAP. 2011. *PAMAP - The Digital Base Map of Pennsylvania* [Online]. Available: <http://www.dcnr.state.pa.us/topogeo/pamap/index.aspx> [Accessed January 2011].
- PASDA. 2011. *Pennsylvania Spatial Data Access* [Online]. Available: <http://www.pasda.psu.edu/>.
- PRESSEL, B. & WEISER, M. 2006. A Computer-Based Navigation System Tailored to the Needs of Blind People. In: MIESENBERGER, K., KLAUS, J., ZAGLER, W. & KARSHMER, A. (eds.) *Computers Helping People with Special Needs*. Springer Berlin.
- QUDDUS, M. A. 2006. *High Integrity Map Matching Algorithms for Advanced Transport Telematics Applications*. Ph.D., Imperial College London.

- QUDDUS, M. A., NOLAND, R. B. & OCHIENG, W. 2009. The Effects of Navigation Sensors and Spatial Road Network Data Quality on the Performance of Map Matching Algorithms. *GeoInformatica*, 13, 85-108.
- RANDALL, T. A. & BAETZ, B. W. 2001. Evaluating Pedestrian Connectivity for Suburban Sustainability. *Journal of Urban Planning and Development*, 127, 1-15.
- RENSLOW, M. S. 2001. Predicting NW Forest Stand Structural Characteristics Using Multi-Return LIDAR. Available: <http://proceedings.esri.com/library/userconf/proc01/professional/papers/pap214/p214.htm>
- ROGERS, S., LANGLEY, P. & WILSON, C. 1999. Mining GPS Data to Augment Road Models. *International Conference on Knowledge Discovery and Data Mining*.
- SCHLOSSBERG, M. 2006. From TIGER to Audit Instruments: Measuring Neighborhood Walkability with Street Data Based on Geographic Information Systems. *Journal of the Transportation Research Board*, 1982, 48-56.
- SCHROEDLL, S., WAGSTAFF, K., ROGERS, S., LANGLEY, P. & WILSON, C. 2004. Mining GPS Traces for Map Refinement. *Data Mining and Knowledge Discovery*, 9, 59-87.
- SHEKHAR, S. 2008. *Ground Truth Verification in Urban Planning and Management: A Case Study of Pune City* [Online]. Available: <http://ssrn.com/abstract=1285442> [Accessed December 2009].
- SHI, W., SHEN, S. & LIU, Y. Automatic Generation of Road Network Map from Massive GPS Vehicle Trajectories. the 12th International IEEE Conference on Intelligent Transportation Systems, 2009 St.Louis, MO, USA. 48-53.
- SINNOT, R. W. 1984. Virtues of the Haversine. *Sky and Telescope*, 68, 158.
- SMITH, M. J. D., GOODCHILD, M. F. & LONGLEY, P. A. 2007. *Geospatial Analyst: A Comprehensive Guide to Principles, Techniques and Software Tools*, Matador.
- SOBEK, A. D. & MILLER, H. J. 2006. U-Access: a web-based system for routing pedestrians of differing abilities. *Journal of Geographical Systems*, 8, 269-287.
- SONG, M. & CIVCO, D. 2004. Road Extraction Using SVM and Image Segmentation. *Photogrammetric Engineering & Remote Sensing*, 70, 1365-1371.
- SOUTHWORTH, M. 2005. Designing the Walkable City. *Journal of urban planning and development*, 131, 246-257.
- STARK, A., RIEBECK, M. & KAWALEK, J. 2007. How to Design an Advanced Pedestrian Navigation System: Field Trial Results. *IEEE International Workshop on Intelligent Data Acquisition and Advanced Computing Systems: Technology and Applications*. Dortmund, Germany.
- STEINIGER, S., NEUN, M. & EDWARDES, A. 2006. Lecture notes: Foundations of location based services. *University of zurich*.
- TAO, G. & YASUOKA, Y. 2002. Combining high resolution satellite imagery and airborne laser scanning data for generating bareland DEM in urban areas. *International Archives of the Photogrammetry, Remote Sensing and Spatial Information Sciences*, V.
- THEODORIDIS, Y. 2003. Ten Benchmark Queries for Location-Based Services. *The Computer Journal*, 46, 713-725.
- TITHERIDGE, H., MACKETT, R. & ACHUTHAN, K. 2007. Developing methods for measuring pedestrian accessibility. *10th International Conference on Computers in Urban Planning and Urban Management (CUPUM'07)*. Iguassu Falls, BRAZIL.

- TOMTOM. 2010. *TeleAtlas Map* [Online]. Available: <http://licensing.tomtom.com/OurProducts/MapData/index.htm>.
- USGS 2009. The National Map-Orthoimagery. In: INTERIOR, U. S. D. O. T. (ed.).
- VAPNIK, V. N. 1995. *The nature of Statistical Learning Theory*, New York, Spring-Verlag.
- VOLKER, T. & WEBER, G. 2008. RouteCheck: Personalized Multicriteria Routing for Mobility Impaired Pedestrians. *the 10th international ACM SIGACCESS conference on Computers and accessibility*. Halifax, Nova Scotia, Canada: ACM.
- WALTER, V., KADA, M. & CHEN, H. Shortest Path Analyses in raster maps for pedestrian navigation in location based systems. International Symposium on Geospatial Databases for sustainable development, 2006 Goa, India. ISPRS Technical Commission IV.
- WANG, S., MIN, J. & YI, B. K. Location-Based Services for Mobiles: Technologies and Standards. IEEE International Conference on Communication (ICC'08), 2008 Beijing, China.
- WANG, Y., TIAN, Y., TAI, X. & SHU, L. 2006. Extraction of Main Urban Roads from High Resolution Satellite Images by Machine Learning. *Lecture Notes in Computer Science*, 3851, 236-245.
- WANG, Z. & ZHANG, H. Edge Linking Using Geodesic Distance and Neighborhood Information. International Conference of Advanced Intelligent Mechatronics, IEEE, 2008 Xi'an, China. 151-155.
- WASHINGTONSTATELEGISLATURE. 2003. *RCW 46.04.400 Pedestrian* [Online]. Available: <http://apps.leg.wa.gov/RCW/default.aspx?cite=46.04.400> [Accessed July 5 2009].
- WIEDEMANN, C. 2003. External Evaluation of Road Networks. *ISPRS Archives*, XXXIV, 93-98.
- WIKILOC. 2010. *WikiLoc* [Online]. Available: <http://wikiloc.com/wikiloc/home.do>.
- WIKIMAPIA. 2011. *WikiMapia* [Online]. Available: <http://www.wikimapia.org>.
- WILLIAMS, E. 2008. *Aviation Formulary Version 1.44* [Online]. Available: <http://williams.best.vwh.net/avform.htm> [Accessed May 2009].
- WORRALL, S. & NEBOT, E. 2007. Automated Process for Generating Digitised Maps through GPS Data Compression. *2007 Australasian Conference on Robotics & Automation* Brisbane, Australia.
- YOUN, J. H. 2006. *Urban Area Road Extraction from Aerial Imagery and LiDAR*. Doctor of Philosophy, Purdue University.
- ZHAO, Y. 1997. *Vehicle location and navigation systems*, Artech House, Inc.
- ZHENG, Y., LI, Q., CHEN, Y., XIE, X. & M, W.-Y. M. Understanding mobility based on GPS data. Proceedings of the 10th international conference on Ubiquitous computing (UbiComp '08), 2008. ACM, New York, NY, USA, 312-321.
- ZHU, C., SHI, W., PESARESI, M., LIU, L., CHEN, X. & KING, B. 2005. The Recognition of Road Network from High-Resolution Satellite Remotely Sensed Data Using Image Morphological Characteristics. *International Journal of Remote Sensing*, 26, 5493-5508.